TITLE

Synthesis and biological investigation of antifungal peptides and benzimidazoles

DISSERTATION

Synthese und biologische Untersuchung antifungisch wirkender Peptide und Benzimidazole

der Mathematisch-Naturwissenschaftliche Fakultät der Eberhard-Karls- Universität Tübingen
zur Erlangung des Grades eines Doktors der Naturwissenschaften

2017

vorgelegt von

Clàudia R. Aunós

This dissertation was carried out from October 2013 to October 2016 at EMC microcollections GmbH, Tübingen and at the Institute of Organic Chemistry, Eberhard Karls Universität Tübingen under the supervision of:

Prof. Dr. Karl-Heinz Wiesmüller

and

Prof. Dr. Martin E. Maier

To my parents

Acknowledgments

I would like to start to thank my supervisors Prof. Dr. Karl-Heinz Wiesmüller and Prof. Dr. Martin E. Maier.

I thank to EMC microcollections GmbH to allow me do my PhD; to Dr. Holger Eickhoff and to Dr. Renate Spohn.

I acknowledge Dr. Steffen Rupp (Fraunhofer Institute, Stuttgart), Prof. Dr. Karl Kuchler (Medical University Vienna, Max F. Perutz Laboratories, Vienna) and Dr. Concha Gil (Universidad Complutense de Madrid, Madrid) for letting me use their facilities to test my compounds. To all the rest of the PI's involved in this ImResFun project, thank you as well for all the good times we have spent together during the meetings and for the value discussions. It has been a truly pleasure!

Being part of this Marie-Curie Initial Training Network (ITN) has been the best part during my PhD. I met so amazing people from around the world that I am happy to treasure them for life. To all of you: Nathalie Uwamahoro, Raju Shivarathri, Andreas Küchbacher, Débora Teixeira Duarte, Fitz Gerald Silao, Emilia Gómez Molero, Mariana Blagojevic, Vicent Llopis Torregrosa, Catarina Oliveira Vaz, Tanmoy Chakraborty, Enrst Thür, Leonel Pereira and Nitesh Kumar Singh, thank you so much from the deepest of my heart. Sharing experiences, life and jokes with you has been the best time ever. I love our ImResFun family and I can only wish you all the best in your professional and personal life.
I don't know if our paths will meet again, but I want you to know that you can always count on me and don't forget… you have a home in Barcelona anytime you want!
I would like to include in my ImResFun family two of the people I had to collaborate with during this journey: Filomena Nogueira and Fabian Istel, which they have helped me and taught me a lot and I could only learn in the easiest and best way possible: enjoying every second of it.

Being here at this moment it wouldn't have been possible without my master supervisor Prof. Dr. Francesc Rabanal. His blind trust on me has shown me that you can reach your goals if there is always passion and hard work. I had one of my best professional times in that lab and it is thanks to him and mostly because of my little lab group in Barcelona. Ari (sorry to not

add your Doctor designation here, to me you are plain Ari), Helena and Natàlia, we started as a lab's workmates and we have ended up being friends. Can I ask for more?
To you Ari, I can't describe how grateful I am. Your help always in the worst moments has been much appreciated it. You might not know, but you have taught me so many things (not only about science) that I will always be grateful that life brought me in that lab when you were there. I believe that sometimes, unexpected things happen in life to give us the change to learn, grow up and enjoy better what has to come. Ari, your friendship is the best example! Thank you so much to you and your family, don't forget to tell them so!

To all my friends that I left in Barcelona or around the world, when I moved to Tübingen which they gave me all the support from distance but as much as if they were here with me, thank you. Thanks to all of you to always find a moment to meet me when I am home. I am very lucky to have you all in my life. To Débora, Daniel (my D&D couple) and Joan, my three big pillars in Germany, thank you for making my time there more enjoyable and less homesick. You have given me strength to keep forward from those moments when I was in low mood but mostly, for all your selflessly help all the times I needed without asking. To Mariana, since the moment we met, you became a very important sweet person in my life. I am very fortunate to call you my friend (and Raviolo!!).

My mental me wouldn't have survived without my closest and dearest bestfriends, Lídia, Elisabet and Laura. To all of you, thank you so much for just simply being there, not only during this PhD but also through my life. To me, you define the meaning of a true friend and I hope to keep growing up by your sides as long as life lets us. I know I don't say it very often, but I love you so much, I can't imagine my life without you, girls!

Finally but not the least, I reserve my last paragraph and therefore a change of language, to the most important people in my life, my lovely family.

A mi gran familia Aunós decirles que qué placer de familia, oye! Dicen que la familia no se escoge pero qué suerte la mía la de haber nacido en ésta. Adoro los momentos y las risas con vosotros, no cambéis nunca. A mi tíos, muchas gracias por todos los ánimos durante este trayecto y por celebrar mis éxitos cómo si fueran vuestros.

En momentos así no puedo dejar de pensar en mis abuelitos, que me han querido mucho, mucho, muchísimo. Me da pena que no puedan disfrutar de éste momento conmigo, pero me gusta pensar que allí dónde estén, puedan verme y se sientan orgullosos de lo que he conseguido hasta ahora.

Finalment, agrair a la meva petita i més pròxima família: ha estat un camí molt dur, ho sabeu molt bé, però he aconseguit arribar on estic i ser com sóc gràcies a vosaltres. Sempre ens heu ensenyat que hem de ser pacients ja que en algun moment l'esforç acaba sent recompensat, que cal quedar-se només amb les coses bones i que cal extreure experiència de les dolentes. Durant aquest camí hi ha hagut masses moments dels últims i ha costat seguir els vostres consells, però espero haver-ho fet el millor que he pogut degudes les circumstàncies. Creieu-me quan us dic que aquest camí ple d'entrebancs i que semblava sense fi, no hagués estat possible d'avançar sense el vostre amor, suport i ànims diaris i des de la distància. Ens heu dit molts cops l'orgullosos que esteu de nosaltres, però haig de dir-vos que em considero una de les persones més afortunades en aquesta vida, i no sabeu el que m'omple a mi d'orgull ser part d'aquesta meravellosa família.
Mama, Papa i Víctor, aquesta tesi està dedicada a vosaltres. Us estimo molt!

"*Nothing in life is to be feared, it is only to be understood. Now is the time to understand more, so that we may fear less.*" – **Marie Curie**, 1973.

List of abbreviations

Aa	Amino acids
ACN	Acetonitrile
Ac_2O	Acetic anhydride
AcOH	Acetic acid
AMPs	Antimicrobial peptides
anh	Anhydrous
APS	Ammonium persulfate
aq	Aqueous
ATCC	American type culture collection
atm	Atmosphere
Boc	*tert*-Butyloxycarbonyl
BOP	(Benzotriazol-1-yloxy)tris(dimethylamino)phosphonium hexafluorophosphate
tBu	*tert*-Butyl
tBuLi	*tert*-Butyl lithium
°C	Degrees celsius
CASY	Cell counting system
CC_{50}	50 % Cytotoxic concentration
CDI	Carbonyldiimidazole
CFU	Colony-forming unit
$CHCl_3$	Chlorofom
d	Day(s); doublet (spectral)
DCM	Dichloromethane
DHR	Dihydrorhodamine
DIC	Diisopropylcarbodiimide
DIPA	Diisopropylamine
DIPEA	Diisopropylethylamine
DMF	Dimethylformamide
DMFDMA	Dimethylformamide dimethyl acetal
DMSO	Dimethyl sulfoxide
DTT	Dithiothreitol
ECF	Ethyl chloroformate
EDTA	Ethylenediaminetetraacetate
eq	Equivalent(s)
ESI	Electrospray ionization
Et	Ethyl
EtAc	Ethyl acetate
Et_3N	Triethylamine
Et_2O	Diethyl ether
EtOAc	Ethyl acetate
EtOH	Ethanol
EUCAST	European committee on antimicrobial susceptibility testing
f	Functionalization
FBS	Fetal bovine serum
FCS	Fetal calf serum
FDA	Food and drug administration; Fluorescein diacetate
Fmoc	9-Fluorenylmethoxycarbonyl
HeLa	HeLa cells (Henrietta Lacks)
HOBt	Hydroxybenzotriazole
HPLC	High-performance liquid chromatography
iBu	*Iso*-butyl
IC_{50}	50 % Inhibitory concentration
iPro	*Iso*-propyl

MeNHOMe	N,O-Dimethyldidroxylamine
NBS	N-Bromosuccinimide
NMM	N-Methylmorpholine
NMP	N-Methyl-2-pyrrolidone
NMR	Nuclear magnetic resonance
O^{t}Bu	*tert*-Butyl ester
Oxyma Pure	Ethyl cyano(hydroxyimino)acetate
Pbf	Pentamethyl-2,3-dihydrobenzofuran-5-sulfonyl
PBS	Phosphate-buffered saline
PI	Propidium iodide
PMSF	Phenylmethane sulfonyl fluoride
ROS^{+}	Reactive oxygen species
ppm	Part per milion
RPMI	Roswell Park Memorial Institute medium
rt	Room temperature
s	Singulet, seconds
SDS	Sodium dodecyl sulfate
TBAc	*tert*-Butyl acetate
TCTU	*N,N,N',N'*-Tetramethyl-*O*-(6-chloro-1*H*-benzotriazol-1-yl)uranium tetrafluoroborate
TEA	Triethanolamine
TEMED	Tetramethylethylenediamine
TFA	Trifluoroacetic acid
THF	Tetrahydrofuran
TIS	Triisopropylsilane
Trt	Trityl
UV	Ultraviolet
YP	Yeast peptone
YPD	Yeast peptone dextrose
Z	Benzyloxycarbonyl

ANNEX I
Benzimidazole compound collection

EMC120B12

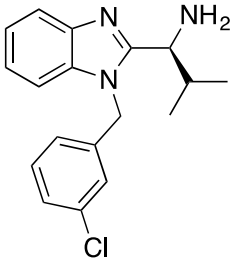

BE1

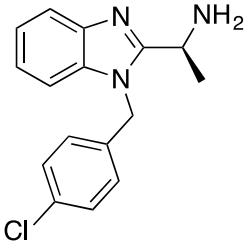

BE2

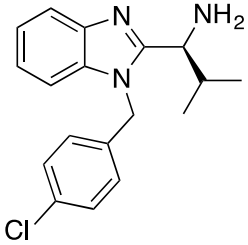

BE3

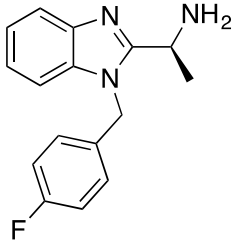

BE4

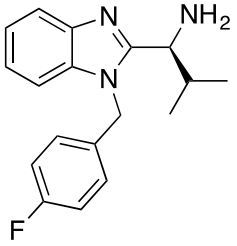

BE5

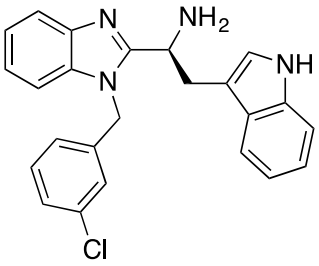

BE6

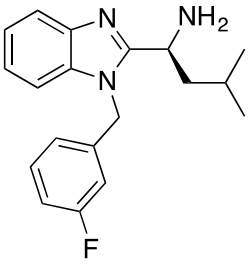

BE7

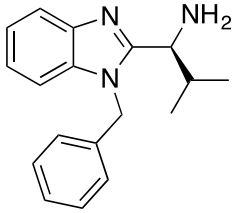

BE8

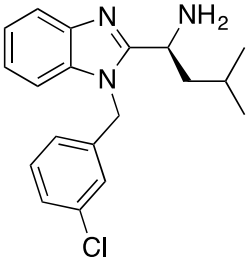

BE9

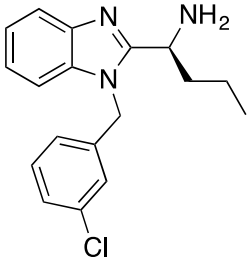

BE10

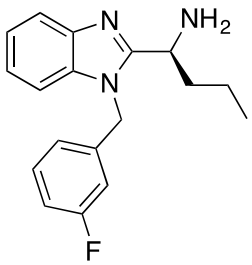

BE11

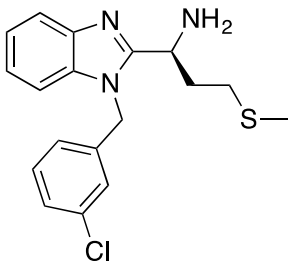

BE12

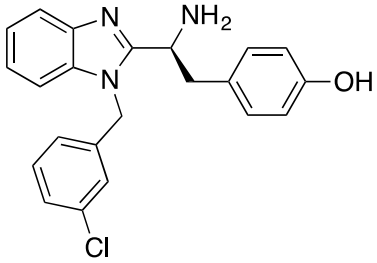

BE13

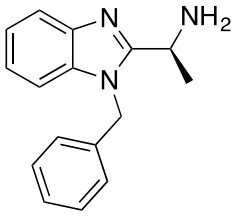

BE14

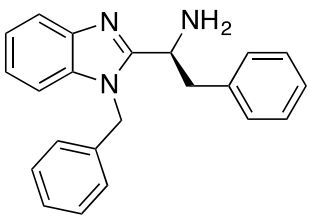

BE15

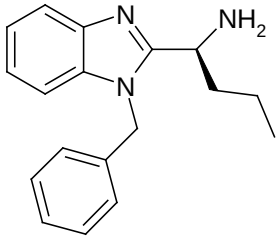

Triazole compound collection

TR1

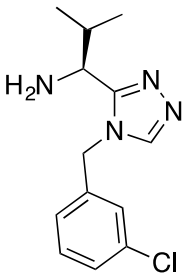

TR2

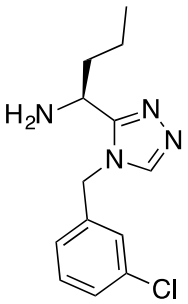

TR3

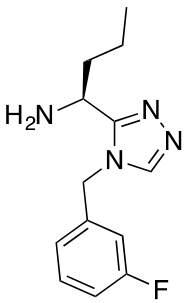

TR4

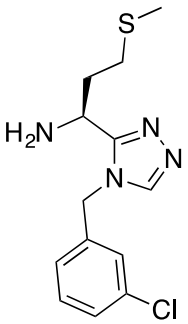

TR5

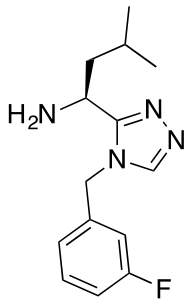

TR6

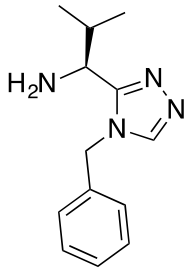

TR7

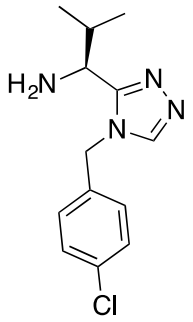

TR8

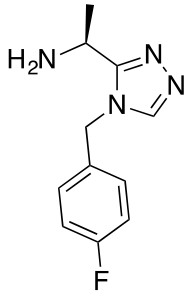

Indole compound collection

IN0

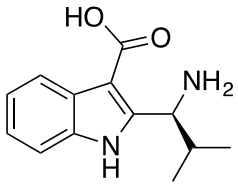

IN1

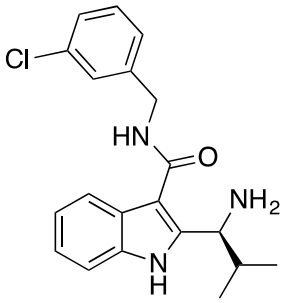

IN2

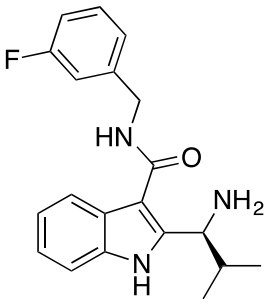

IN3

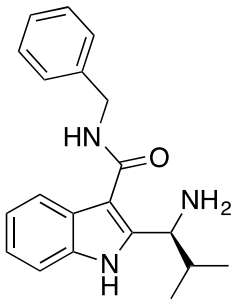

IN4

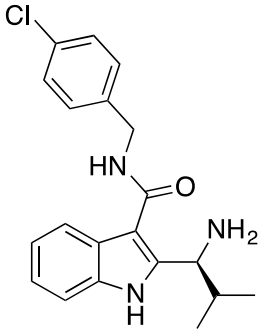

IN5

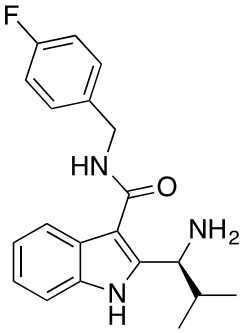

IN6

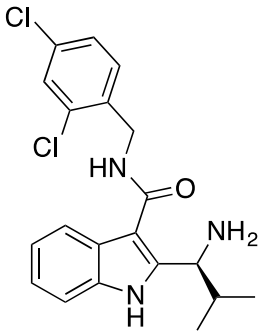

IN7

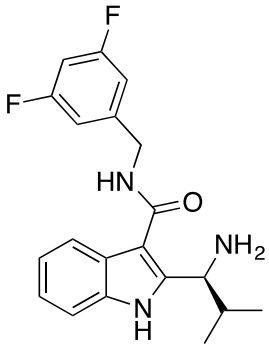

Imidazo[1,2-a]pyridine compound

ImPn1

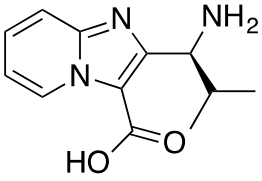

Imidazo[1,2-a]pyrimidine compound

ImPm1

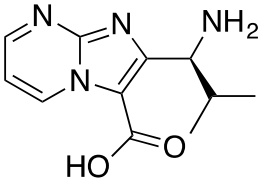

ANNEX II

Table of LL-37 and analogues. Green letter refers to hydrophilic amino acids; Black and underlined refers to positive charged amino acids; Purple and italics refers to negative charged amino acids; Blue corresponds to polar amino acids; Orange refers to special amino acids; Red refers to the modifications done. The names of the analogues are designed with the first two letters of the sequence followed by the modified residue with the position within the sequence (red). The pale pink background is the controls synthesized. The blue background corresponds to the disruption of the hydrophilic zone by amino acid Ser. The pale orange background refers to where the bench is located in the peptide sequence. Yellow background is the minimum sequence needed to obtain biological activity by literature. Bright pink background refers to C-terminal modification by an amide termination. **Ac-KS-30**; **Ac-KS-30-NH_2** and **KS-30-NH_2** have the C-terminal, N-terminal or both modified by acetylation (brown) or/and amidation (bright pink). [a]Net charge at pH = 7.

Sequences

ID	Name	1	2	3	4	5	6	7	8	9	10	11	12	13	14	15	16	17	18	19	20	21	22	23	24	25	26	27	28	29	30	31	32	33	34	35	36	37	Charge[a]
LL-37	LL-37	L	L	G	*D*	F	F	R	K	S	K	*E*	K	I	G	K	*E*	F	K	R	I	V	Q	R	I	K	*D*	F	L	R	N	L	V	P	R	T	*E*	S	+ 6
FK-13	FK-13																	F	K	R	I	V	Q	R	I	K	*D*	F	L	R									+ 4
KR-12	KR-12																		K	R	I	V	Q	R	I	K	*D*	F	L	R									+ 4
RK-31	RK-31							R	K	S	K	*E*	K	I	G	K	*E*	F	K	R	I	V	Q	R	I	K	*D*	F	L	R	N	L	V	P	R	T	*E*	S	+ 7
KS-30	KS-30								K	S	K	*E*	K	I	G	K	*E*	F	K	R	I	V	Q	R	I	K	*D*	F	L	R	N	L	V	P	R	T	*E*	S	+ 6
KR-20	KR-20																		K	R	I	V	Q	R	I	K	*D*	F	L	R	N	L	V	P	R	T	*E*	S	+ 4
(11)	AS-30								A	S	K	*E*	K	I	G	K	*E*	F	K	R	I	V	Q	R	I	K	*D*	F	L	R	N	L	V	P	R	T	*E*	S	+ 5
(12)	KF-30								K	F	K	*E*	K	I	G	K	*E*	F	K	R	I	V	Q	R	I	K	*D*	F	L	R	N	L	V	P	R	T	*E*	S	+ 6
(13)	KSA_7-30								K	S	K	*E*	K	I	A	K	*E*	F	K	R	I	V	Q	R	I	K	*D*	F	L	R	N	L	V	P	R	T	*E*	S	+ 6
(14)	KSR_8-30								K	S	K	*E*	K	I	G	R	*E*	F	K	R	I	V	Q	R	I	K	*D*	F	L	R	N	L	V	P	R	T	*E*	S	+ 6
(15)	KSG_8-30								K	S	K	*E*	K	I	G	G	*E*	F	K	R	I	V	Q	R	I	K	*D*	F	L	R	N	L	V	P	R	T	*E*	S	+ 5
(16)	KS-30- NH_2								K	S	K	*E*	K	I	G	K	*E*	F	K	R	I	V	Q	R	I	K	*D*	F	L	R	N	L	V	P	R	T	*E*	S	+ 6
(17)	Ac-KS-30						CH_3	CO	K	S	K	*E*	K	I	G	K	*E*	F	K	R	I	V	Q	R	I	K	*D*	F	L	R	N	L	V	P	R	T	*E*	S	+ 6
(18)	Ac-KS-30- NH_2						CH_3	CO	K	S	K	*E*	K	I	G	K	*E*	F	K	R	I	V	Q	R	I	K	*D*	F	L	R	N	L	V	P	R	T	*E*	S	+ 6
(19)	KK-31							K	K	S	K	*E*	K	I	G	K	*E*	F	K	R	I	V	Q	R	I	K	*D*	F	L	R	N	L	V	P	R	T	*E*	S	+ 7

Continuation: table of LL-37 and analogues. Green letter refers to hydrophilic amino acids; Black and underlined refers to positive charged amino acids; Purple and italics refers to negative charged amino acids; Blue corresponds to polar amino acids; Orange refers to special amino acids; Red refers to the modifications done. The names of the analogues are designed with the first two letters of the sequence followed by the modified residue with the position within the sequence (red). The pale pink background is the controls synthesized. The blue background corresponds to the disruption of the hydrophilic zone by amino acid Ser. The pale orange background refers to where the bench is located in the peptide sequence. Yellow background is the minimum sequence needed to obtain biological activity by literature. Bright pink background refers to C-terminal modification by an amide termination. **Ac-KS-30**; **Ac-KS-30-NH_2** and **KS-30-NH_2** have the C-terminal, N-terminal or both modified by acetylation (brown) or/and amidation (bright pink). [a]Net charge at pH = 7.

Sequences

ID	Name	1	2	3	4	5	6	7	8	9	10	11	12	13	14	15	16	17	18	19	20	21	22	23	24	25	26	27	28	29	30	31	32	33	34	35	36	37	Charge[a]
(20)	KSA_3-30								K	S	A	*E*	K	I	G	K	*E*	F	K	R	I	V	Q	R	I	K	*D*	F	L	R	N	L	V	P	R	T	*E*	S	+ 5
(21)	KSF_{17}-30								K	S	K	*E*	K	I	G	K	*E*	F	K	R	I	V	Q	R	F	K	*D*	F	L	R	N	L	V	P	R	T	*E*	S	+ 6
(22)	KS-22								K	S	K	*E*	K	I	G	K	*E*	F	K	R	I	V	Q	R	I	K	*D*	F	L	R									+ 6
(23)	KS-26								K	S	K	*E*	K	I	G	K	*E*	F	K	R	I	V	Q	R	I	K	*D*	F	L	R	N	L	V	P					+ 6
(24)	KSA_{29}-30								K	S	K	*E*	K	I	G	K	*E*	F	K	R	I	V	Q	R	I	K	*D*	F	L	R	N	L	V	P	R	T	A	S	+ 7
(25)	KSA_9-30								K	S	K	*E*	K	I	G	K	A	F	K	R	I	V	Q	R	I	K	*D*	F	L	R	N	L	V	P	R	T	*E*	S	+ 7
(26)	KS-27								K	S	K	*E*	K	I	G	K	*E*	F	K	R	I	V	Q	R	I	K	*D*	F	L	R	N	L	V	P	R				+ 7
(27)	KE-23															K	*E*	F	K	R	I	V	Q	R	I	K	*D*	F	L	R	N	L	V	P	R	T	*E*	S	+ 4
(28)	FF-22																F	F	K	R	I	V	Q	R	I	K	*D*	F	L	R	N	L	V	P	R	T	*E*	S	+ 4
(29)	SK-29									S	K	*E*	K	I	G	K	*E*	F	K	R	I	V	Q	R	I	K	*D*	F	L	R	N	L	V	P	R	T	*E*	S	+ 5
(30)	KE-28										K	*E*	K	I	G	K	*E*	F	K	R	I	V	Q	R	I	K	*D*	F	L	R	N	L	V	P	R	T	*E*	S	+ 5
(31)	FK-21																	F	K	R	I	V	Q	R	I	K	*D*	F	L	R	N	L	V	P	R	T	*E*	S	+ 4
(32)	KF-22																K	F	K	R	I	V	Q	R	I	K	*D*	F	L	R	N	L	V	P	R	T	*E*	S	+ 5

(33)	FKG_{13}-13		F	K	R	I	V	Q	R	I	K	*D*	F	L	G	+ 3
(34)	FK$F_{12}G$-13		F	K	R	I	V	Q	R	I	K	*D*	F	F	G	+ 3
(35)	FKN_{3}-13		F	K	N	I	V	Q	R	I	K	*D*	F	L	R	+ 3

INDEX

INTRODUCTION

1. INTRODUCTION

1.1. Fungal infections

Fungi have become a major issue in critically ill patients and, in the latest years, invasive fungal infections have risen as one of the major causes of morbidity and mortality for immunocompromised patients. [1] Fungi can grow in two forms, i.e. yeast and moulds, and appear as either endogenous or exogenous infections (Figure 1). [2,3]

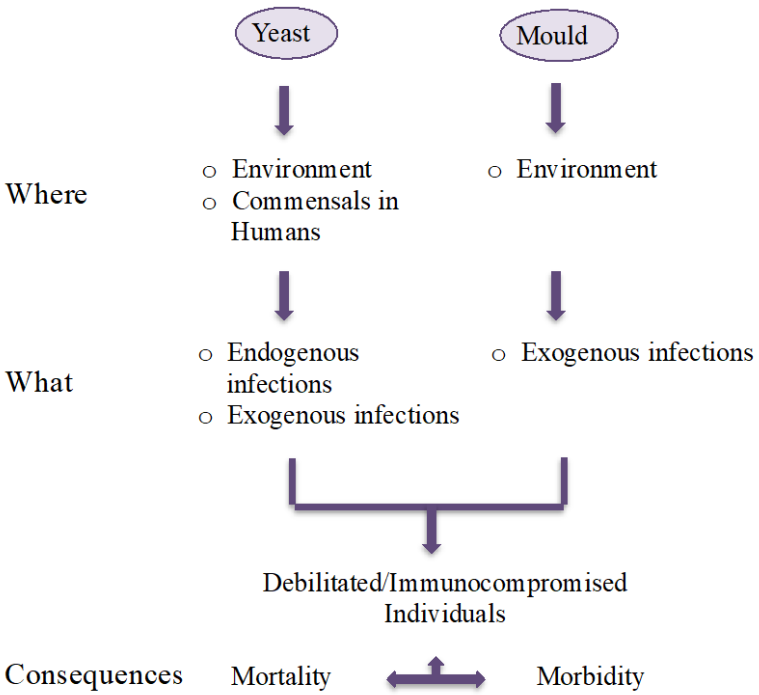

Figure 1. Flow chart representing source and consequences of invasive fungal infections: where they can be found, what kind of infections they can develop and the consequences of those infections for immunocompromised patients.

Fungal infections are often classified as opportunistic or primary. [4] The main difference between those types of infections is that the opportunistic ones take advantage of a weakened immune system, while the primary ones can occur in patients with a healthy immune system.

The most common opportunistic pathogenic fungi are *Candida albicans*, *Aspergillus fumigatus* and *Cryptococcus neoformans* among others. [5,6]

Candida albicans exists as a harmless commensal pathogen in oral cavities as well as in gastrointestinal and genitourinary tracts, behaving as normal flora. Although bacteria present in those tracts control the growth of *Candida* in such areas, the use of antibiotics may allow fungi to grow unchecked, thus causing the infection. Normally, the balance is restored once bacteria grow back and hence the infection usually resolves with no further problems. That

would be the case of the typical vaginal candidiasis, of which according to some studies almost 75 % of reproductive-age women will be affected at least once in their life. [7] Although these superficial infections are quite common and produce no major harm, they may become severe in immunocompromised individuals, such as HIV-infected or chemotherapy patients, transplant recipients and low birth weight infants. Damage caused by *Candida albicans* infection, generally known as candidiasis, may range from superficial to life-threating. [8, 9]

Thus, *Candida* has become a serious medical problem, specially due to the high level of resistance it exhibits against most clinically used antifungals drugs, which has been related to its ability to form biofilms. [10]

1.2. Fungal resistance and antifungal drugs

The World Health Organization recognizes the antifungal resistance as one of the three major threats to human health. [11] Basically, emerge of drug-resistance, poor diagnosis and lack of effective antifungal drugs are the main factors for the high mortality and morbidity. [12]

Developing effective antifungal drugs and therapies is quite challenging, as fungi are eukaryotes. They share many similarities with the host, except for the cell wall, which limits the exploitation of fungal-specific targets. [13]

Compared to the wide range of antibacterial drugs present in the pharmaceutical market, the number of available drugs against fungi is considerably limited. Antifungal drugs target various stages of metabolic pathways and they can be classified in different groups depending on their structure: [5, 6]

- Polyenes: the most known polyene drug is called Amphotericin B (AmB). Polyenes target the ergosterols and thus destabilize the plasma membrane of fungal cells and they initiate cell lysis. One of the advantages of AmB is that fungi rarely develop resistance, although AmB is compromised with high toxicity to the host. [14]

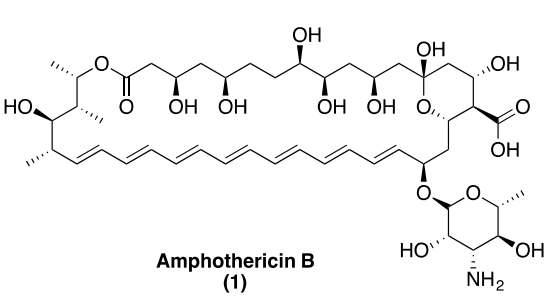

Amphothericin B
(1)

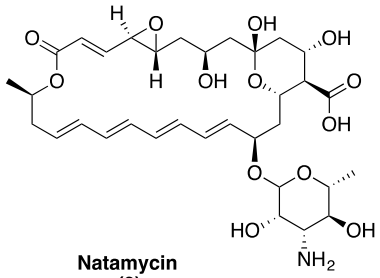

Natamycin
(2)

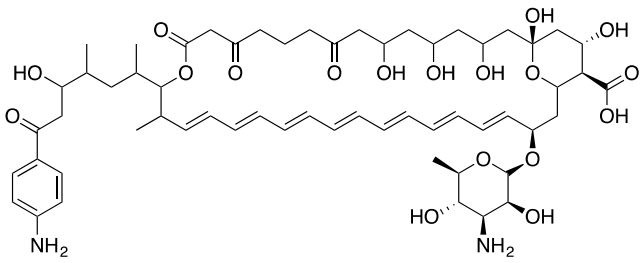

Candicidin
(3)

- Azoles: this group can be divided in two groups, the azoles with one or two nitrogen atoms (indole, benzimidazole, imidazole, etc…) and the ones with three nitrogen atoms like triazoles. They target the ergosterol biosynthesis pathway by blocking a key enzyme (Erg11p), hence killing the fungi. Fluconazole (**6**) or Voriconazole (**7**) are the most common antifungal drugs belonging in this group. [15]

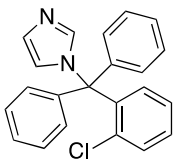

Clotrimazole
(4)

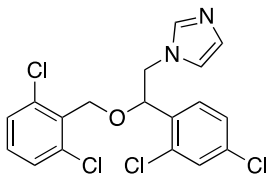

Isoconazole
(5)

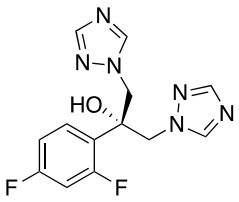

Fluconazole
(6)

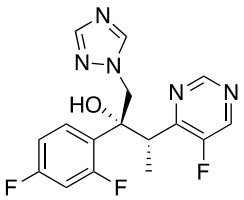

Voriconazole
(7)

- Echinocandins: a new type of antifungals with a lipocyclopeptide structure. The most known is caspofungin B (**8**). Echinocandins inhibit the synthesis of β-D-glucan, a cell-wall component. One of their main advantages is their lower toxicity compared to that of polyenes. [16, 17]

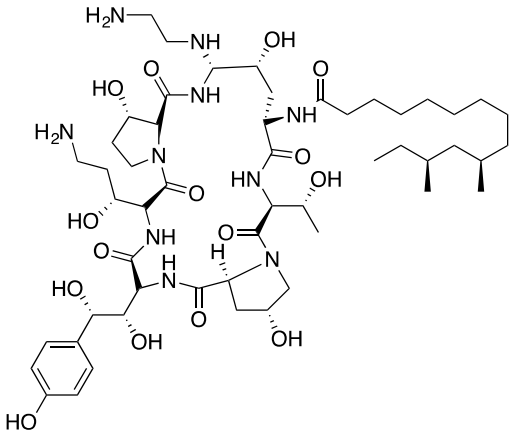

Caspofungin (8)

- Allylamines: this kind of antifungals inhibit squalene epoxidase, an enzyme required for ergosterol synthesis. Naftifine (**9**) and Terbinafine (**10**) belong to this group. [6]

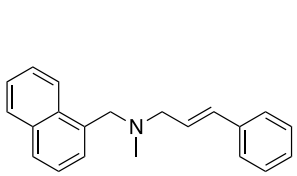

Naftifine (9)

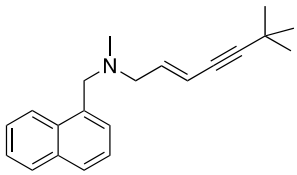

Terbinafine (10)

It is worth noting that the number of antimicrobial and antifungal agents approved by the United States Food and Drug Administration (FDA) and the European Medicines Agency (EMA) has sharply decreased over the last 25 years. [18] The last antifungal drug approval by the FDA dates from March 2015, when Cresemba was accepted for the treatment of invasive *aspergillosis* and invasive mucormycoses in adults. Therefore, the finding of new antifungals or new strategies to restore the effectiveness of known antifungals has become a major issue. [19, 20]

1.3. Identification of new antifungal drugs

Historically, many drugs present in the pharmaceutical market were originally isolated from natural sources. Nowadays, in contrast, biologically relevant compounds are usually generated by means of synthetic medicinal chemistry and computational design, which has vastly increased the efficiency of the drug-discovery process. [21, 22]

Combinatorial chemistry is a useful technology in medicinal chemistry. Its basic principle is the preparation of a large number of related compounds by parallel synthesis, which is followed by high-throughput screening to identify the most promising compounds for further development.

However, the screening of a large number of structurally diverse drugs is neither economical nor efficient.

Then, “how can we design economically viable drugs maintaining or improving efficacy?” [23]

The approval of “scaffold hopping” is a valuable tool in drug development to generate focused compound collections by modifying the core structure of known active compounds.

In this way, there is no need to synthesize a large numbers of compounds, but rather to progressively improve hit rates by exploring molecular space. [24, 25]

Within this strategy there is a subcategory, the target-family oriented collections that consist of compounds specifically designed to target certain protein families. This new focused collection may potentially be more effective than the initial active compound.

OBJECTIVES

2. OBJECTIVES

The aim of this work is the design, synthesis and evaluation of novel lead structures, which provide better biological activities and lower cytotoxicities compared to a previously found lead structure against *Candida* species.

The design and synthesis of novel lead compounds was based on focused target-family design and supported by solid phase and solution phase combinatorial organic chemistry.

This work is divided in two sections each with a starting lead compound.

The first section (**A**) is focused on the human antimicrobial peptide belonging to the cathelicidin family, called **LL-37**. Its characteristics are discussed in the next chapter.

In section (**B**), a series of (S)-2-aminoalkyl benzimidazoles, which are non-toxic to cell lines and exhibit antifungal activity against a set of significant clinical isolates of *Candida* spp, were synthesized. They were investigated for biological activity using a high-throughput activity-selectivity assay carried out at the Fraunhofer Institute in Stuttgart in 2011. [26] After screening, it was found that the active (S)-2-(1-aminoisobutyl)-1-(3-chlorobenzyl) benzimidazole, gave IC_{50} (half inhibitory concentration) and CC_{50} (half cytotoxicity concentration) values of 0.75 µM and 97.5 µM respectively (Figure 2). [20] This lead molecule was used for designing new (S)-2-aminoalkyl-benzimidazole analogues.

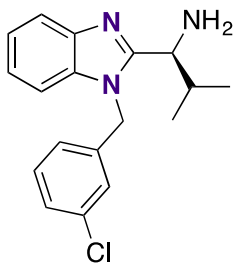

Figure 2. The antifungal compound (S)-2-(1-aminoisobutyl)-1-(3-chlorobenzyl)-benzimidazole structure (or EMC120B12). Initial hit identified on a previous high-throughput activity-selectivity assay.

Based on the scaffold hopping approach, indoles **a**, triazoles **b** and imidazo[1,2-a]pyridines **c** (Figure 3), have been synthesized. These scaffolds have been selected for their high probability to exhibit biological activity.

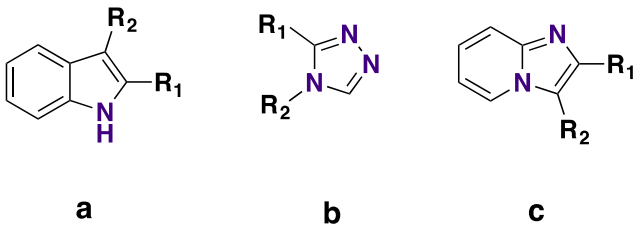

Figure 3. General structures of the investigated scaffolds

At the end of each of the two sections **(A)** and **(B)**, there is a full chapter summarizing the biological screenings of all compounds designed and synthesized in this work against several *Candida* species in collaboration with project partners.

ANTIMICROBIAL PEPTIDES

3. ANTIMICROBIAL PEPTIDES – SECTION A

3.1 Introduction Antimicrobial Peptides (AMPs)

Antimicrobial peptides can be mostly found in the host defence systems of a wide range of species, including amphibians, mammals, bacteria and fungi. [27]

To date, there are more than thousand peptides identified in nature and listed in the Antimicrobial Peptides Database (http://aps.unmc.edu/AP/main.php). These natural weapons, also called host defence peptides are very diverse in their sequences, length (normally short) and structures (linear or cyclic due to intramolecular bridges, with a variety of secondary structures) but generally they seem to adopt an amphipathic conformation with opposing hydrophobic and polar or charged faces that allows them to interact and disrupt selectively negatively charged microbial membranes. [28, 29] The functions of AMPs are very wide. They can be antibacterial, antiviral or antifungal or exhibit anticancer properties. They have been presented as promising noble class of antibiotics. [30]

It is known that humans produce three natural classes of AMPs, histatins, defensins and cathelicidins. [31]

- Histatins: expressed in saliva, are peptides rich in histidine residues and with good fungicidal activity. [32]
- Defensins: expressed in epithelia cells, are small, cysteine-rich (allowing them to form disulfide bonds) cationic and amphipathic peptides with good antimicrobial and fungicidal activity. [33]
- Cathelicidins: like defensins, are expressed in epithelia and in phagocytic cells are small, cationic and amphipathic peptides with high heterogeneous structural features in comparison to the two others AMPs groups. [34]

Whilst other mammals secrete several peptides from all three families, in mice and humans only one example of cathelicidin peptide is produced. For mice it is named CRAMP (Cathelin-Related Antimicrobial Peptide) and for humans, it is named **LL-37**. Its importance is not only in its antimicrobial properties but also in its modulation of the immune system.

3.2. Cathelicidins

Cathelicidins are a large family of antimicrobial and immunostimulatory peptides. [35, 36] The term cathelicidin was introduced in 1995 by Zanetti [37] to describe molecules both containing the cathelin domain and a C-terminal antimicrobial domain. Its name comes from an acronym

for Cathepsin L Inhibitor but also can be named as CAMP, referring to Cathelicidin Antimicrobial Peptide.

All members of this family are synthesized as a preproprotein comprising a signal peptide, a highly conserved N-terminal prosequence termed cathelin domain and a highly variable C-terminal peptide domain in which the antimicrobial activity is located (Figure 4). [35, 38, 39]

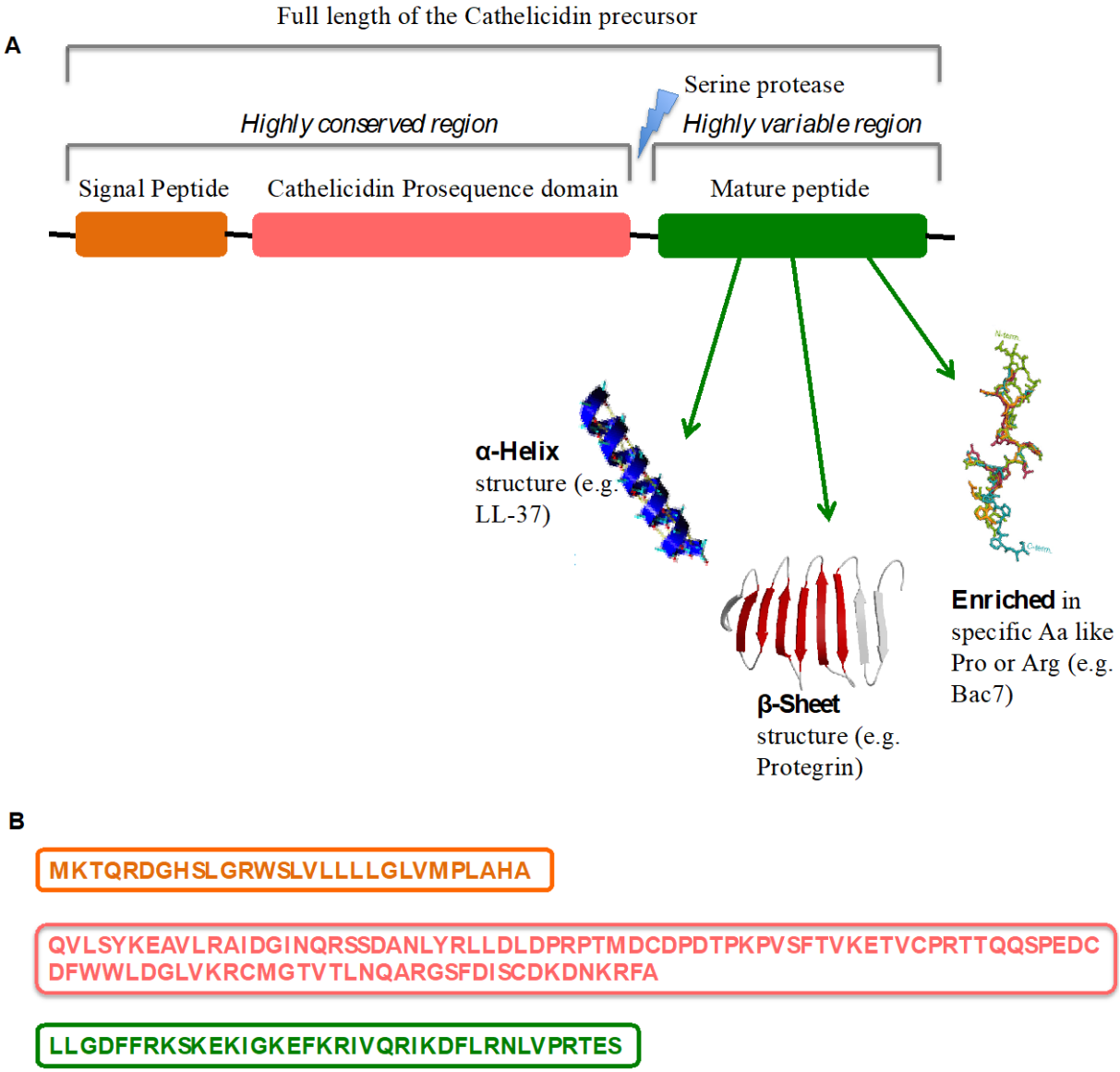

Figure 4. Sequence of the CAMP (**C**athelicidin **A**nti**M**icrobial **P**rotein) gene product. **A)** Full length of the Cathelicidin precursor composed by a signal peptide (orange, ≈ 30 Amino acids, aa), N-terminal Cathelin domain (pink, ≈ 94-144 aa) and a C-terminal Antimicrobial peptide **LL-37** (green, ≈ 12-100 aa). **B)** The Amino acid sequences for each of the three parts that formed the Cathelicidin precursor.

The mature C-terminal antimicrobial peptide ranges from 12-100 amino acid residues and diverse secondary structures are mostly found. The most common are the linear antimicrobial

peptides with an α-helix amphipathic structure like the human AMP **LL-37**, but also the are two other groups being flat β-sheet structures stabilized by disulfide bonds (e.g. Protegrin) and peptides rich in one amino acid like proline, arginine or tryptophan (e.g. Bac7, rich in proline and Indolicidin, rich in tryptophan).

Natural Killer (NK) cells and mast cells constitutively express the cathelicidin protein and store the precursor in granules. Activation of TLR(s) (Toll-like Receptors), immune receptors that recognize pathogens, and cell damage provides a trigger that activates the cell to degranulate. This leads to the release of the inactive peptide precursor in the extracellular environment where it can be processed by specific proteases into the active antimicrobial peptide. [40]

3.3. Human antimicrobial peptide LL-37

3.3.1. Introduction

LL-37 (name based on the first two amino acids in the sequence followed by the number of total residues in the peptide), also designed hCAP18 (terminology applied as an alternative to **LL-37**; containing a mass of 18 kDa before processing) is generated from the proprotein form hCAP18 encoded by the CAMP gene [41] hCAP18. Following the excision of the signal peptide, this proprotein is stored in neutrophil granules and epithelial cells until activated through cleavage by the serine protease, specifically, proteinase 3. [42]

Interestingly, after cleavage of **LL-37**, the cathelin domain has shown antimicrobial properties highlighting how evolution has maximised the antimicrobial function of hCAP18. [43]

As its name indicates, **LL-37** contains a sequence of 37 amino acid residues: LLGDFFRKSKEKIGKEFKRIVQRIKDFLRNLVPRTES adopting an α-helical structure in lipid membranes, micelles and ions but being a random coil in pure water. [44] At physiological pH, 16 of its 37 residues are charged, namely 6 Lys and 5 Arg residues carry 11 positive charges, while 3 Glu and 2 Asp residues bear 5 negative charges. Based on that, the resulting net charge at physiological pH is positive (6+).

Although **LL-37** is described as the sole human cathelicidin, other cleavage sites exist leading to different mature peptides. For example, peptides **KR-20**, **RK-31** and **KS-30** (table listing peptides in appendix) are found in human sweat and skin cells and they are a shorter version

of **LL-37**. [42] Despite being shorter, they still show biological activity which has opened a new aspect of study.

LL-37 has been shown to have multitude roles in our body. It is well known for its antibacterial effects [45, 46] but also has other antimicrobial properties including antifungal, [42, 47] antiviral, [48 - 49] anticancer, [50 - 51] and inhibition of biofilm formation. [52]

LL-37 has also been associated with modulation of the expression profiles of elements of the immune system, regulation of the inflammatory response, stimulation of wound healing, chemotaxis, apoptosis, angiogenesis and cancer tumourgenesis. [53 - 54]

LL-37 is sometimes referred as "alarmin" due to many of these immunomodulatory functions, which appear to occur at concentrations below the levels required for antimicrobial activities suggesting that the immune response may arise form interactions with more specific receptor proteins. [55]

3.3.2. Structure

LL-37 is a classical amphiphilic α-helical peptide. At low concentrations ($< 10^{-5}$ M) it is a largely unfolded monomeric peptide but at higher concentrations it adopts the α-helical oligomeric structure. [56] It is believed that the hydrophobic effect involving shielding of the hydrophobic face from the bulk medium is the cause of this switch. [57]

Some NMR studies in micelles with **LL-37** have shown some flexibility within the central helical core, this part of the sequence is described as a bent helix [58] and corresponds to an area of high glycine content in related primate orthologs. [59]

The existence of this helical bend between residues 14-16 within **LL-37** (Figure 5) allows classifying the human cathelicidin into three structural and functional regions:

1. The N-terminal unit (residues 1-13, labelled as **I** in Figure 5) is a relatively disordered non-polar / hydrophobic section which has been implicated in chemotaxis, in peptide oligomerization, in proteolytic resistance and hemolytic activity. [60, 61, 44]

2. The central bulk of the peptide (residues 17-31, labelled as **II**) is α-helical and contains the antimicrobial, antifungal and antiviral effect. [60, 62, 63]

3. The C-terminal end (residues 32-37, labelled as **III**) is described as a short hydrophilic tail unit that facilities the tetramer formation at physiological pH. [64, 65]

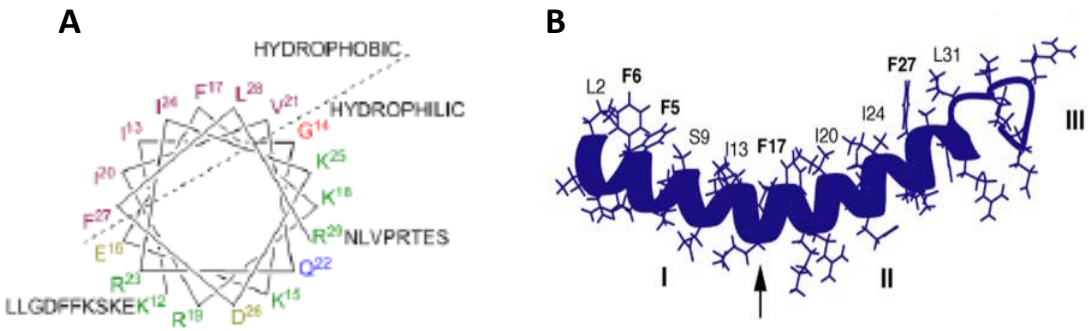

Figure 5. A) Helical wheel diagram for **LL-37**. **B)** *Ribbon representation* of the **LL-37** structure with hydrophobic side chains labelled. The helical bend is indicated by an arrow and the three structural regions are labelled **I**, **II** and **III**. Figures extracted from Wang, G.S. *J. Biol. Chem.*, **2008**, *283*, 32637-32643.

By using NMR techniques it is possible to show that the predominance of hydrophobic residues in the N-terminal region and the hydrophilic amino acids at the C-terminus make terminal sections of **LL-37** unstructured in lipid micelles and therefore not essential for antibacterial activity. [64, 66]

3.3.3. Mode of action

LL-37 has high diversity compared to other α-helical AMPs due to the lack of specificity when it easily binds to both microbial and mammalian membranes. [67 - 68]

In general, antimicrobial peptides target bacterial membranes rather than mammalian, simply, due to the fundamental difference in the composition of the cell wall. Mammalian cells contain only a cell membrane formed by a phospholipid bi-layer, being hydrophilic to the external part of the membrane and hydrophobic in the inner wall.

Bacteria, though, contain a cell membrane and an other outer membrane called cell wall. A sub-classification within bacteria cell walls exists: Gram-negative and Gram-positive.

Gram-positive bacteria possess a cell wall outside the membrane while Gram-negative bacteria contain an outer secondary membrane (Figure 6). Furthermore, Gram-negative cell walls contain lipopolysaccharides whilst Gram-positive bacteria present a surface of teichoic acids. In both bacteria classes, negatively charged cell surfaces predominate.

In contrast, most mammalian cell membrane have an outer leaflet comprised of zwitterionic phosphatidylcholine (PC) and sphingomyelin phospholipids (SM), whilst the inner leaflet is composed of phosphatidylserine (PS) leading to an essentially neutral surface. [57, 69]

Based on that, the negative charge associated with bacterial cells means that cationic AMPs are primarily attracted to the pathogenic membrane (negatively charged) rather than to that of mammalian cells (neutral charged).

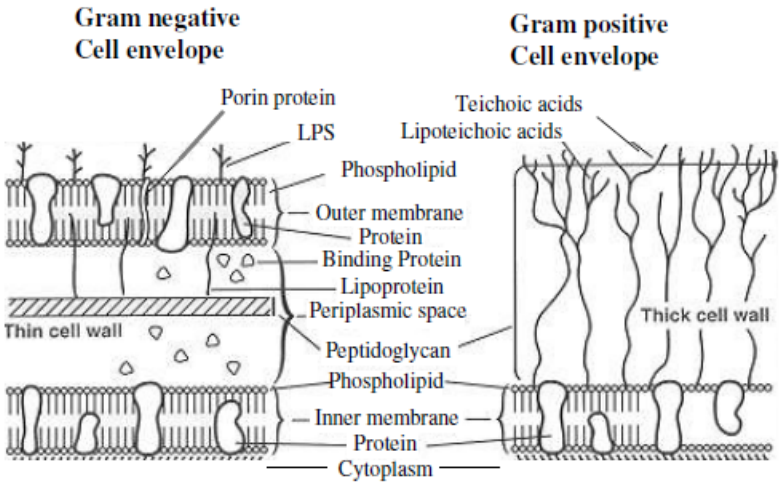

Figure 6. Comparison of the thin cell wall of Gram-negative bacteria (left) with the thick cell wall of Gram-positive bacteria (right). Adapted figure from public domain.

For antimicrobial peptides such as **LL-37**, three mechanisms for disrupting membranes has been proposed: [61, 57]

1) **The barrel-stave model**: this model requires that membrane bound peptides recognise each other, oligomers forming structured transmembrane pores within the membrane through which essential cellular components can escape.

2) "**Carpet-model**": peptides coat the phospholipid membrane surface until a threshold concentration is reached when the peptide either permeates the membrane in a detergent like manner or leads to the formation of toroidal holes. In the former, the peptides bind parallel to the membrane surface such that the positively charged amino acids of the peptide can maintain constant contact with the membrane (Figure 7).

3) **Toroidal-pore mechanism**: follows a similar initial pathway also involving curvature of the membrane. In this case, self-association of the membrane associated peptides leads to the formation of toroidal (doughnut like) holes in the membrane. [70]

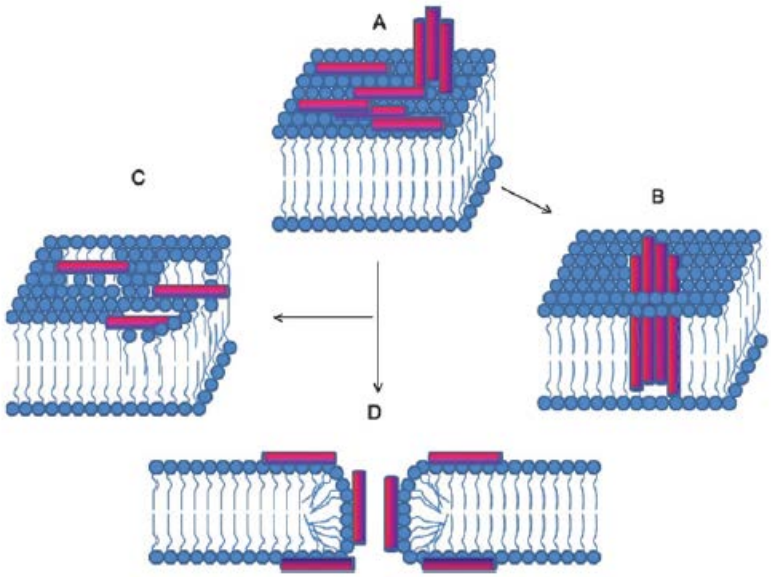

Figure 7. Mechanisms for insertion of **LL-37** into membranes: **A)** Monomers or aggregates of peptides approach to the membranes. **B)** Barrel-stave mechanism: the peptides form a large cylindrical pore lined with peptide oligomers inserting themselves perpendicular to the membrane. **C)** Carpet mechanism: peptides coat the membrane surface until a critical concentration when either the membrane is disrupted in a detergent like manner. **D)** Peptides bind to the phospholipids headgroups that induces such a high degree of membrane curvature forming the toroidal pores. (Burton, M.F and Steel, P; *Nat.Prod.Rep*., **2009**, *26*, 1572-1584).

LL-37 can interact with mammalian cell membranes as well despite not being negatively charged and stimulate a wide range of cell receptors and transcriptional factors. Significantly, it is through stimulating such targets that the human natural product exerts its immunomodulatory effects. [71, 72]

For the mode of action of AMPs two possibilities have been described: either AMPs binding triggers a chain of events leading to the displacement of a signalling molecule which then activates its cognate receptor or insertion of the AMPs into the lipid structure triggers an allosteric change to the receptor structure thus modifying the activity. [73 - 74]

3.3.4. Modifications

Due to its potential roles in many therapeutic areas, **LL-37** has been extensively studied. Fragments of this molecule are usually denoted by the one-letter-code abbreviation of its two initial amino acids followed by the number of residues. Tossi and co-workers [59] have determined more than a dozen cathelicidin sequences, each one with different biological activity. Their conclusion is, that the antimicrobial and immunomodulatory effects of the

peptide are interlinked and dependent on the key properties of charge, helicity and amphipathicity.

3.3.4.1. Modification of the N-terminus

As described in Section *3.3.2. Structure*, the predominance of hydrophobic residues in the N-terminal region is not essential for antibacterial activity considering the absence of affinity for membranes interaction. Johansson et al., [44] along with their studies of the wild type peptide, investigated two truncated variants, **FF-33** and **SK-29**, which lacked 4 and 8 residues on the N-terminus, respectively, making the fragments more hydrophilic than the full-length peptide but less effective in killing bacteria. However, despite not being biologically active against bacteria or fungi, they were crucial for the immunological activity of **LL-37**.

RK-31 and **KS-30** fragments lacking the hydrophobic N-terminal region, were found in human sweat and skin cells. They showed activity against some bacteria (*S. aureus* and *E. coli*) and some fungi (*C. albicans*) but also hemolytic activity. [42]

Our synthetic analogues were based on those two fragments and especially on **KS-30**, which gave the best inhibitory activity against *Candida*. [42] Therefore, most of the analogues start with KS followed by the rest of the **LL-37** sequence, varying some other regions of the main peptide.

Ac-KS-30 (**17**) and **Ac-KS-30-NH$_2$** (**18**), which were N-acetylated at the N-terminus (**17**) and also C-modified by an amide at the C-terminus (**18**) were designed in order to possible enhance the stability against exoproteases.

3.3.4.2. Modification of the C-terminus

It is considered that the short hydrophilic tail unit of the **LL-37** facilities the tetramer formation at physiological pH and therefore the better affinity to the cell membranes. [40] Majority of all analogues used in this work maintain the C-terminus untouched. **KS-30-NH$_2$** (**16**) and **Ac-KS-30-NH$_2$** (**18**) are peptide amides with no change in the sequence. **KS-22** (**22**), **FKG$_{13}$-13** (**33**), **FKF$_{12}$G-13** (**34**), **FKN$_3$-13** (**35**) and **KS-26** (**23**), are C-terminally truncated peptides.

3.3.4.3. **Modification of the bend section**

NMR studies have shown that between residues 14 to 16 a small bend exists, which gives some flexibility to the peptide. [58]

The flexibility might due to the high glycine content. The region was modified by:

- Changing glycine by hydrophobic alanine: **KSA$_7$-30** (**13**) and **KSA$_9$-30** (**25**)
- Adding an additional glycine residue: **KSG$_8$-30** (**15**)
- Moving the bend to the N-terminus of the peptide: **KE-23** (**27**)

3.3.4.4. **Modification in the net charge**

LL-37 at physiological pH has a positive net charge of + 6. It is well known that antimicrobial peptides with different net charge have different biological activity. [40] Therefore, the immunomodulotary and antimicrobial effects of peptides may be interlinked and dependent on their charge.

To address this subject, we have designed some analogues with more and less positive net charge than + 6: **KK-31** (**19**), **KSA$_{29}$-30** (**24**) and **KS-27** (**26**) (charge + 7); **KSA$_3$-30** (**20**), **SK-29** (**29**), **AS-30** (**11**), **KE-28** (**30**) and **KF-22** (**32**) (charge + 5); **KE-23** (**27**), **FF-22** (**28**) and **FK-21** (**31**) (charge + 4); **FKG$_{13}$-13** (**33**), **FKF$_{12}$G-13** (**34**) and **FKN$_3$-13** (**35**) (charge + 3).

3.3.4.5. Modification of the core section

Wang's group [58] using also NMR, identified the smallest active peptide within **LL-37** sequence which still gives antimicrobial activity. Called **FK-13**, it was designed as the "core" of the **LL-37** structure. Based on that, the residues that comprise the core of the long analogues were not varied. Only a few analogues, in which the length coincided with **FK-13** or **KR-12**, have been slightly modified. The only variations done were focused on changing the positive net charge, **FKG$_{13}$-13** (**33**), adding hydrophobic residues, **FKF$_{12}$G-30** (**34**) or adding polar side chains, **FKN$_3$-13** (**35**).

3.3.4.6. Other modifications

The presence of the residue serine in position 9 in the full sequence of **LL-37** disrupts the hydrophobic region of the peptide. To study this disruption and its effects on the biological activity, the analogue **KF-30** (**12**) was designed.

The aromatic hydrophobic phenyl residues of F5, F6, F17 and F27 of **LL-37** could have an essential role for the interaction with phosphatidylglycerols in the bacteria membrane. [58] Mostly all the analogues are based on **KS-30**, which lack of F5 and F6 but not F17 and F27. We assumed that F5 and F6 were less important, as the shortest analogues of **LL-37** (**KR-12** and **FK-13**) still produce some biological activity despite the absence of F5 and F6.

3.4. Synthesis of LL-37 analogues

3.4.1. Solid phase peptide synthesis

Bruce Merrifield pioneered in 1963 the solid phase synthesis, for which he won the Nobel Prize in 1984. [75] His concept has spread in many fields, including in parallel organic chemistry.

The basic of the technique consists in constructing the peptide through successive addition of protected amino acids, anchored to an insoluble polymer through its C-terminus (Figure 8).

The most benefits of SPPS are the separation of the intermediate polymer-bounded peptides from soluble reagents and solvents by filtration and washing; excess of reagents can be employed to help to drive reactions to completion and the physical losses can be minimized as the peptide remains attached to the support throughout the synthesis. There are several limitations. By-products arising from incomplete reactions or side reactions can accumulate on the resin during chain assembly and contaminate the final product. Also, the yield of the reaction will decrease in longer peptides. [76, 77]

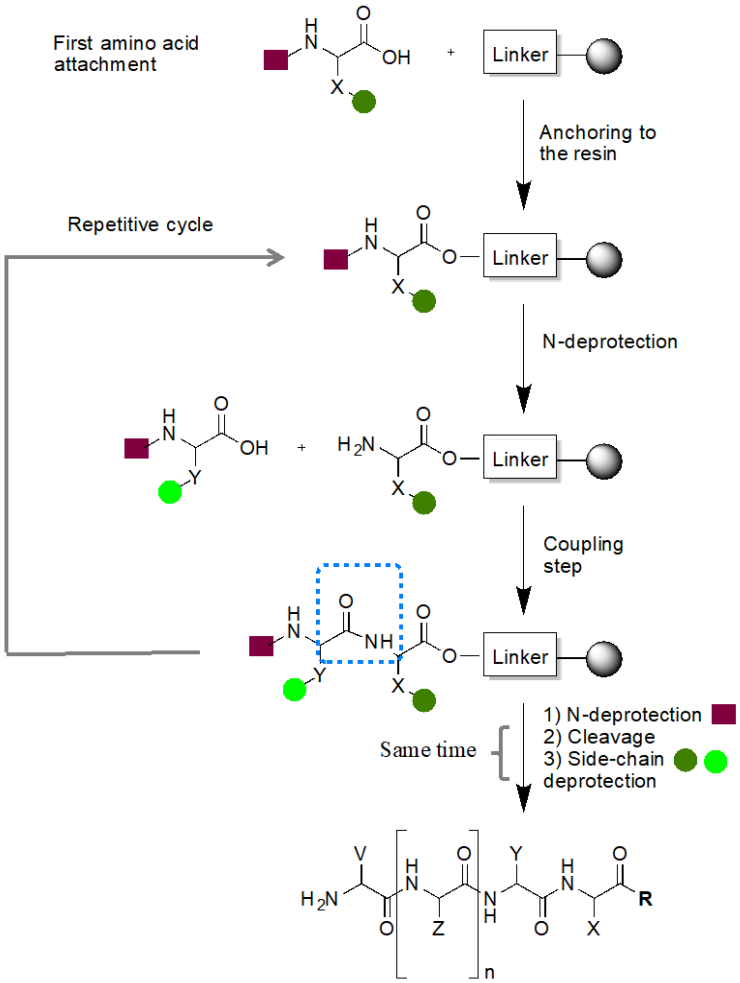

Figure 8. The solid phase peptide synthesis (SPPS) principle. [78]

The C-terminal amino acid residue of the target peptide is attached to an insoluble support (resin) through a linker via its carboxy group (Figure 8). Any functional groups in amino acid side chains must be protected with *permanent* protecting groups that are not affected by the reactions conditions employed during the peptide chain assembly. The *temporary* protecting group masking the α-amino group during the initial resin loading is removed. The next amino acid is introduced with the carboxy group of this amino acid being activated with coupling reagents for amide bond formation. After coupling, excess of reagents are removed by washing and the protecting group from the N-terminus of the last amino acid is also removed. This process is repeated until the desired peptide sequence is assembled. In a final step, the peptide is released form the support and the side-chain protecting groups are removed at the same time using appropriate conditions.

The analogues were synthesized using a fully automated parallel synthesizer (SyroII) and following a standard Fmoc/tBu procedure.

In all cases the linker used was 2-chlorotrityl to a crosslinked divinylbenzene-polystyrene. For peptides **KS-30-NH_2** and **Ac-KS-30-NH_2**, Rink Amide linker was used in order to obtain the C-terminal end of the peptide as a carboxamide.

The permanent protecting groups of the amino acids side chains were the following: Trt for Asn and Gln; Boc for Lys; Pbf for Arg; OtBu for Asp and Glu and tBu for Ser and Thr.

The amino acids were dissolved in DMF and with OxymaPure® (0.5 M) to minimize racemization and using as activating reagents DIC and TCTU. SyroII instrument followed the protocol (described in *"6.1.2.3." Experimental part*, Section A) composed by flushing the needle for two cycles (2 times), removing the Fmoc group (N-protection) with a solution of 30 % piperidine in DMF and adding DIPEA, activating reagent (1^{st} coupling: DIC 3 M in DMF, and 2^{nd} coupling: TCTU 0.4 M in DMF) and the Fmoc-amino acids (0.5 M). This procedure was repeated until the sequence was finished.

Once the last amino acid was coupled, the Fmoc protecting group was split off. Simultaneous, cleavage and full deprotection of the linear peptides was carried out by acidolysis with a mixture of TFA/TIS/H_2O or TFA/Reagent K for 90 min.

The filtrate was collected and the resin was washed with DCM and the peptides were precipitated from TFA solution with diethyl ether, isolated by centrifugation and the supernatant was removed by decantation. This procedure was repeated at least three times to assure the removal of the acidolytic mixture from precipitated peptides.

The pellets were redissolved from tBuOH:H_2O (4:1, v/v) and lyophilized.

Finally, the crude peptides were purified by preparative HPLC and the products (purity > 95 %) were characterized with analytical HPLC and MS.

3.5. Antifungal screenings – AMPs

3.5.1. Objective

The objective in this part was to determinate the biological effect of the synthetic **LL-37** and analogues against *Candida* species. Several biological assays for antifungal activity were carried out with all peptides. These compounds were investigated by high-throughput screening, to define the minimum inhibitory concentration (MIC) and to evaluate their antifungal activity against clinical isolates of *Candida* species.

3.5.2. High-throughput screening (HTS)[1]

The fluorimetric high-throughput screening (HTS) was based on published procedures [26] and should give a general overview of the effect of the compounds against *Candida albicans* SC5314.

The assay mimics the natural interaction of host-pathogen by incubation of the pathogen (this case *Candida albicans* SC5314) in the presence of a host cell line (e.g. HeLa cells). In parallel, this assay is able to control the tolerability of antifungal agents by host cells and the antifungal activity. Therefore, the survival of the HeLa cells culture (host) in the presence of *Candida albicans* (pathogen) and the respective compounds (**LL-37** and analogues) is measured directly instead of measuring the inhibition of enzymatic functions of *Candida albicans* or the growth retardation alone. This screening assay covers potential *in vitro* targets of both the pathogen and the host (Figure 9). [79]

HeLa cells were chosen in this assay due to their characteristic robust growth behaviour and reproducible sensitivity to *Candida albicans* strain SC5314. Amphotericin B was used as a positive control.

[1] In collaboration with Project partner, Fraunhofer IGB, Stuttgart.

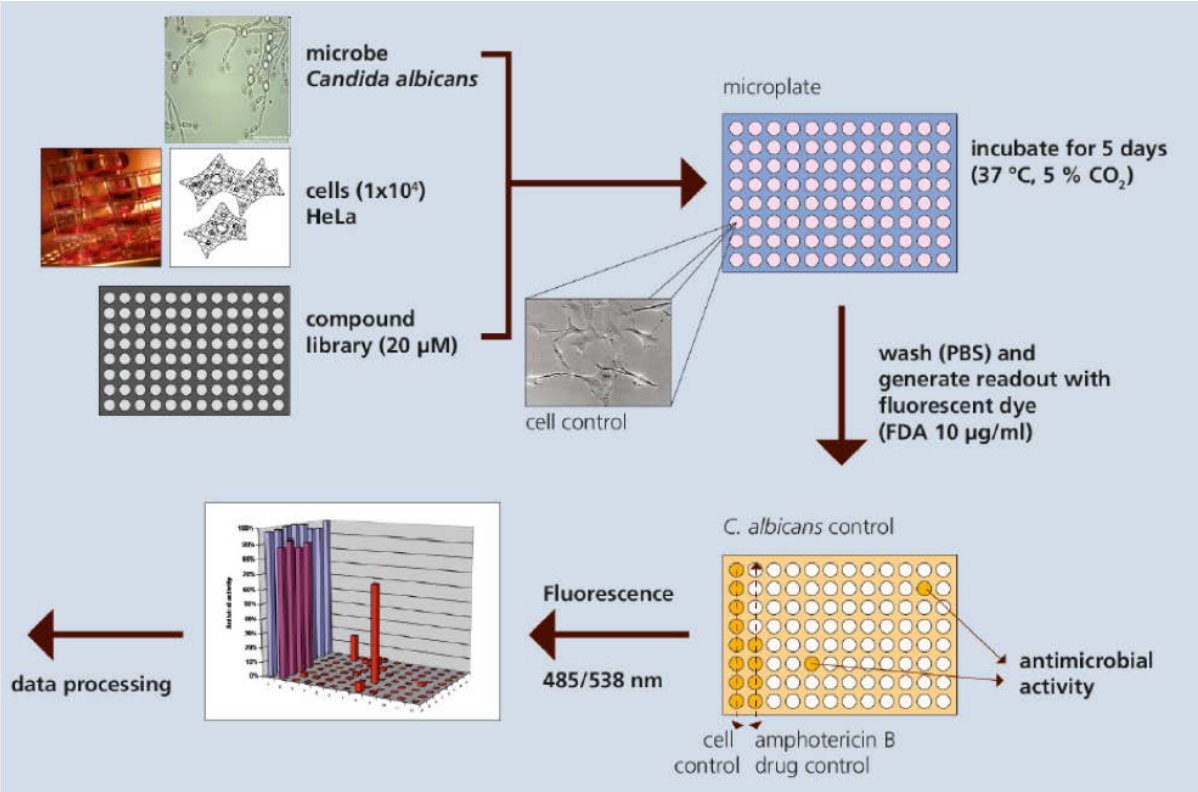

Figure 9. HTS used in Fraunhofer Institute. Plates were incubated for 5 days, 5 % CO_2 at 37 °C. After washings with PBS, the dye FDA (Fluorescein diacetate) was added and the fluorescence was immediately read by spectrofluorometer. The results were shown as a chart calculated by software. Figure handed over by Fraunhofer IGB.

Basically, in a 96 well plate, HeLa cells were previously grown before starting the assay. Afterwards, in each well *Candida albicans* SC5314 (50 CFU) and 10 µM concentration for initial screening of the peptides were added. The plates then were incubated for 5 days at 37 °C in a 5 % CO_2 humidified incubator.

After that time, the plates were washed with PBS and the dye FDA was added to each well. The plates were immediately read in a spectrofluorometer (λ = 485 – 535 nm, sensitivity 50), every 60 seconds for 3 minutes.

The read out is an area under the curve, calculated by the software that gives the amount of HeLa cells that are alive measured by the FDA released. The values obtained for the cell vitality control were defined as 100 % cell viability and all the samples were normalized to this cell vitality control (Table 1).

Table 1. Layout of the plate. Cell viability control contained only HeLa cells. Fungus control contained HeLa cells and *C. albicans*. Positive control contained HeLa cells, *C. albicans* and Amphotericin B. Each peptide was studied in duplicate.

	1	2	3	4	5	6	7	8	9	10	11	12
A	Cell viability control	Fungus control	Pep 1									
B												
C			Pep 2									
D												
E		Drug Control	Etc…									
F												
G												
H												

3.5.2.1. Results

Screening graph

Table 2. Results obtained from the fluorometer readings for all **LL-37** analogues. The percentage represents the amount of HeLa cells alive.

	1	2	3	4	5	6	7	8
A	**LL-37 13 %**	**RK-31 3.5 %**	**KSA_7-30 (13) 0 %**	**KSA_3-30 (20) 12 %**	**KSA_9-30 (25) 0 %**	**SK-29 (29) 7 %**	**FKG_{13}-13 (33) 7 %**	**Ac-KS-30 (17) 8.2 %**
B								
C	**FK-13 11 %**	**KS-30 8.5 %**	**KSR_8-30 (14) 0 %**	**KSF_{17}-30 (21) 4 %**	**KS-27 (26) 2 %**	**KE-28 (30) 4 &**	**$FKF_{12}G$-13 (34) 8 %**	**Ac-KS-30-NH_2 (18) 13 %**
D								
E	**KR-12 16.5 %**	**AS-30 (11) 0 %**	**KSG_8-30 (15) 0 %**	**KS-22 (22) 11 %**	**KE-23 (27) 3 %**	**FK-21 (31) 12.6 %**	**FKN_3-13 (35) 7 %**	**KS-26 (23) 1.3 %**
F								
G	**KR-20 7 %**	**KF-30 (12) 2 %**	**KK-31 (19) 7 %**	**KSA_{29}-30 (24) 7 %**	**FF-22 (28) 24.5 %**	**KF-22 (32) 31 %**	**KS-30-NH_2 (16) 47 %**	
H								

The analogue that showed some activity (almost 50 % of cell viability) was **KS-30-NH_2** (**16**) (Table 2). This analogue corresponds to the control **KS-30** with an amide C-terminus.

3.5.3. Minimum inhibitory concentration (MIC)

To explore their antifungal activity only on *Candida* species (pathogens) without the presence of any host, the minimum inhibitory concentration (MIC) was studied.[2]

Minimum inhibitory concentration is described as the lowest concentration of antifungal agent that inhibits the visible growth of a microorganism in 18-24 h.

The species used for this assay were *C. glabarata* ATCC2001, *C. parapsiolosis* ATCC22019 and *C. krusei* ATCC6258 beside the *C. albicans* SC5314. Those species were selected due to their resistance to azoles and other antifungal drugs, such as fluconazole and voriconazole, which were used as controls.

All peptides were titrated at 8 different concentrations and coincubated with the yeast cells for 24 h at 30 °C.

The range of peptide concentrations was from 64 - 0.125 µg/ml (0.05 – 40 µM).

After incubating the plates for 24 h at 30 °C the OD_{600} values were measured using a plate reader (Victor[3], Biotek,Winooski, USA) (Table 3):

- Translation of readouts in percentage of fungi growth:

Table 3. Translation of the crude data from the plate reader values into percentages. E.g: cell A1 after the readings, indicates that the compound was not able to inhibit the growth of *C. albicans* SC5314 because the growth was 99.7 %.

		Relative Growth									
		1	2	3	4	5	6	7	8	9	10
SC5314	A	99,7	101,7	100,4	100,3	99,6	99,9	100,1	99,3	99,2	99,4
SC5314	B	100,3	100,8	100,0	99,8	100,2	100,0	101,0	100,6	100,0	99,8
ATCC2001	C	100,6	100,6	99,8	99,9	99,3	99,3	99,7	100,0	99,9	99,9
ATCC2001	D	100,2	100,5	99,6	99,7	99,7	99,0	100,1	99,9	99,5	99,7
ATCC22019	E	104,4	101,3	96,3	97,5	100,9	101,9	101,6	98,8	97,9	99,0
ATCC22019	F	103,6	101,0	95,8	97,4	100,1	101,2	102,6	100,2	99,7	98,1
ATCC6258	G	106,2	102,5	100,0	100,6	100,3	100,2	100,8	99,5	99,8	100,9
ATCC6258	H	106,1	103,1	100,3	106,8	100,5	101,6	101,0	100,6	100,2	100,0
µg.ml-1		64	32	16	8	4	2	1	0,5	0,25	0,125

[2] This study was carried out at the Medical University Vienna, Max F. Perutz Laboratories Vienna.

3.5.3.1. RESULTS

The MIC curves were calculated for each peptide based on the plate read out at OD_{600}.

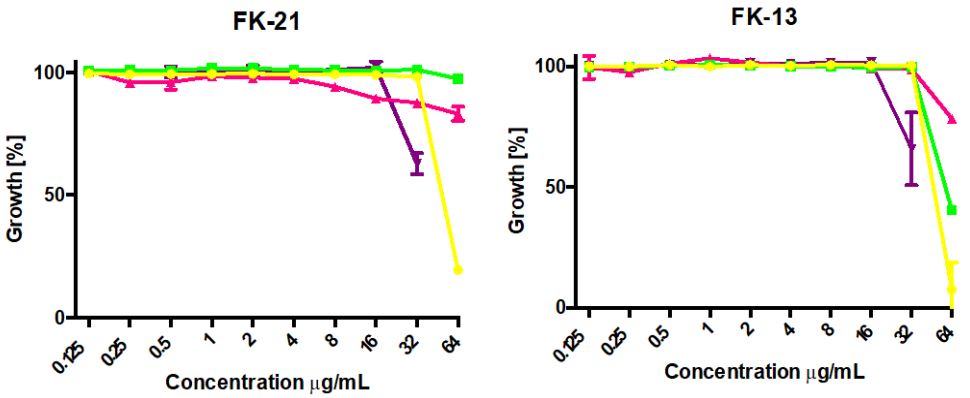

Figure 10. Minimum inhibitory concentration (MIC) representation, showing the biological effect of the synthetic analogues against *Candida* species. Yellow line *C. albicans* SC5314; Green line *C. glabrata* ATCC2001; Pink line *C. parapsilosis* ATCC22019 and purple line *C. krusei* ATCC6258.

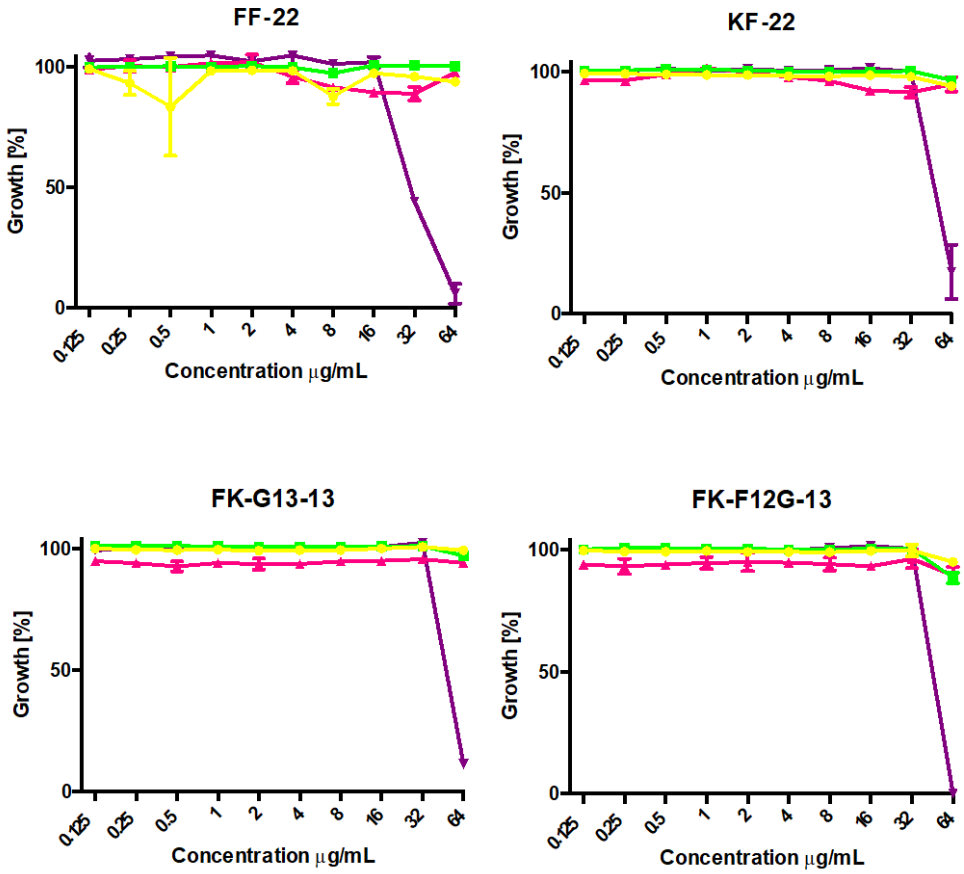

Figure 11. Minimum inhibitory concentration (MIC) representation, showing the biological effect of the synthetic analogues against *Candida* species. Yellow line *C. albicans* SC5314; Green line *C. glabrata* ATCC2001; Pink line *C. parapsilosis* ATCC22019 and purple line *C. krusei* ATCC6258.

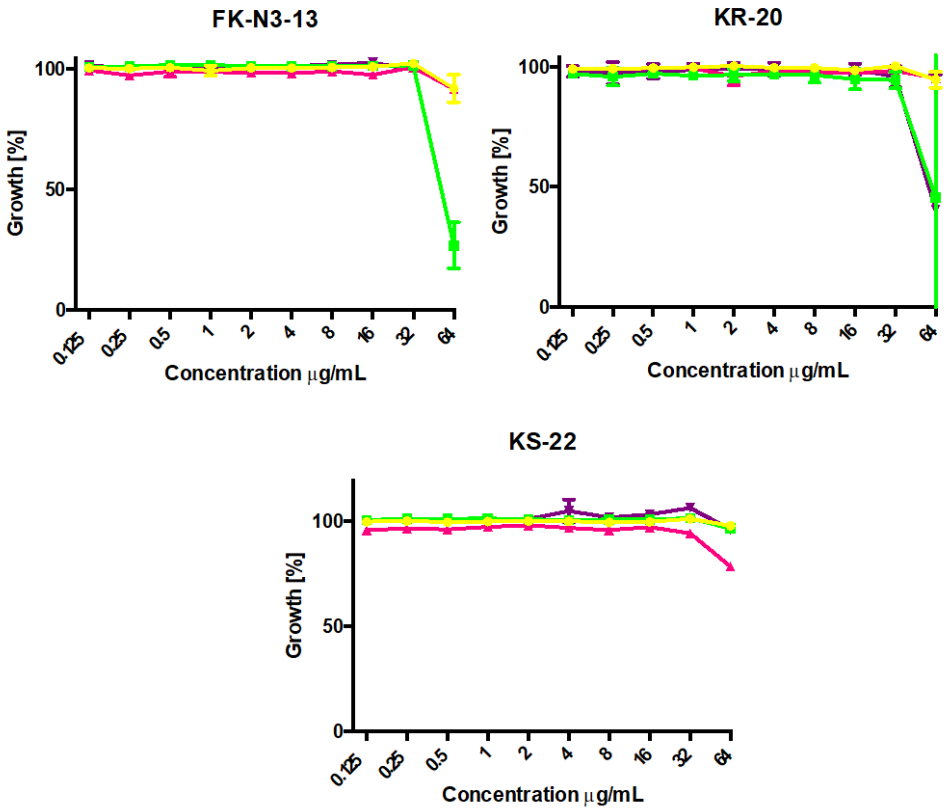

Figure 12. Minimum inhibitory concentration (MIC) representation, showing the biological effect of the synthetic analogues against *Candida* species. Yellow line *C. albicans* SC5314; Green line *C. glabrata* ATCC2001; Pink line *C. parapsilosis* ATCC22019 and purple line *C. krusei* ATCC6258.

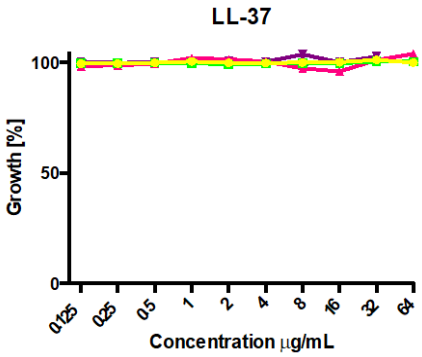

Figure 13. Minimum inhibitory concentration (MIC) representation, showing the biological effect of the **LL-37** against *Candida* species. Yellow line *C. albicans* SC5314; Green line *C. glabrata* ATCC2001; Pink line *C. parapsilosis* ATCC22019 and purple line *C. krusei* ATCC6258.

To resume these graphs:

Table 4. Concentration of the analogues that showed activity against *Candida* spp at the minimum inhibitory concentration (MIC).

	Fungi			
Peptides	***C.albicans* SC5314**	***C.glabrata* ATCC2001**	***C.parapsilosis* ATCC22019**	***C.krusei* ATCC6258**
LL-37	-	-	-	-
FK-13	64 µg/ml	64 µg/ml	64 µg/ml	32 µg/ml
KR-20	-	64 µg/ml	-	64 µg/ml
FK-21 (31)	64 µg/ml	-	64 µg/ml	32 µg/ml
KF-22 (32)	-	-	-	64 µg/ml
FF-22 (28)	-	-	-	64 µg/ml
KS-22 (22)	-	-	64 µg/ml	-
FKG_{13}-13 (33)	-	-	-	64 µg/ml
$FKF_{12}G$-13 (34)	-	-	-	64 µg/ml
FKN_3-13 (35)	-	64 µg/ml	-	-

The control peptide **FK-13** was the only compound that showed some growth inhibition for all four *Candida* species tested. **FK-21** (**31**) analogue was also active to all *Candida* species but *C. glabrata*. Both compounds, **FK-13** and **FK-21** (**31**), were active at the highest concentration 64 µg/ml (37.2 and 24.5, µM, respectively) and both compounds inhibited the growth of *C. krusei* at 32 µg/ml (18.6 and 12.2 µM) (Table 4).

FF-22 (**28**), **$FKF_{12}G$-13** (**34**), **KF-22** (**32**) and **FKG_{13}-13** (**33**) analogues were active only against *C. krusei* at highest concentration (64 µg/mL, 23.2, 38.7, 23.2 and 39.5 µM, respectively).

FKN_3-13 (**35**) analogue was active only against *C. glabrata* at highest concentration (64 µg/ml, 38.2 µM). **KS-22** (**22**) analogue was active only to *C. parapsilosis* and at highest concentration 64 µg/ml (23.2 µM) and control **KR-20** was active for two *Candida* species, *glabrat*a and *krusei* at highest concentration (64 µg/ml, 26 µM).

LL-37 was not active for the *Candida* spp we tested and neither at the range of concentration we used (Table 4).

3.5.4. Screening of clinical *Candida* spp isolates

Compounds exhibiting growth inhibition during the MIC analysis were selected for further screening. These compounds were tested against several clinical isolates of *Candida* spp. Therefore, clinical isolates were arrayed in a 96 well pattern shown in Figure 14.

	1	2	3	4	5	6	7	8	9	10	11	12
A	SC5314	KK017	ATCC2001	KK060	ATCC22019	KK136	ATCC6258	KK264	KK268	KK014	KK158	KO1054 ypk1Δ
B	KK001	KK018	KK003	KK070	KK002	KK190	KK107	KK273	KK007	KK036	KK170	KO519 slt2Δ
C	KK005	KK019	KK004	KK079	KK012	KK196	EMPTY	KK166	KK067	KK038	KK181	KO172 wsc1Δ
D	KK008	KK020	KK006	KK088	KK030	KK207	KK147	KK198	KK112	KK062	KK189	
E	KK009	KK021	KK033	KK113	KK041	KK209	KK163	KK251	KK162	KK063	KK167	
F	KK010	KK024	KK045	KK114	KK048	KK210	KK165	KK252	KK187	KK130	KK073	
G	KK011	KK025	KK047	KK115	KK056	KK212	KK197	KK253	KK240	KK132	#26 HTL	
H	KK013	KK026	KK059	KK122	KK096	KK213	KK246	KK254	KK016	KK142	KO160 pdr1Δ	

Figure 14. Layout of clinical *Candida* spp isolates screening plate. Columns 1-2, *C. albicans* isolates; Columns 3-4, *C. glabrata*; Columns 5-6, *C. parapsilosis* and columns 7-8, *C. krusei*. Purple background corresponds to lab strains. The remaining columns show results of different *Candida* species like *tropicalis* or *lusitaniae*. All clinical isolates come from Vienna General Hospital expect blue background cells that come from Karl Kuchler lab, specific for azole resistance.

The screening plates with 100 µl of medium YPD were supplemented with 100 µl of the respective antifungal peptide diluted in medium and distilled H_2O (all wells except the last 4 of the plates, see Figure 14) with the concentration determined in MICs assay (Table 4). To assure the stress of all standard strains without inhibiting their growth completely, the concentration used for all compounds was the highest, 64 µg/ml.

The clinical isolates were arrayed in a 96 well pattern on a solid media square. Using a Singer RoTor HDA robot, they were transferred to the 96 well plate holding the 200 µl (YPD media + peptide) and incubated 24 h at 30 °C.

The readings were carried out after those 24 h of incubation by measuring the OD_{600} on the Victor^3 plate reader.

The empty wells contained only media as a blank. The average of their values was subtracted from the readouts of all walls prior to analysis.

3.5.4.1. Results

The results of the screening of clinical *Candida* spp isolates were summarized in a table specifying the grade of growth of the fungi with the peptide (Table 5).

Table 5. Summarized results for the growth of the fungi cells with the peptides at their MIC concentration. Red colour indicates that the growth of the fungi was over 50 %. The pink colour indicates that the effect of the peptide was very poor and the growth of the fungi was between 30-50 %. Bright green indicates that the growth of the fungi was between 0-30 %. The other green colour collects the other different *Candida* species and corresponding to the growth of the fungi between 0-50 %.

Fungi	*C. albicans* Isolates	*C. glabrata* Isolates	*C. parapsilosis* isolates	*C. krusei* isolates	Other species
Peptides					
FK-13 (37.2 µM)	Poor effect	None effect	None effect	Strong effect	Some species: *C. tropicalis* *C. lusitaniae* *C. kefyr*
KR-20 (26 µM)	Poor effect	None effect	None effect	Poor effect, only lab strain	Some species: *C. Kefyr* *C. tropicalis*
FF-22 (23.1 µM)	None effect	None effect	None effect	Poor effect, only lab strain	None effect
FK-21 (24.5 µM)	None effect	None effect	None effect	Poor effect	None effect / Only *C. tropicalis*
KF-22 (23.2 µM)	None effect	None effect	None effect	Poor effect	Only *C.lusitaniae*
FK-G_{13}-13 (39.5 µM)	None effect	None effect	Very poor effect	Poor effect, only lab strain	None effect
FK-$F_{12}G$-13 (38.7 µM)	Not studied	Not studied	Not studied	Not studied	Not studied
FK-N_3-13 (38.2 µM)	None effect	None effect	Very poor effect	Poor effect, only lab strain	Some species: *C. lusitaniae* *C. kefyr*
KS-22 (25.8 µM)	None effect	None effect	Very poor effect	None effect	None effect

3.6. DISCUSSION SECTION A

After the synthesis of **LL-37** (plus controls) and analogues, the peptides were biologically studied[3] and the results obtained were summarized here.

- **Chemical synthesis**: The synthesis of all peptides was carried out by automated solid phase peptide synthesis. The yields of some analogues were affected not only due to length of the sequence but also for the presence of hydrophobic residues.

- **High-throughput screening**: All synthesized peptides were screened at a concentration of 10 µM against *Candida albicans*. Only **KS-30-NH_2** (**16**) showed some activity, with cell viability over 40 %. Its structure is based on the control **KS-30** but with an amide C-terminal. In comparison to control **KS-30**, this C-terminal modification showed to be more active against *Candida albicans* SC5314 than the control. This modification might be reinforcing the sequence by making it less sensible to degradation. [42] Unexpectedly, the other analogue with amide C-terminal, **Ac-KS-30-NH_2** (**18**) and expected to have similar action, it did not show much activity (13 % cell viability). Probably, the effect of the acetyl N-terminal modification is counteracting the C-terminal action. This hypothesis was validated with the analogue **Ac-KS-30** (**17**), which only had the N-terminal modified but not the C-terminal. **Ac-KS-30 (17)** showed to be less active (8.2 % cell viability) than the N,C-modified peptide, **Ac-KS-30-NH_2** (**18**).

- **Minimum inhibitory concentration (MIC)**: The minimum inhibitory concentration assay was carried out for all the synthesized peptides and showed that only two peptides were able to inhibit the growth of all the tested *Candida* spp: **FK-21** (**31**) and **FK-13**. Both peptides inhibited the growth for all *Candida* species at the highest concentration tested (64 µg/ml; 24.5 and 37.2 µM, respectively), except for the species *C. krusei* ATCC6258, which was inhibited at 32 µg/ml (12.2 and 18.6 µM). The structural difference between the two peptides is the hydrophilic tail unit of the **FK-21** (**31**). This C-terminal hydrophilic tail has minor influence on the activity of the core region.

  Several other peptides inhibited the growth of at least one *Candida* species such as:

[3] Supported by ImResFun partners.

- **FF-22** (**28**), **KF-22** (**32**), **FKG$_{13}$-13** (**33**) and **FKF$_{12}$G-13** (**34**). They inhibited only the growth of the species, *C. krusei* at high concentration tested (64 µg/ml; 23.1, 23.2, 39.5 and 38.7 µM, respectively). Their structure is very similar, lacking the N-terminal unit, a disordered non-polar / hydrophobic section.
- **FKN$_3$-13** (**35**) was active only against *C. glabrata* at high concentration (64 µg/ml, 38.2 µM); **KS-22** (**22**) was active against *C. parapsilosis* at 64 µg/ml (23.3 µM) and the control **KR-20** was active against both *C. glabrata* and *C. krusei* also at its high concentration (64 µg/ml, 26 µM).

For the rest of the peptides, even **LL-37** and other controls, no activity was observed at those concentrations. The structure for all the non active peptides mimics the control **KS-30**. They lack the N-terminal unit that is partially responsible for the peptide oligomerization and proteolytic resistance. [60]

In this assay, the analogue **KS-30-NH$_2$** (**16**), which was active during the high-throughput screening, showed no activity for all *Candida* species tested at highest concentration (64 µg/ml, 17.5 µM).

- **Screening of clinical *Candida* spp isolates**: In this screening, only the peptides that showed activity in the MIC assay were further studied. Their antifungal activity was evaluated in a screening with different clinical *Candida* spp isolates. The concentration used was the one obtained in MIC assay. To assure a visual effect for all the compounds, the concentration chosen was 64 µg/ml, although the control **FK-13** was active at lower concentration (32 µg/ml).

  FK-13 (37.2 µM) showed to be the most active peptide so far, inhibiting the growth of *C. krusei* clinical isolates over 70 % and *C. albicans* between 50 – 70 %. For *C. glabrata* and *C. parapsilosis* species, they were weakly inhibited for **FK-13**, with less than 50 %. The rest of the active peptides did not show any notable inhibition against any of *Candida* species.

  It was observed that the clinical isolates from *C. krusei* species were more sensitive to inhibition (50 – 70 %) for all peptides tested but **KS-22** (**22**). Other *Candida* species studied like *C. tropicalis* or *C. lusitane* were also inhibited by almost all the analogues except for **FF-22** (**28**), **FK-21** (**31**) (both with identical sequence but differing only in one extra phenyl residue), **KS-22** (**22**) and **FKG$_{13}$-13** (**33**).

FKF$_{12}$G-13 (**34**) was not studied.

HETEROCYCLIC DRUGS

4. HETEROCYCLIC DRUGS – SECTION B

4.1. Scaffold hopping

The aim of scaffold hopping in medicinal chemistry is the discovery of structurally novel compounds based on a known active compound. The core structure of a biologically active compound is modified to improve chemical properties and to generate novel compounds. [21, 80] For example, a replacement of a lipophilic scaffold by a more polar one will increase the solubility of the compound; or a change in the scaffold can lead to an improved binding affinity in interaction with the target protein; or from the business point of view, a change in the central scaffold can lead to a novel structure that can be patentable. [81 - 82]

Usually, the rational basis for scaffold hopping comes from computational calculations, which help to design new potential hits. Many different software programs can offer combinations of several approaches like shape matching, pharmacophore searching or fragment replacement (Figure 15). [83]

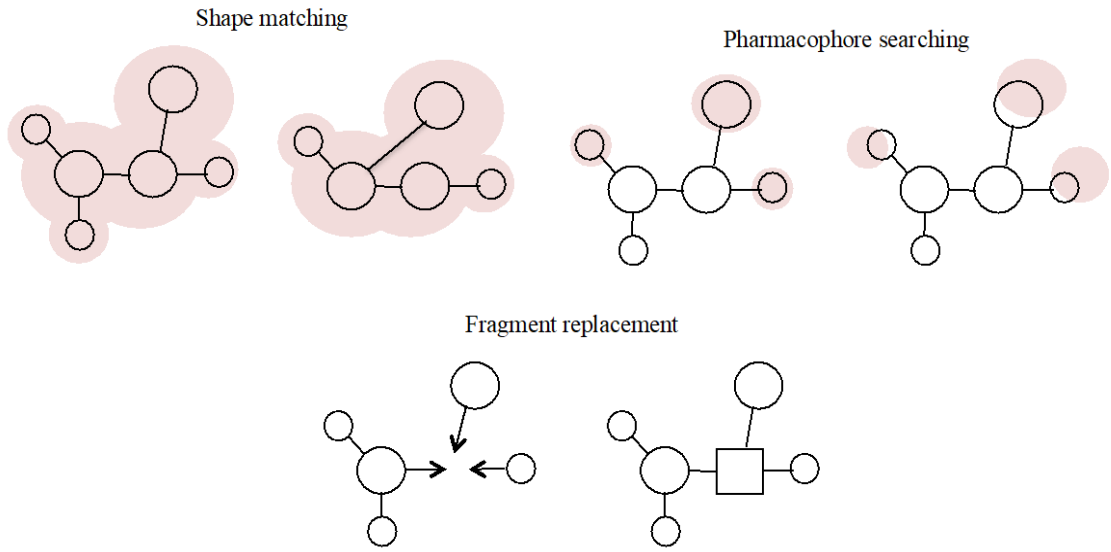

Figure 15. Schematic representation of principal computational approaches to scaffold hopping. [83]

In this work, the scaffold hopping approach has been used to develop novel scaffolds for antifungal treatment on *Candida* species.

4.2. Nitrogen containing heterocyclic drugs

Nitrogen heterocycles are common drug components in the pharmaceutical market and play a central role in the design of therapeutic molecules. A wide range of natural products such as amino acids, vitamins or nucleic acids, contain nitrogen heterocycles as core structure elements, so there are strong efforts in medicinal chemistry to find analogues of these structural motifs. The presence of a heterocyclic moiety in a molecule gives the compound pharmacokinetic and toxicological properties that can be modulated and therefore utilized to optimize potency and selectivity through different strategies like bioisosteric replacements, polarity, lipophilicity or aqueous solubility. [84] In addition to this information, Njardarson et al. [85] compiled a database of all U.S FDA approved pharmaceuticals focused only on structurally unique small-molecule drugs with heterocyclic structure. This analysis of the structural diversity among heterocycles showed that at least 60 % of these compounds contained N-heterocycles.

4.3. Benzimidazoles

Benzimidazole is a well-known heterocyclic compound consisting of a benzene and an annulated imidazole ring.

The broad interest for benzimidazoles in medicinal chemistry is well expanded due to their diverse biological activity and clinical applications. [86 - 87] Benzimidazole core has five positions that can be substituted. Very common are positions 1 and 2, but positions 5 to 7, located in the phenyl ring are also easily substituted (Figure 16, A).

The optimization of benzimidadozole-based structures has resulted in various drugs that are currently on the market, such as Omeprazole (proton pump inhibitor, **39**), Candesartan (hypertension treatment (AstraZeneca), **36**), Emedastine or Astemizole (antihistaminic activity (Alcon), **37** and **38**) (Figure 16, B).

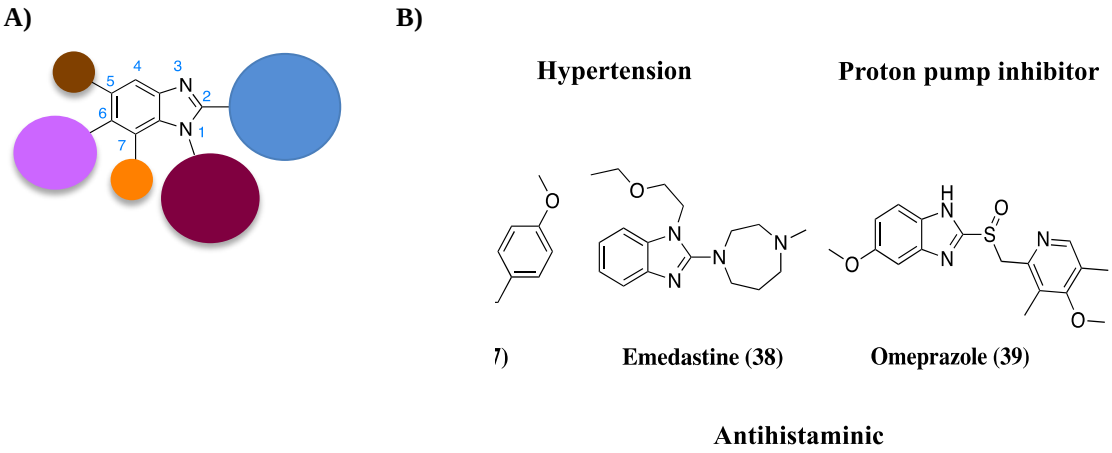

Figure 16. A) Preferred substitution patterns. B) Pharmaceuticals containing a benzimidazole scaffold.

4.3.1. EMC120B12 - *(S)-2-(1-aminoisobutyl)-1-(3-chlorobenzyl) benzimidazole*

The result of a high-throughput screening, which combined the tolerability of human cells (HeLa) with the activity against *Candida albicans*, (*S*)-2-(1-aminoisobutyl)-1-(3-chlorobenzyl) benzimidazole (**EMC120B12**) (Figure 17) exhibited an IC_{50} and CC_{50} of 0.75 µM and 97.5 µM, respectively. [26]

On the contrary, further SAR studies showed that the (*R*)-enantiomer was completely inactive.

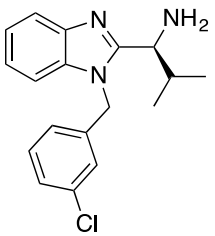

EMC120B12

Figure 17. Structure of the active (S)-2-(1-aminoisobutyl)-1-(3-chlorobenzyl)benzimidazole (**EMC120B12**).

4.3.2. Synthesis of substituted benzimidazoles

Based on **EMC120B12**, a small collection of compounds was synthesized by systematically varying two regions of the core structure without affecting the essential (*S*)-configuration and without changing the free primary amino group. The synthesis was carried out by methods of parallel solid phase organic synthesis and based on published procedures. [20] The synthesis is summarized in Scheme 1.

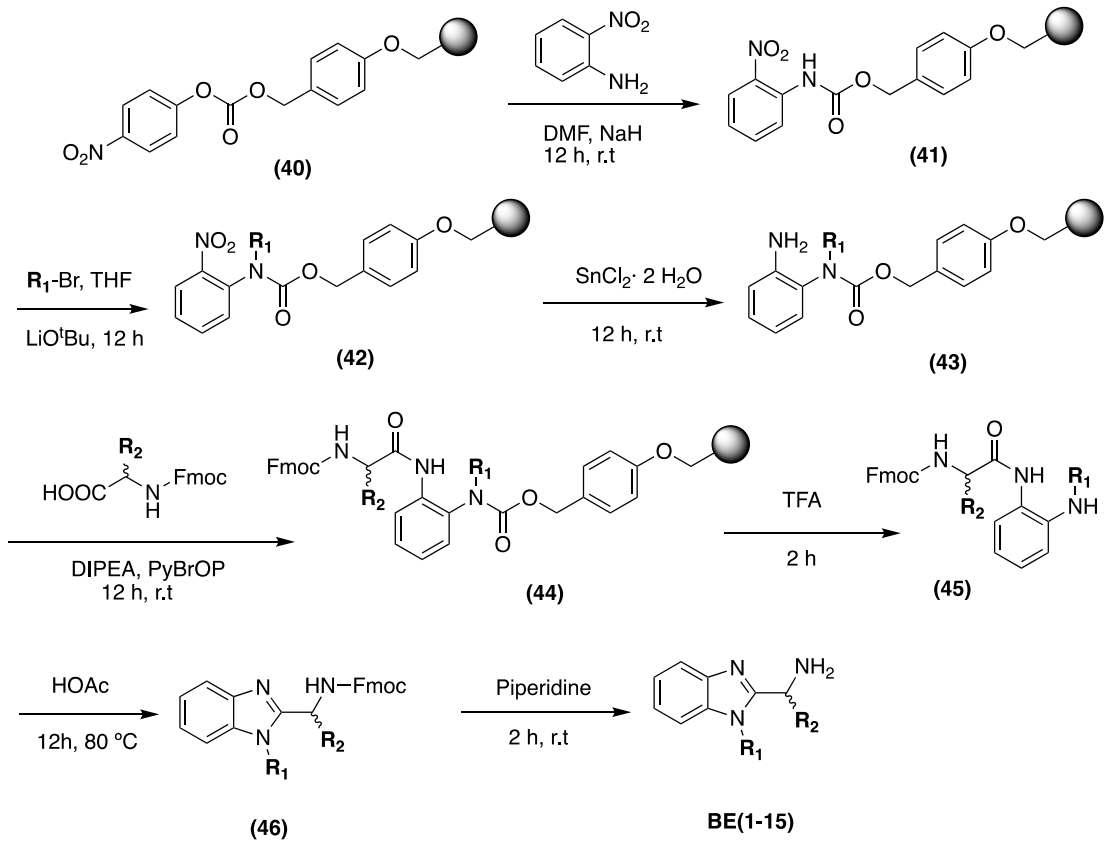

Scheme 1. Synthesis of the **EMC120B12** analogues (Table 6).

Table 6. List of the **EMC120B12** analogues synthesized.

Compound	R_1	R_2	Yield (%)	Purity (%)*
EMC120B12	3-Chloro-phenyl	iPr	65	98
BE1	4-Chloro-phenyl	Methyl	85	94
BE2	4-Chloro-phenyl	iPr	66	95
BE3	4-Fluoro-phenyl	Methyl	82	90
BE4	4-Fluoro-phenyl	iPr	76	91
BE5	3-Chloro-phenyl	Indolyl	26	88
BE6	3-Fluoro-phenyl	iBu	77	94
BE7	H-Phenyl	iPr	74	97
BE8	3-Chloro-phenyl	iBu	73	89
BE9	3-Chloro-phenyl	Propyl	55	98
BE10	3-Fluoro-phenyl	Propyl	54	98
BE11	3-Chloro-phenyl	3-Methylthioethyl	31	95
BE12	3-Chloro-phenyl	4-Hydroxyphenyl	34	97
BE13	H-Phenyl	Methyl	86	85
BE14	H-Phenyl	Phenyl	46	98
BE15	H-Phenyl	Propyl	68	95

*Purities were determined by HPLC-ESI-MS after purification.

After reaction of the Wang resin **40**, with 2-nitro-aniline, the first substituent was introduced by alkylation of the carbamate **41**. After reduction of the nitro group in **42**, the acylation with varying Fmoc-amino acids was carried out to yield **44**. The intermediate, **45**, was cleaved from the resin and cyclized at elevated temperature to yield the benzimidazole **46**. The last step was the cleavage of the Fmoc protecting group to give the desired **EMC120B12** analogues (**BE (1-15)**, Scheme 1, Table 6).

All compounds (Table 6) were characterized by HPLC-MS and ^{1}H-NMR, (example shown in Figure 18).

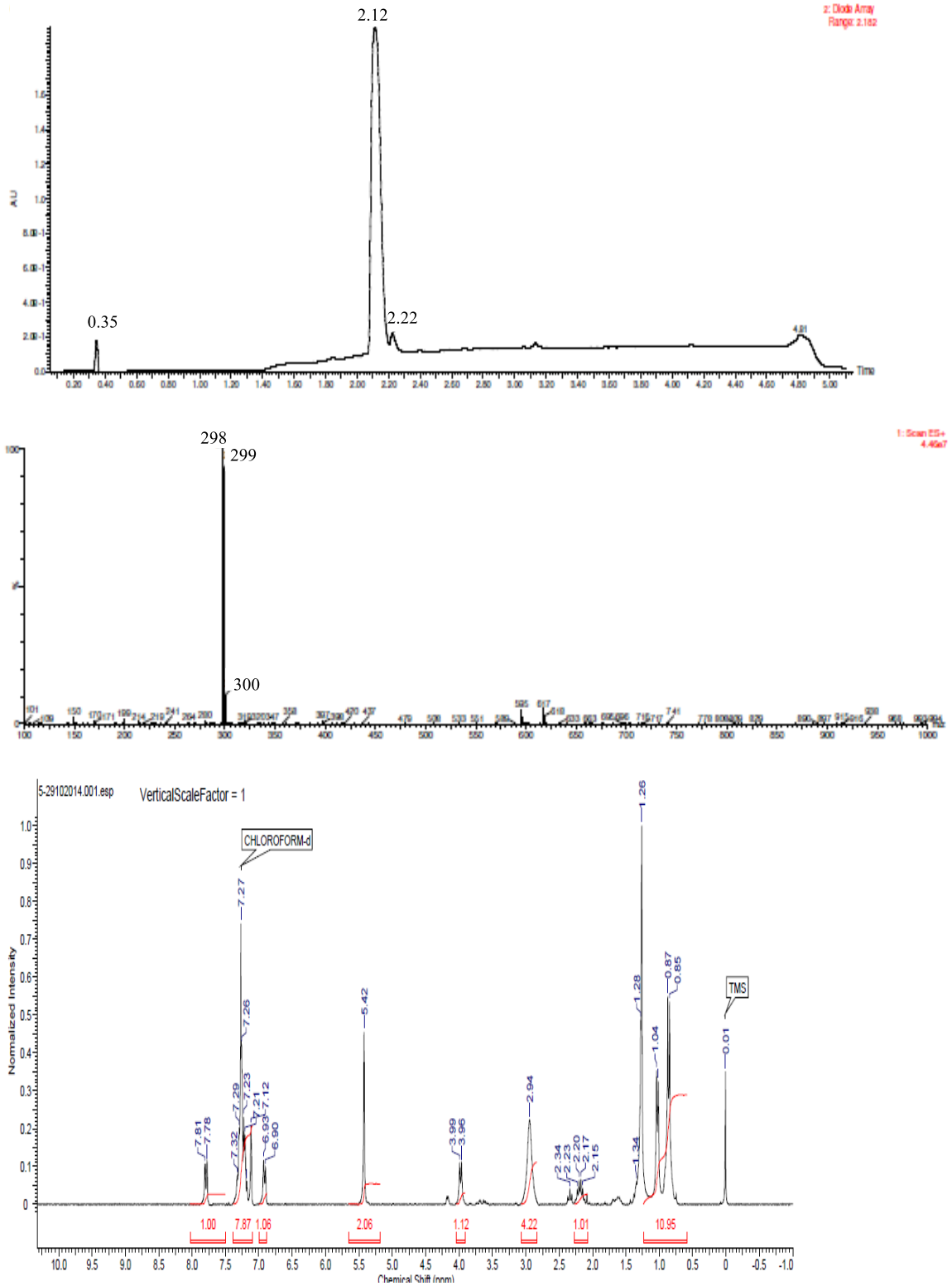

Figure 18. Characterization of compound **BE10** by HPLC-MS (214 nm) and ^{1}H-NMR (400 MHz).

4.4. Indoles

The indole structure has been referred to as “privileged structure” due to its presence in natural products, indole is part of the essential amino acid tryptophan and a key structural component of value in pharmaceuticals. [88, 89] In medicinal chemistry, indole belongs to the top five commonly used heterocycles, among them, thiazoles, benzimidazoles, tetrazoles and imidazoles.

The interest in the use of indole derivatives as bioactive molecules against several disorders in the human body was recently boosted by their activities against cancer cells and microbes. [90,91]

The indole core has seven positions that can be substituted. Position 3, located in the pyrrole ring is the most frequented substituted position followed by position 5 (located in the phenyl ring) and position 2 (also, located in pyrrole ring) (Figure 19). [85]

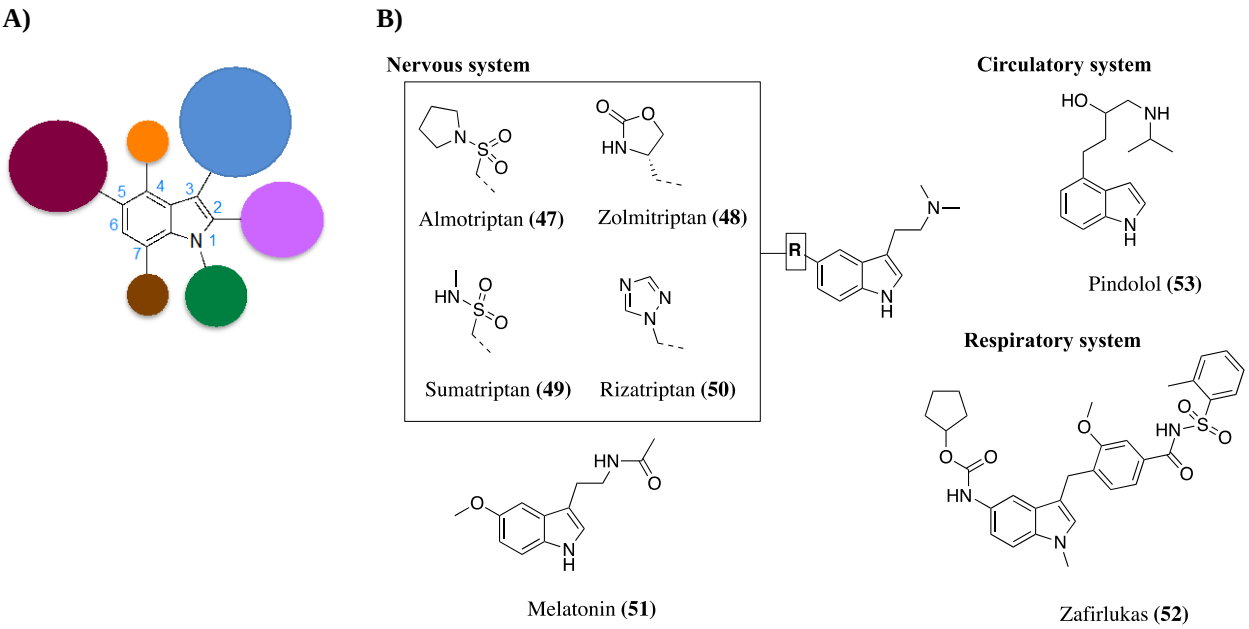

Figure 19. A) Preferred substitution patterns. B) Pharmaceuticals containing indole structure.

A closer look reveals that indoles tend to be more often disubstituted than monosubstituted. Trisubstituted indoles are as frequent as disubstituted indoles.

For example, Figure 19, part B shows some of the pharmaceutical drugs containing the indole scaffold. All of them but Pindolol (**53**) and Zafirlukas (**52**) are disubstituted, while Pindolol is monosubtituted and Zafirlukas is trisubstituted.

In conclusion, disubstituted compounds with indole core were synthesized for investigation of potential antifungal activity.

4.4.1. Synthesis of substituted indoles

The indole compounds were synthesized as it is described in Scheme 2. The approach started by the synthesis of the intermediate β-aminoketoester (**54**), which was reacted with 2-iodoaniline and CuI as a catalyst of the reaction to give the indole **55**. Intermediate compound **55** was obtained from compound **55** by acidic cleavage of the Boc-protecting group and purified by precipitation.

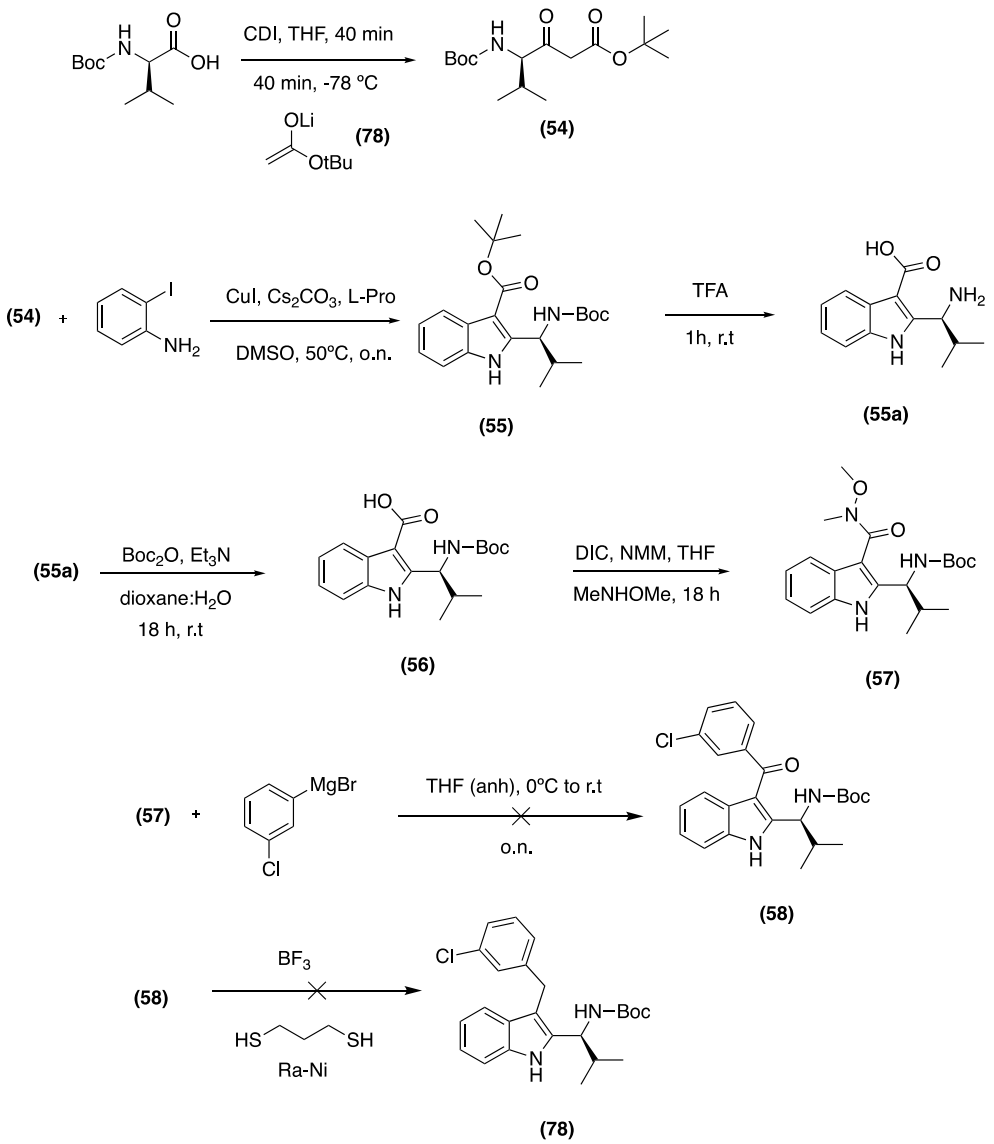

Scheme 2. Planned synthesis of the indole analogues of **EMC120B12**.

The deprotected amino group of **55a** (65 % yield, 98 % pure) was reprotected (**56**) and the activation of the carbxy group was achieved by using N,O-dimethylhydroxylamine (Weinreb's amine) in THF for 18 h to yield compound **57**. All variations of the Grignard

reaction failed for the generation of compound **58** and consequently, the final product **78**. Therefore it was decided to change the synthesis route (Scheme 3) by amidation of **56** with different amines using ethyl cyano(hydroxyimino)acetate (Oxyma Pure) and EDC hydrochloride as coupling reagents to give the product **59**. Finally, the deprotection of the amino group and the further purification yielded compounds **IN-(1-7)** (Table 7).

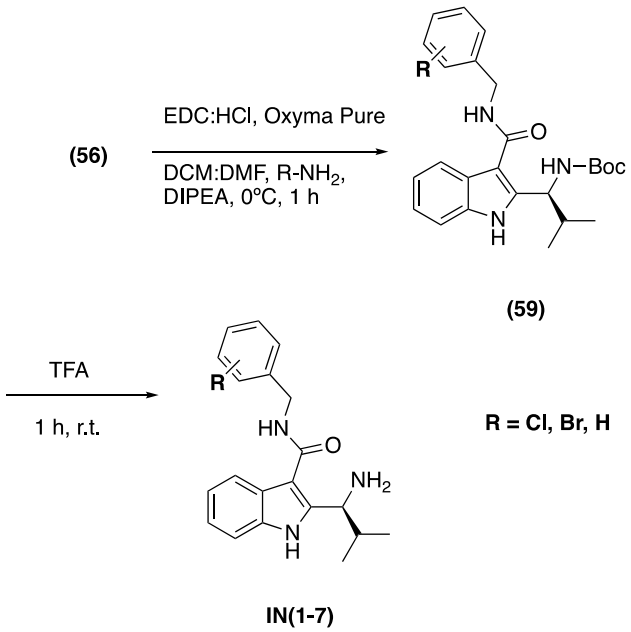

Scheme 3. Final synthetic route for indole compounds (Table 7).

Table 7. Synthesized compounds with an indole scaffold core.

Compound	R	Yield (%)	Purity (%)*
IN1	3-Chloro-phenyl	85	94
IN2	3-Fluoro-phenyl	66	95
IN3	Phenyl	82	98
IN4	4-Chloro-phenyl	76	93
IN5	4-Fluoro-phenyl	26	96
IN6	2,4-Dichloro-phenyl	77	95
IN7	3,5-DifluoroPhenyl	74	89

*Purities were determined by HPLC-MS (214 nm) after purification

A selection of compounds was characterized by HPLC-MS and ^{1}H-NMR and further tested for antifungal activity (Figure 20 and 21).

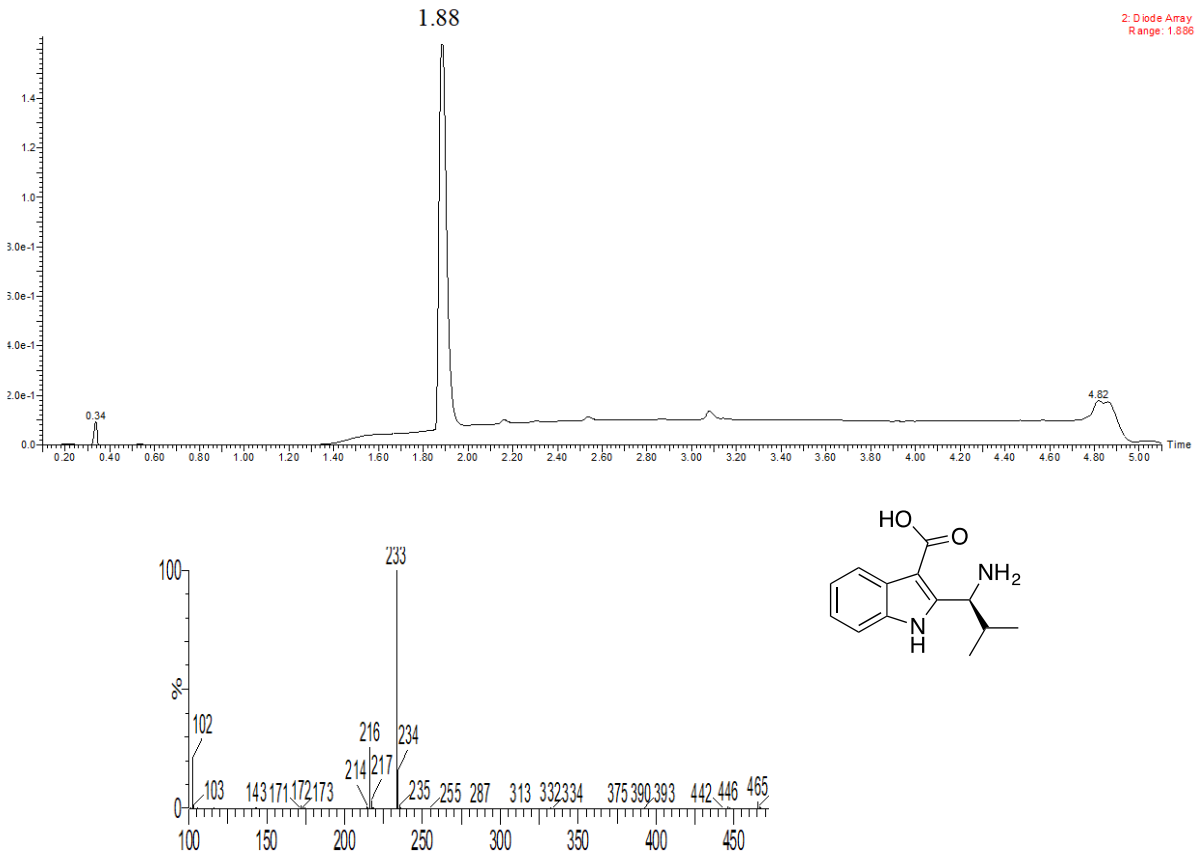

Figure 20. HPLC-MS analysis of indole **55a**

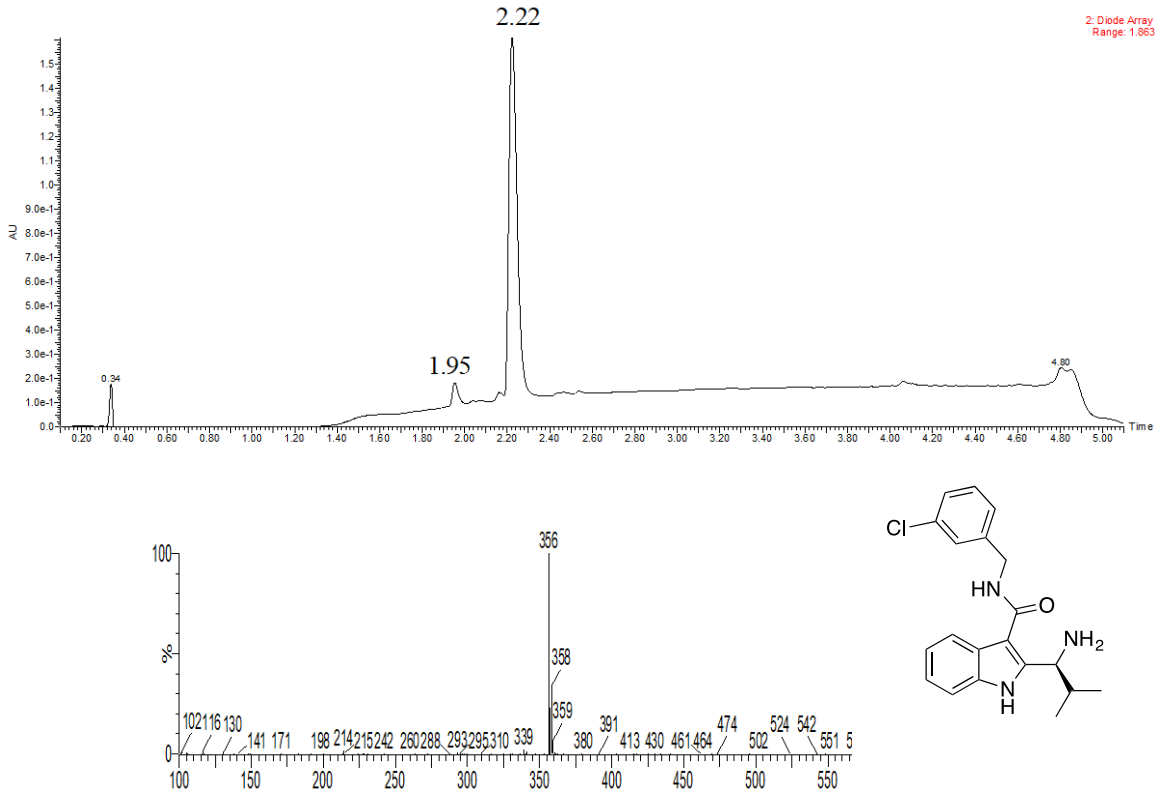

Figure 21. HPLC-MS of one of the final indole compounds synthesized, **IN1**.

4.5. Triazoles

Triazoles are used as pharmaceuticals as well as for plant protection in agriculture. The core is a five-membered ring with three nitrogens. Two isomers are possible, either 1,2,3- or 1,2,4-triazole.

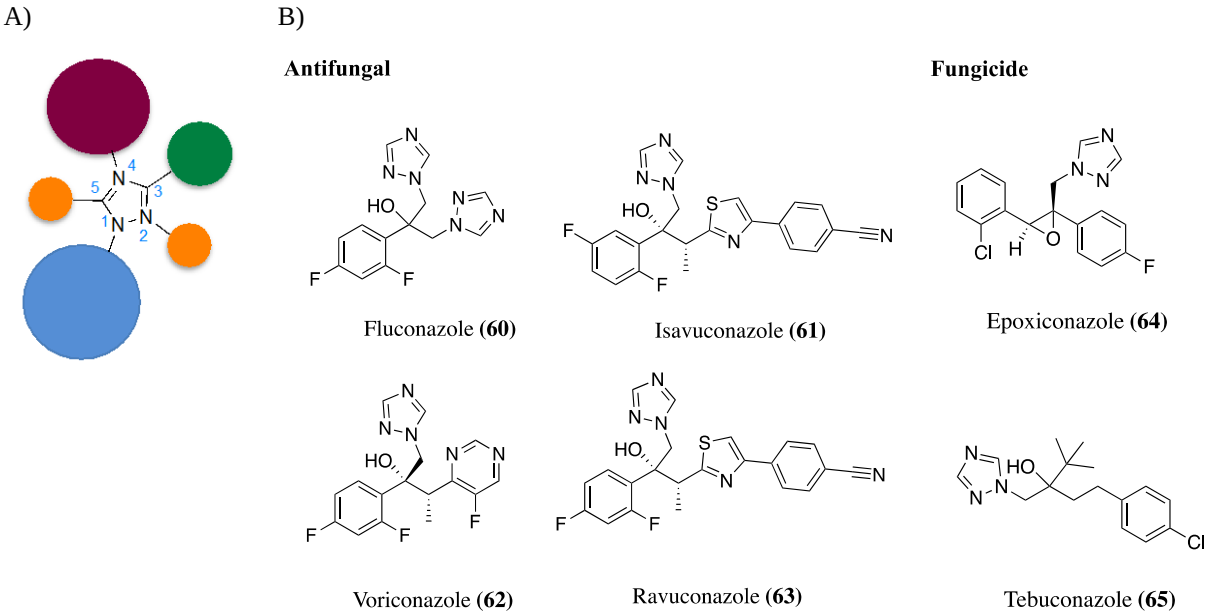

Figure 22. A) Preferred substitution patterns. B) Pharmaceuticals and fungicides containing triazole structure.

The 1,2,4-triazole ring and its tautomer differ in the position of the hydrogen (position 1 or position 4). The nomenclature serves to address this subject as for example: Fluconazole, which its IUPAC named is: 2-(2,4-difluorophenyl)-1,3-*bis*(***1H***-1,2,4-triazol-1yl)propan-2-ol. The N-monosubstituted 1,2,4-triazole seems to be the most common structure over the disubstituted and trisubstituted triazole in most of the drugs (Figure 22). [92]

4.5.1. Synthesis of substituted triazoles

A number of synthetic methods have been investigated to generate the 1,2,4-triazole ring of interest.

The main objective has been to mimic the **EMC120B12** structure by modification of the scaffold. The synthesis proposed here is a two-step reaction (Scheme 4), which starts with the formation of N-protected α-amino acid hydrazide **68** by addition of ethyl chloroformate (ECF) at low temperature for 1 h to N-protected α-amino acid. $Et_3N{\cdot}HCl$ was filtered off and then hydrazine hydrate was added at low temperature and warmed up to room temperature, the desired N-protected α-amino acid hydrazide **68** was obtained. The second step was the

addition of dimethyl formamide dimethyl acetal at 50 ºC for 1 h and the selected primary amine in HOAc and 50ºC to achieve the triazole molecule **69**. The acidolytic deprotection of the amino group yielded compounds **TR-(1-8)**. All compounds were purified and characterized by HPLC-MS (Table 8).

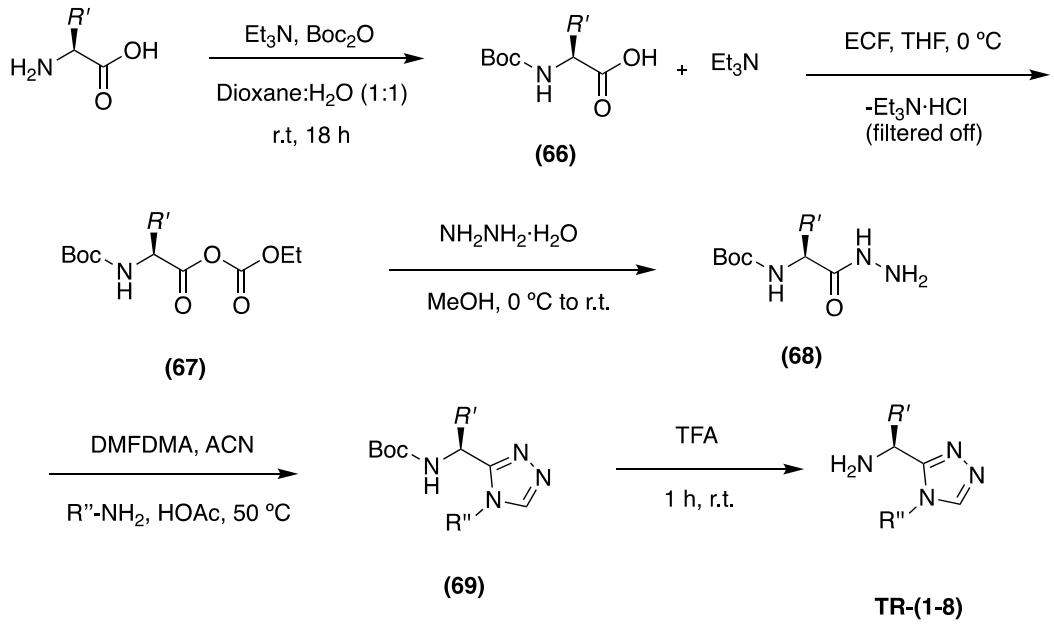

Scheme 4. Synthesis of triazole compounds.

Table 8. List of substituted triazoles.

Compound	R'	R''	Yield (%)	Purity (%)*
TR1	iPr	3-Chloro-phenyl	65	97
TR2	Propyl	3-Chloro-phenyl	87	97
TR3	Propyl	3-Fluoro-phenyl	88	98
TR4	3-Methylthioethyl	3-Chloro-phenyl	89	94
TR5	iBu	3-Fluoro-phenyl	71	95
TR6	iPr	Phenyl	54	93
TR7	iPr	4-Chloro-phenyl	77	97
TR8	Methyl	4-Fluoro-phenyl	85	96

*Purities were determined by HPLC-MS (214 nm).

Selected compounds were characterized by ^{1}H-NMR and tested for antifungal activity (Figure 23).

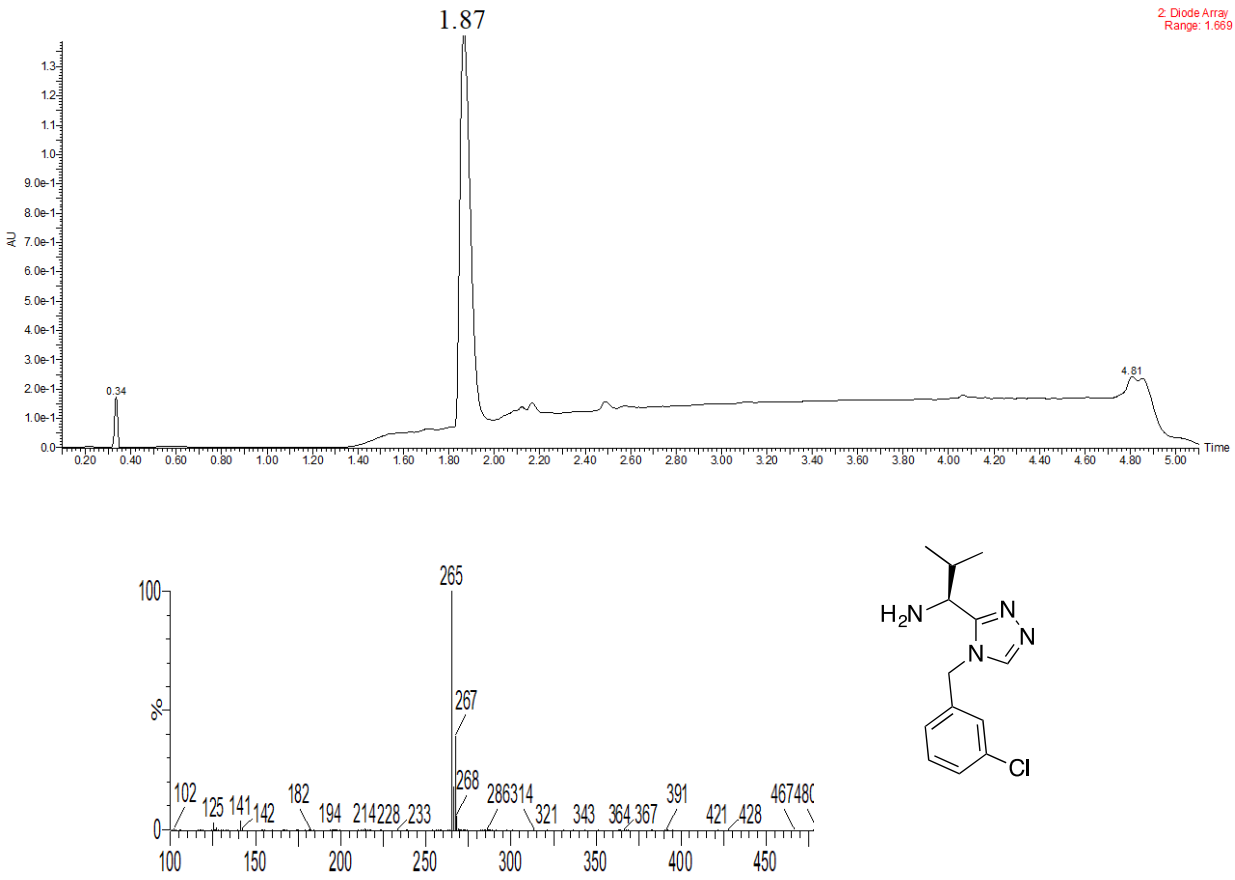

Figure 23. HPLC-MS (214 nm) analysis of triazole compound **TR1**.

4.6. Imidazo[1,2-a]pyridines and imidazo[1,2-a]pyrimidines

The two bicyclic systems contain an imidazole core and occur in numerous natural products and pharmaceuticals. Among the imidazole core derivatives, the most important ones are the imidazo[1,2-a]pyridine and the imidazo[1,2-a]pyrimidine. The imidazo[1,2-a]pyridine derivatives show a wide range of biological activities such as antifungal, anti-inflammatory, antitumor, anticancer or antiviral. [93, 94]

The main difference between these two ring systems is the six membered ring connected to the imidazole moiety which in one case is a pyridine and the other a pyrimidine (Figure 24).

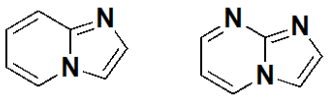

Figure 24. Structure of imidazo[1,2-a]pyridine and imidazo[1,2-a]pyrimidine respectively.

Positions 2 and 3, located in the imidazole ring, are the most substituted positions. However, the positions 5 to 8 of the pyridine moiety can be substituted as well (Figure 25, A). Not very common is the substitution of the imidazole nitrogen in position 1.

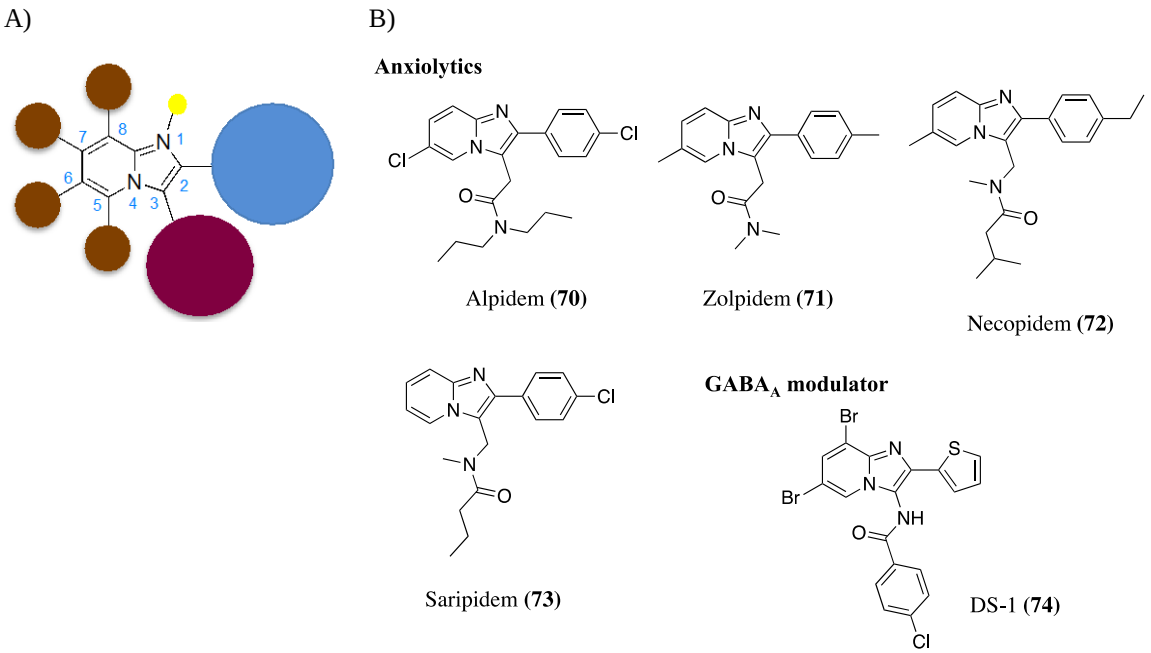

Figure 25. A) Preferred substitution patterns. B) Pharmaceuticals containing the imidazo[1,2-a]pyridine structure.

Examples in Figure 25, B, Alpidem (Sanofi-Aventis, **(70)**), Zolpidem **(71)** and Necopidem **(72)** are trisubstituted in positions 2, 3 and 6, while Saripidem **(73)** is disubstituted at positions 2 and 3. The $GABA_A$ modulator drug, DS-1 **(74)**, is tetrasubstituted in positions 2, 3 and 6, and additionally in position 8 (phenyl ring).

4.6.1. Synthesis of imidazo[1,2-a]pyridine and imidazo[1,2-a]pyrimidine

These structures were designed by scaffold hopping to match the **EMC120B12** molecule, as closely as possible.

Both compounds, **ImPn1** and **ImPm1** were synthesized following the same route. The differing step was the addition of 2-aminopyridine for **ImPn1** and pyrimidin-2-amine for **ImPm1** to the α-bromo-amino-β-ketoester **75**.

Tert-butyl β-ketoester (**54)** was obtained from valine. The bromination of (**54**) by N-bromosuccinimide in MeOH at very low temperature yielded **75**.

2-Aminopyridine and 2-aminopyrimidine were added in parallel to obtain the imidazo[1,2-a]pyridine **(76)** and imidazo[1,2-a]pyrimidine **(77)** respectively (Scheme 5 and 6).

Deprotection of the amino group under acidolytic conditions yielded compounds **ImPn1** and **ImPm1** in reasonable yields (Table 9).

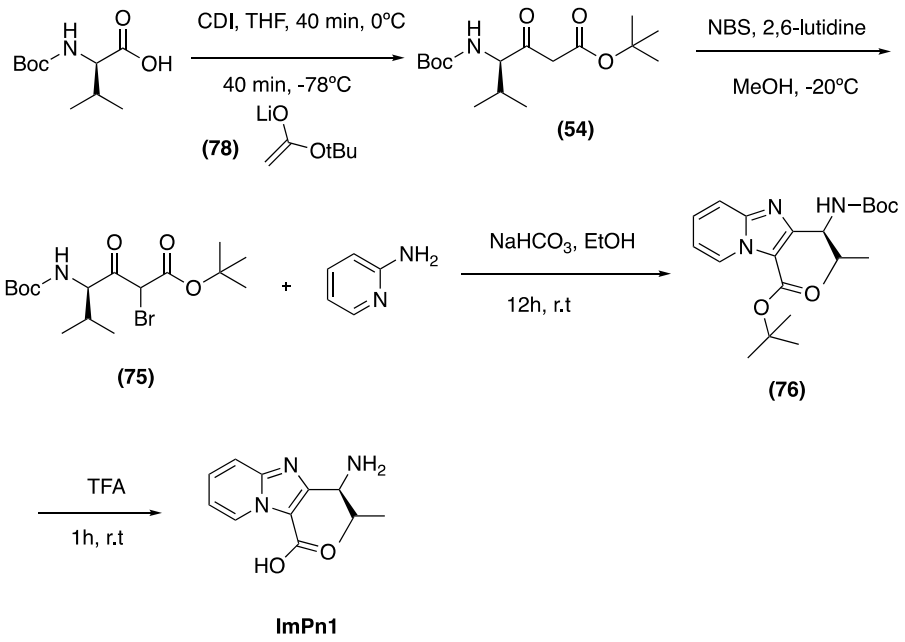

Scheme 5. Synthesis of imidazo[1,2-a]pyridine.

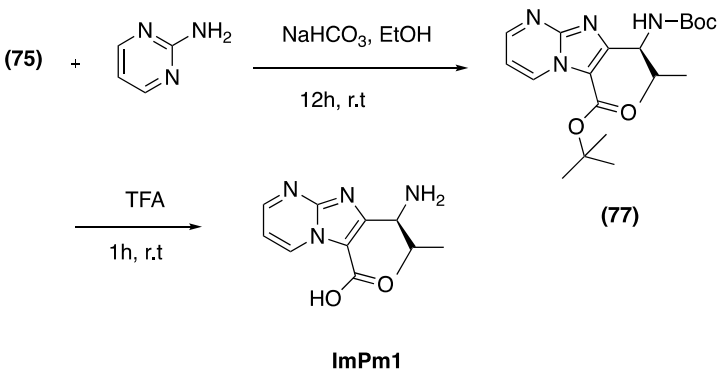

Scheme 6. Synthesis of the imidazo[1,2-a]pyrimidine.

Table 9. Purities and yields of ImPn1 and ImPm1.

Compound	Yield (%)	Purity (%)*
ImPn1	72	84
ImPm1	56	61

*Purities were determined by HPLC-MS (214 nm) after purification.

4.7. Study of antifungal activity

4.7.1. Objective

The objective of this part was to investigate the biological effect of the new heterocyclic compounds against *Candida* species. Several biological assays were carried out and most of the assays have been previously used for the investigation of peptides (Section A). Only the dose-response assay and the proteomic analysis were described because these assays are not described so far. The following assays have been carried out: high-throughput screening, dose-response assay (IC_{50} and CC_{50}), determination of the minimum inhibitory concentration (MIC), evaluation of the antifungal activity of all compounds against clinical isolates of *Candida* species and the proteomic study for two of the most active compounds.

B.4.7.2. High-throughput screening (HTS)

The screening was carried out at the same conditions as described in *"3.6. High-throughput screening (HTS)"* in Section A for peptide compounds.

B.4.7.2.1. Results for benzimidazole drivatives

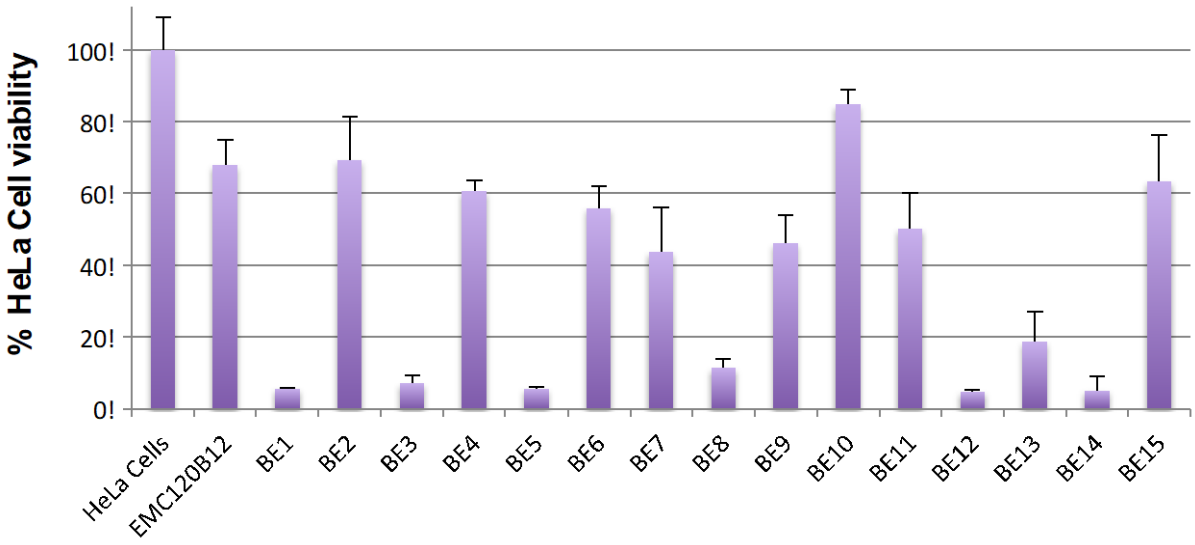

Figure 26. Graphic representation of the screening showing the cell viability of benzimidazole compounds at 10 µM. All compounds over 40 % cell viability were further studied. **BE** (2, 4, 6, 7, 9, 10, 11 and 15).

4.7.2.2. Results for indole derivatives

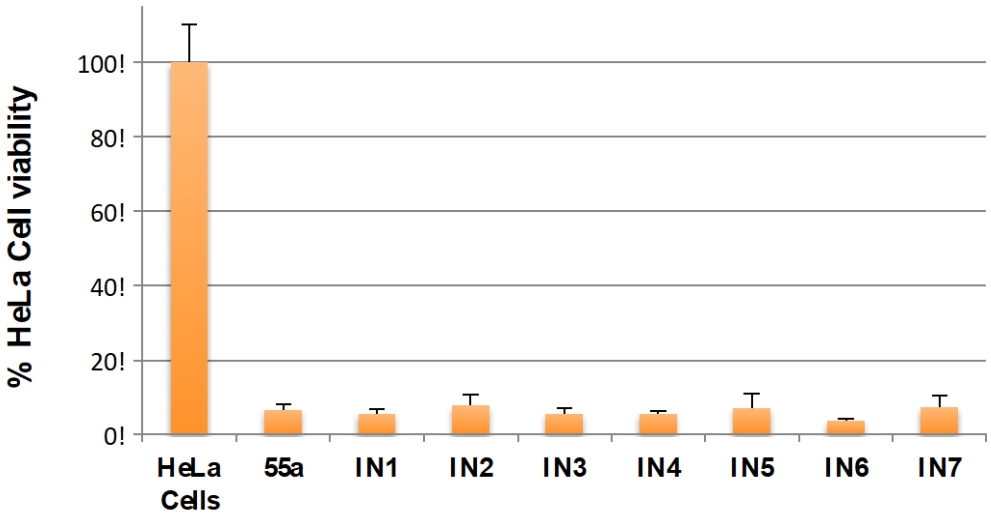

Figure 27. Graphic representation of the screening showing the cell viability of indole compounds at 10 µM.

4.7.2.3. Results for triazole derivatives

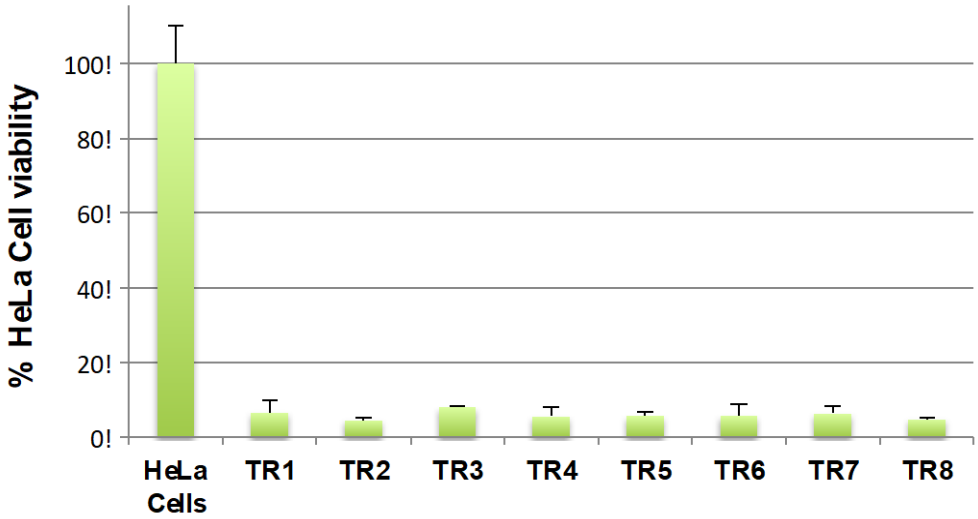

Figure 28. Graphic representation of the screening showing the cell viability of triazole compounds at 10 µM.

4.7.2.4. Results for imidazo[1,2-a]pyridine and imidazo[1,2-a]pyrimidine

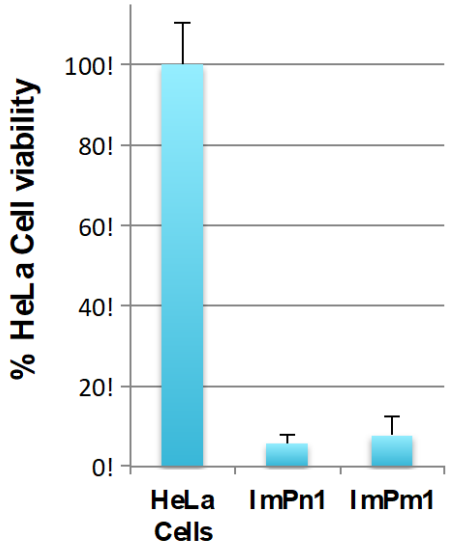

Figure 29. Graphic representation of the screening showing the cell viability of both imidazo[1,2-a]pyridine and imidazo[1,2-a]pyrimidine compounds at 10 µM.

4.7.3. Inhibitory and cytotoxicity assay

A dose-response curve was determined to describe the relationship between the drug treatment response and drug dose (concentration).

From the dose-response assay carried out, IC_{50} (half maximal inhibitory concentration) and CC_{50} (half maximal cytotoxicity concentration) were calculated only for the positive control **EMC120B12**, and analogues **BE2**, **BE4**, **BE6**, **BE7**, **BE9**, **BE10** and **BE11**.

We considered that a compound was active when the cell viability of HeLa cells was high (over 80 %) at the lowest concentration (2 µM). All compounds with high cell viability at 2 µM, were considered as non active compounds and therefore, their IC_{50} and CC_{50} were not studied.

Initially, a dose-response assay was carried out in a range of concentration 250 – 2 (µM). The results from that first assay encouraged investigating the compounds in a second dose-response assay at lower concentrations (4 – 0.03125 µM). The objective of this repetition was to calculate their IC_{50} and CC_{50}. To confirm those results a software program was used (OriginPro9) fitting the Hill equation, a sigmoidal dose-response curve (Table 26).

The experimental conditions for those assays were the following:

- Inhibitory concentration: HeLa cells (50 µl; 10.000 cells/well) + *C. albicans* (50 µl; 50 CFU) + 100 µl of compound in a 96 well plate.

- Cytotoxicity concentration: HeLa cells (50 µl; 10.000 cells/well) + 100 µl compound in a 96 well plate.

4.7.3.1. Results

⇒ *Inhibitory concentration **EMC120B12***:

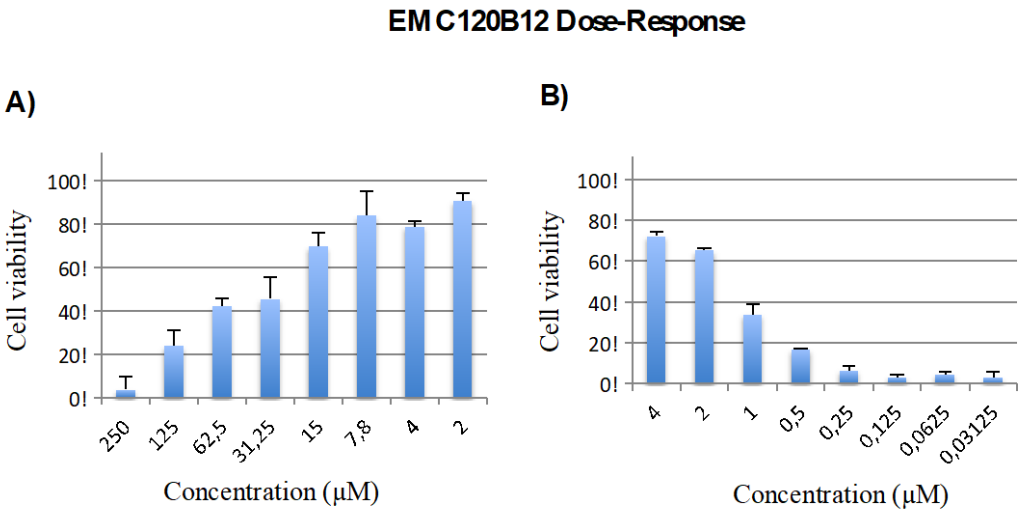

Figure 30. Graphic representation of dose-response assay for **EMC120B12** to calculate the 50 % inhibitory concentration. A) Range of concentration: 250 – 2 µM. B) Range of concentration: 4 – 0.03125 µM.

Table 10. Cell viability (%) at different concentrations during inhibitory assay for **EMC120B12**.

Inhibitory dose-response			
EMC120B12			
Concentration (µM)	% Cell viability	Concentration (µM)	% Cell viability
250	4	4	74
125	23	2	67
62.5	44	1	36
31.25	46	0.5	18
15	73	0.25	8
7.8	84	0.125	4
4	77	0.0625	6
2	92	0.03125	3

⇒ *Cytotoxicity concentration* **EMC120B12**:

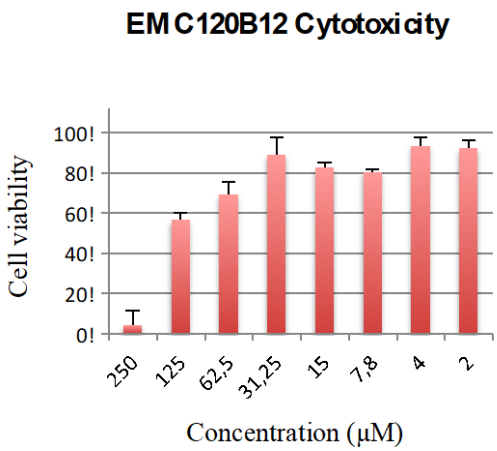

Figure 31. Graphic representation of dose-response assay for **EMC120B12** to calculate the 50 % cytotoxicity concentration. Range of concentration: 250 – 2 µM.

Table 11. Cell viability (%) at different concentrations during cytotoxicity assay.

Cytotoxicity dose-response	
EMC120B12	
Concentration (µM)	% Cell viability
250	4
125	58
62.5	69
31.25	88
15	82
7.8	80
4	93
2	93

EMC120B12 showed over 50 % cell viability at 2 µM but it was toxic to HeLa cells between 125 – 250 µM.

⇒ *Inhibitory concentration* **BE2**:

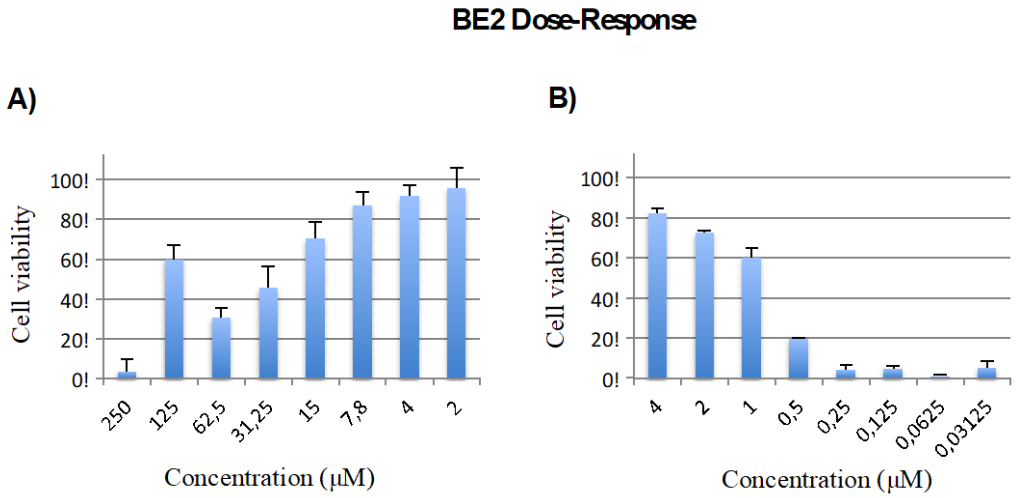

Figure 32. Graphic representation of dose-response assay for **BE2** to calculate the 50 % inhibitory concentration. A) Range of concentration: 250 – 2 µM. B) Range of concentration: 4 – 0.03125 µM.

Table 12. Cell viability (%) at different concentrations during inhibitory assay for **BE2**.

Inhibitory dose-response			
BE2			
Concentration (µM)	% Cell viability	Concentration (µM)	% Cell viability
250	4	4	82
125	60	2	74
62.5	29	1	60
31.25	44	0.5	19
15	75	0.25	3
7.8	90	0.125	4
4	94	0.0625	1
2	98	0.03125	5

⇒ *Cytotoxicity concentration* **BE2**:

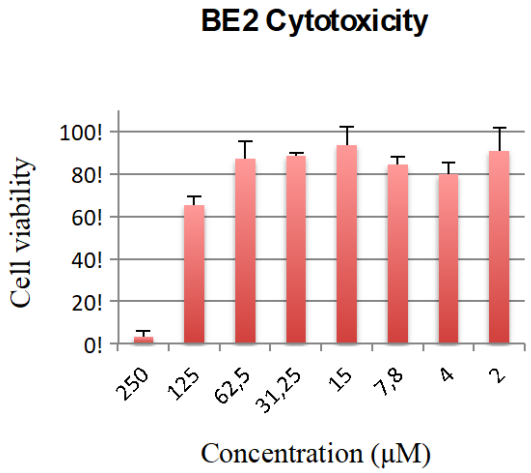

Figure 33. Graphic representation of dose-response assay for **BE2** to calculate the 50 % cytotoxicity concentration. C) Range of concentration: 250 – 2 µM.

Table 13. Cell viability (%) at different concentrations during cytotoxicity assay for **BE2**.

Cytotoxicity dose-response	
BE2	
Concentration (µM)	% Cell viability
250	2
125	62
62.5	87
31.25	89
15	96
7.8	88
4	80
2	91

BE2 showed similar results as **EMC120B12**, as it was active over 50 % cell viability at 2 µM but toxic to HeLa cells between 125 – 250 µM.

⇒ *Inhibitory concentration* **BE4**:

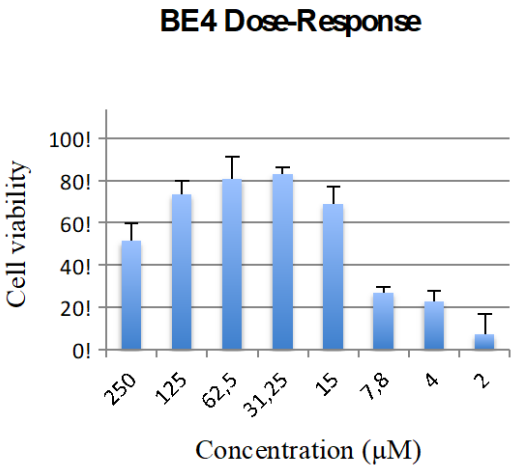

Figure 34. Graphic representation of dose-response assay for **BE4** to calculate the 50 % inhibitory concentration. Range of concentration: 250 – 2 µM

Table 14. Cell viability (%) at different concentrations during inhibitory assay for **BE4**.

Inhibitory dose-response	
BE4	
Concentration (µM)	% Cell viability
250	53
125	67
62.5	80
31.25	80
15	74
7.8	27
4	22
2	7

⇒ *Cytotoxicity concentration* **BE4**:

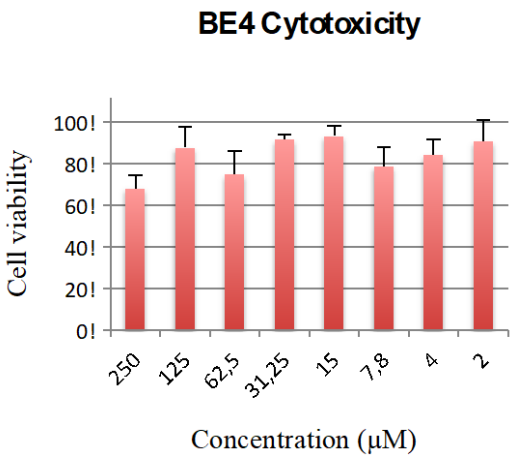

Figure 35. Graphic representation of dose-response assay for **BE4** to calculate the 50 % cytotoxicity concentration. Range of concentration: 250 – 2 µM.

Table 15. Cell viability (%) at different concentrations during cytotoxicity assay for **BE4**.

Cytotoxicity dose-response	
BE4	
Concentration (µM)	% Cell viability
250	68
125	90
62.5	77
31.25	92
15	95
7.8	79
4	83
2	91

BE4 showed over 50 % cell viability at 15 µM but it showed to be not toxic to HeLa cells at any concentration used. Its IC_{50} was not calculated.

⇒ *Inhibitory concentration* **BE6**:

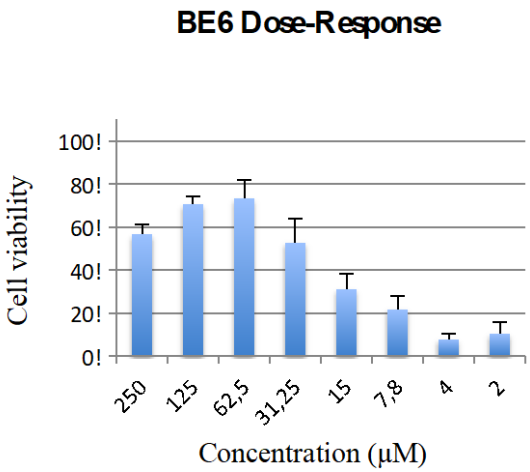

Figure 36. Graphic representation of dose-response assay for **BE6** to calculate the 50 % inhibitory concentration. Range of concentration: 250 – 2 µM.

Table 16. Cell viability (%) at different concentrations during inhibitory assay for **BE6**.

Inhibitory dose-response	
BE6	
Concentration (µM)	% Cell viability
250	58
125	70
62.5	73
31.25	48
15	26
7.8	22
4	5
2	8

⇒ *Cytotoxicity concentration* **BE6**:

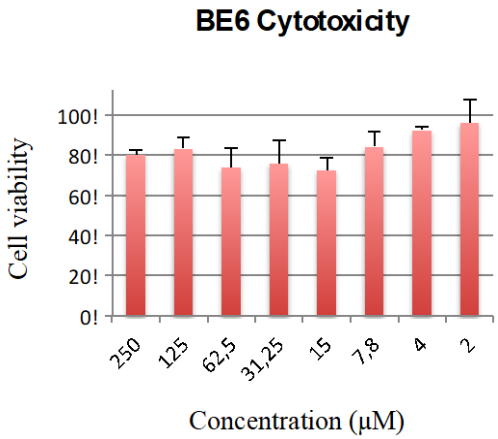

Figure 37. Graphic representation of dose-response assay for **BE6** to calculate the 50 % cytotoxicity concentration. Range of concentration: 250 – 2 µM.

Table 17. Cell viability (%) at different concentrations during cytotoxicity assay for **BE6**.

Cytotoxicity dose-response	
BE6	
Concentration (µM)	% Cell viability
250	81
125	81
62.5	77
31.25	78
15	76
7.8	82
4	91
2	94

BE6 showed over 50 % cell viability at 62.5 µM but, like **BE4**, it showed no toxicity to HeLa cells at any concentration used. Its IC_{50} was not calculated.

⇒ *Inhibitory concentration* **BE7**:

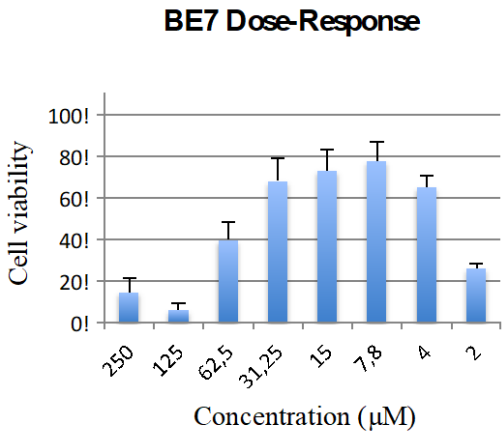

Figure 38. Graphic representation of dose-response assay for **BE7** to calculate the 50 % inhibitory concentration. Range of concentration: 250 – 2 µM.

Table 18. Cell viability (%) at different concentrations during inhibitory assay for **BE7**.

Inhibitory dose-response	
BE7	
Concentration (µM)	% Cell viability
250	14
125	6
62.5	39
31.25	71
15	73
7.8	79
4	65
2	26

⇒ *Cytotoxicity concentration* **BE7**:

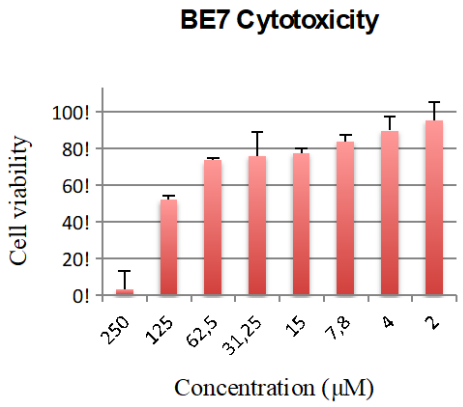

Figure 39. Graphic representation of dose-response assay for **BE7** to calculate the 50 % cytotoxicity concentration. Range of concentration: 250 – 2 µM.

Table 19. Cell viability (%) at different concentrations during cytotoxicity assay for **BE7**.

Cytotoxicity dose-response	
BE7	
Concentration (µM)	% Cell viability
250	4
125	55
62.5	75
31.25	78
15	77
7.8	81
4	86
2	96

BE7 showed over 50 % cell viability at 4 µM but at higher concentration the cell viability decreased. It was toxic to HeLa cells between 125 – 250 µM. Its IC_{50} was not calculated.

⇒ *Inhibitory concentration* **BE9**:

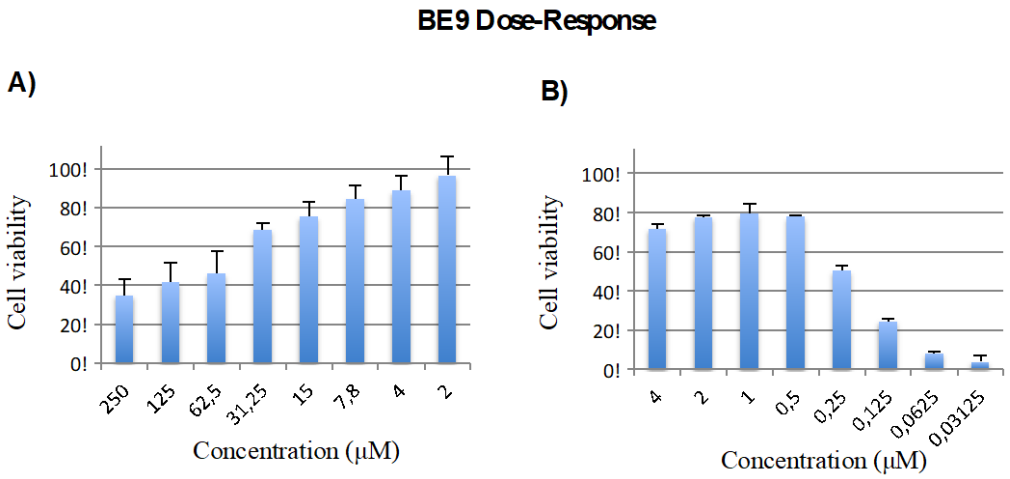

Figure 40. Graphic representation of dose-response assay for **BE9** to calculate the 50 % inhibitory concentration. A) Range of concentration: 250 – 2 µM. B) Range of concentration: 4 – 0.03125 µM.

Table 20. Cell viability (%) at different concentrations during inhibitory assay for **BE9**.

Inhibitory dose-response			
BE9			
Concentration (µM)	% Cell viability	Concentration (µM)	% Cell viability
250	38	4	74
125	40	2	98
62.5	45	1	99
31.25	73	0.5	98
15	76	0.25	53
7.8	84	0.125	24
4	88	0.0625	9
2	98	0.03125	4

⇒ *Cytotoxicity concentration* **BE9**:

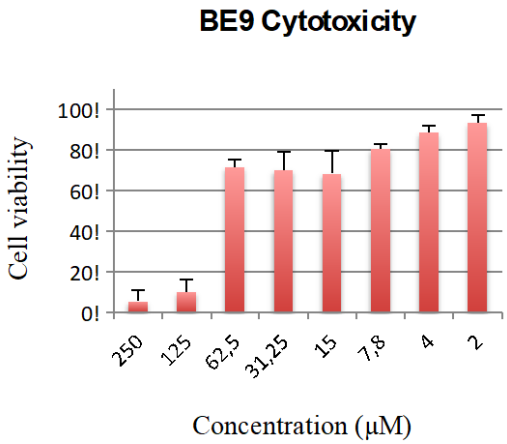

Figure 41. Graphic representation of dose-response assay for **BE9** to calculate the 50 % cytotoxicity concentration. C) Range of concentration: 250 – 2 µM.

Table 21. Cell viability (%) at different concentrations during cytotoxicity assay for **BE9**.

Cytotoxicity dose-response	
BE9	
Concentration (µM)	% Cell viability
250	4
125	8
62.5	74
31.25	72
15	69
7.8	79
4	87
2	93

BE9 showed over 50 % cell viability at 0.25 µM and toxicity towards HeLa cells between 62.5 and 125 µM.

⇒ *Inhibitory concentration* **BE10**:

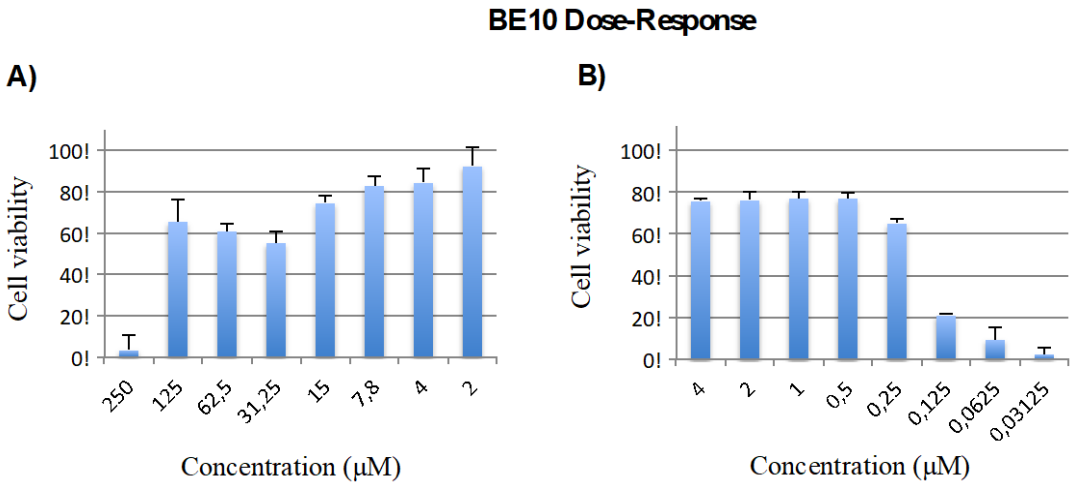

Figure 42. Graphic representation of dose-response assay for **BE10** to calculate the 50 % inhibitory concentration. A) Range of concentration: 250 – 2 µM. B) Range of concentration: 4 – 0.03125 µM.

Table 22. Cell viability (%) at different concentrations during inhibitory assay for **BE10**.

Inhibitory dose-response			
BE10			
Concentration (µM)	% Cell viability	Concentration (µM)	% Cell viability
250	3	4	76
125	66	2	77
62.5	59	1	78
31.25	58	0.5	77
15	77	0.25	65
7.8	84	0.125	21
4	86	0.0625	10
2	93	0.03125	3

⇒ *Cytotoxicity concentration* **BE10**:

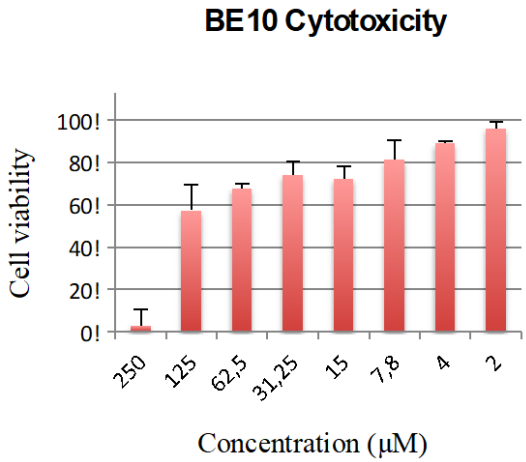

Figure 43. Graphic representation of dose-response assay for **BE10** to calculate the 50 % cytotoxicity concentration. C) Range of concentration: 250 – 2 µM.

Table 23. Cell viability (%) at different concentrations during cytotoxicity assay for **BE10**.

Cytotoxicity dose-response	
BE10	
Concentration (µM)	% Cell viability
250	2
125	58
62.5	67
31.25	73
15	72
7.8	80
4	89
2	98

BE10 showed over 50 % cell viability at 0.25 µM and toxicity towards HeLa cells between 125 – 250 µM.

⇒ *Inhibitory concentration* **BE11**:

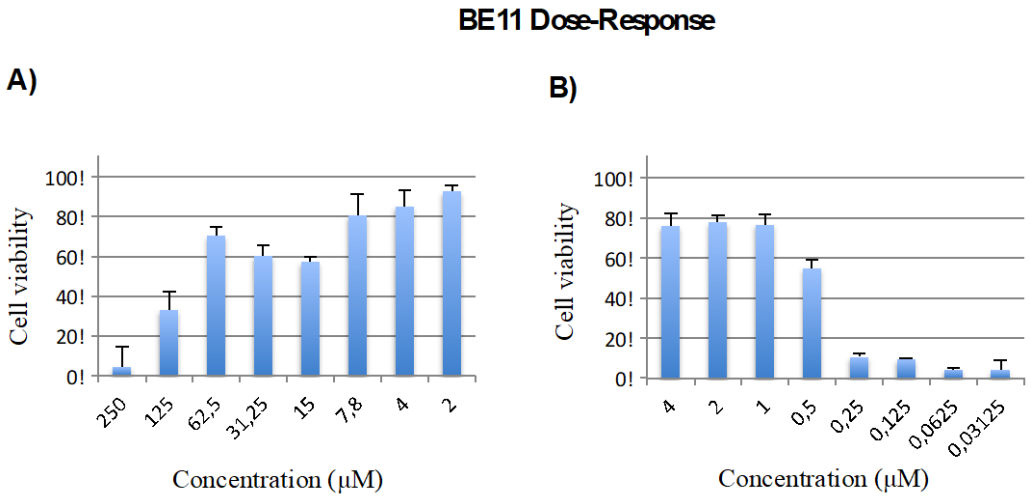

Figure 44. Graphic representation of dose-response assay for **BE11** to calculate the 50 % inhibitory concentration. A) Range of concentration: 250 – 2 µM. B) Range of concentration: 4 – 0.03125 µM.

Table 24. Cell viability (%) at different concentrations during inhibitory assay for **BE11**.

Inhibitory dose-response			
BE11			
Concentration (µM)	% Cell viability	Concentration (µM)	% Cell viability
250	3	4	88
125	31	2	89
62.5	74	1	87
31.25	61	0.5	57
15	59	0.25	12
7.8	81	0.125	10
4	85	0.0625	5
2	89	0.03125	6

⇒ *Cytotoxicity concentration* **BE11**:

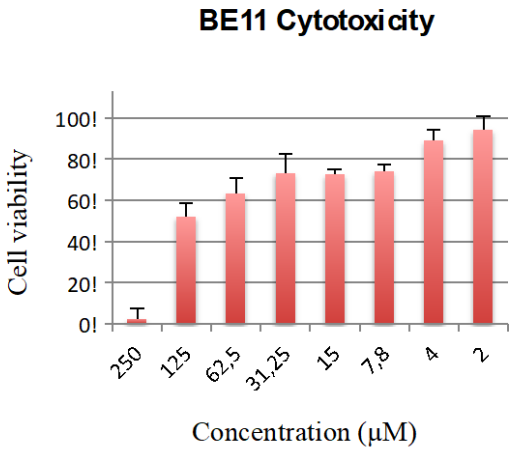

Figure 45. Graphic representation of dose-response assay for **BE11** to calculate the 50 % cytotoxicity concentration. C) Range of concentration: 250 – 2 µM.

Table 25. Cell viability (%) at different concentrations during cytotoxicity assay for **BE11**.

Cytotoxicity dose-response	
BE11	
Concentration (µM)	% Cell viability
250	4
125	52
62.5	61
31.25	72
15	72
7.8	74
4	87
2	96

BE11 showed over 50 % cell viability at 0.5 µM and toxicity towards HeLa cells between 62.5 and 125 µM.

4.7.3.2. IC_{50} and CC_{50} calculation

The software program OriginPro9, fitting Hill equation, was used to obtain the IC_{50} and CC_{50}. The Hill equation is a general equation for a dose-response curve that shows the response as a function of the logarithm of concentration (Figure 46), being X the logarithm of agonist concentration and Y the response.

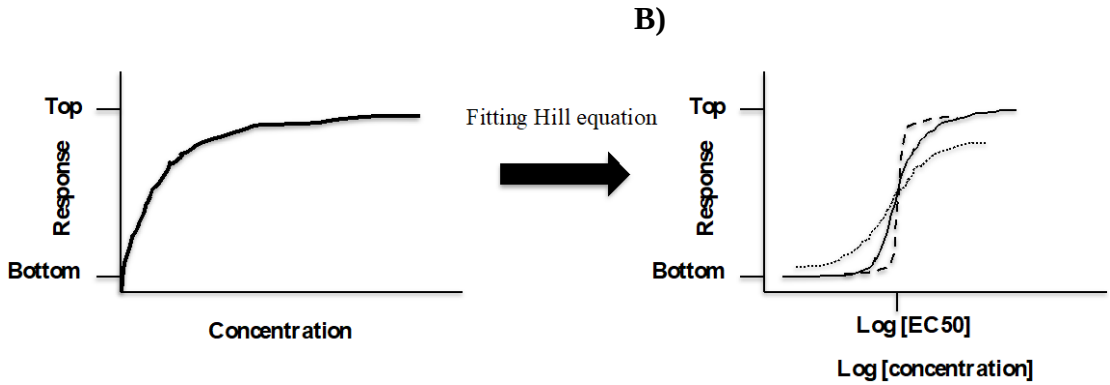

Figure 46. Dose-response curve before and after fitting Hill equation (A and B, respectively). B) Three logarithm curves: discontinuous line curve corresponds to a Hill slope over 1; discontinuous dot curve corresponds to a Hill slope less than 1 and the last curve remain, corresponds to a Hill equation equal to 1.

$$Y = \text{Bottom} + \frac{(\text{Top} - \text{Bottom})}{1 + 10^{(\text{LogEC50} - X) \cdot \text{Hill slope}}}$$

Figure 47. Hill equation

The variable bottom is the Y value at the bottom plateau and the variable top is the Y value at the top plateau (Figure 46). EC_{50} corresponds to X value when the response is halfway between bottom and top and its $LogEC_{50}$ is the logarithm of the EC_{50}. The Hill slope describes the steepness of the curve. This variable, also called slope factor or Hill coefficient, can be positive, negative or standard. The standard sigmoid dose-response curve has a Hill slope of 1, while if it is positive, the curve increases as X increases and the curve is steeper (discontinuous curve). On the opposite, when it is negative, the curve decreases as X increases and the curve is shallower (discontinuous dot curve) (Figure 46, B). [95 - 96]

In the next table, values are summarized based on the IC_{50} and CC_{50} obtained from the dose-response curve fitting Hill equation.

Table 26. IC_{50} and CC_{50} of all active benzimidazole compounds. CI refers to confidence interval and SI to selectivity index.

Compound	IC_{50} (µM)	95 % CI	CC_{50} (µM)	95 % CI	SI
EMC120B12	0.971	0.877 – 1.253	105.12	98.37 – 139.29	108.26
BE2	0.861	0.778 – 0.959	129.32	107.15 – 162.14	150.20
BE9	0.233	0.208 – 0.266	64.91	61.59 – 76.16	278.58
BE10	0.194	0.176 – 0.218	201.31	124.22 – 249.48	1037.68
BE11	0.472	0.434 – 0.515	124.76	102.57 – 162.82	264.32

The selectivity index (SI) shown in Table 26 is the comparison of the amount of the drug inhibiting fungal replication effect to the amount that induces cell death and defined as the ratio between CC_{50} and IC_{50}. The higher this index is, the more antifungal activity with minimal cell cytotoxicity is induced. The confidence interval (CI) consists of an interval that contains the valid value of the corresponding parameter. In this assay carried out, our CI was 95 % confident and the value of our parameter was within our confidence interval. [97]

4.7.4. Minimum inhibitory concentration (MIC)

4.7.4.1. Results

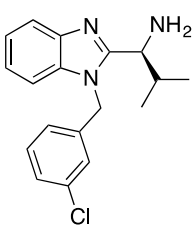

Positive control

EMC120B12

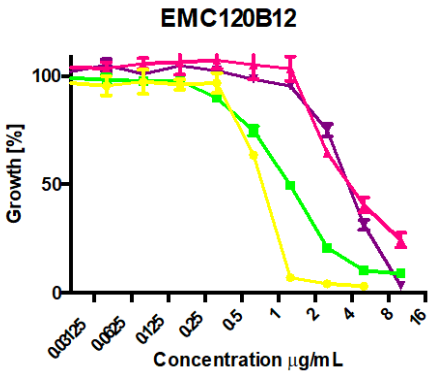

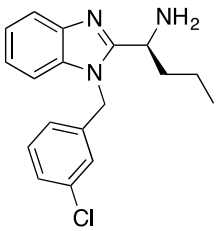

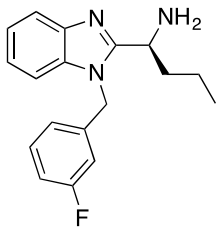

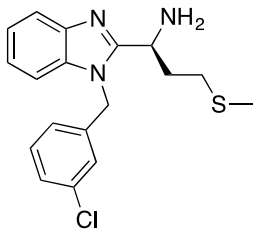

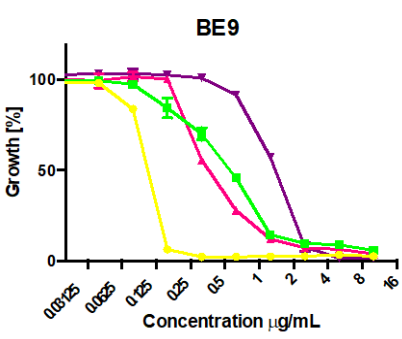

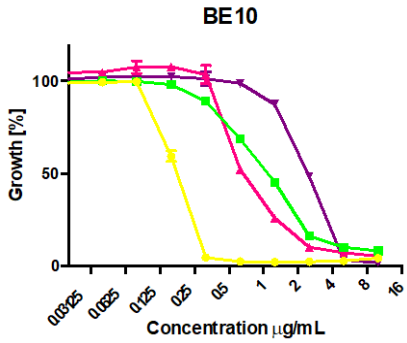

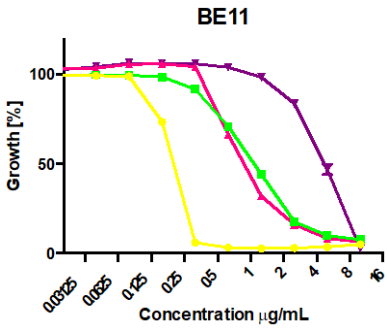

Figure 48. Results extracted from MIC assay. Voriconazole was used as a positive control and EMC120B12 was used to compare with its analogues **BE9**, **BE10** and **BE11**. Yellow corresponds to *C. albicans* SC5314; Green corresponds to *C. glabrata* ATCC2001; Pink corresponds to *C. parapsilosis* ATCC22019 and purple corresponds to *C. krusei* ATCC6258.

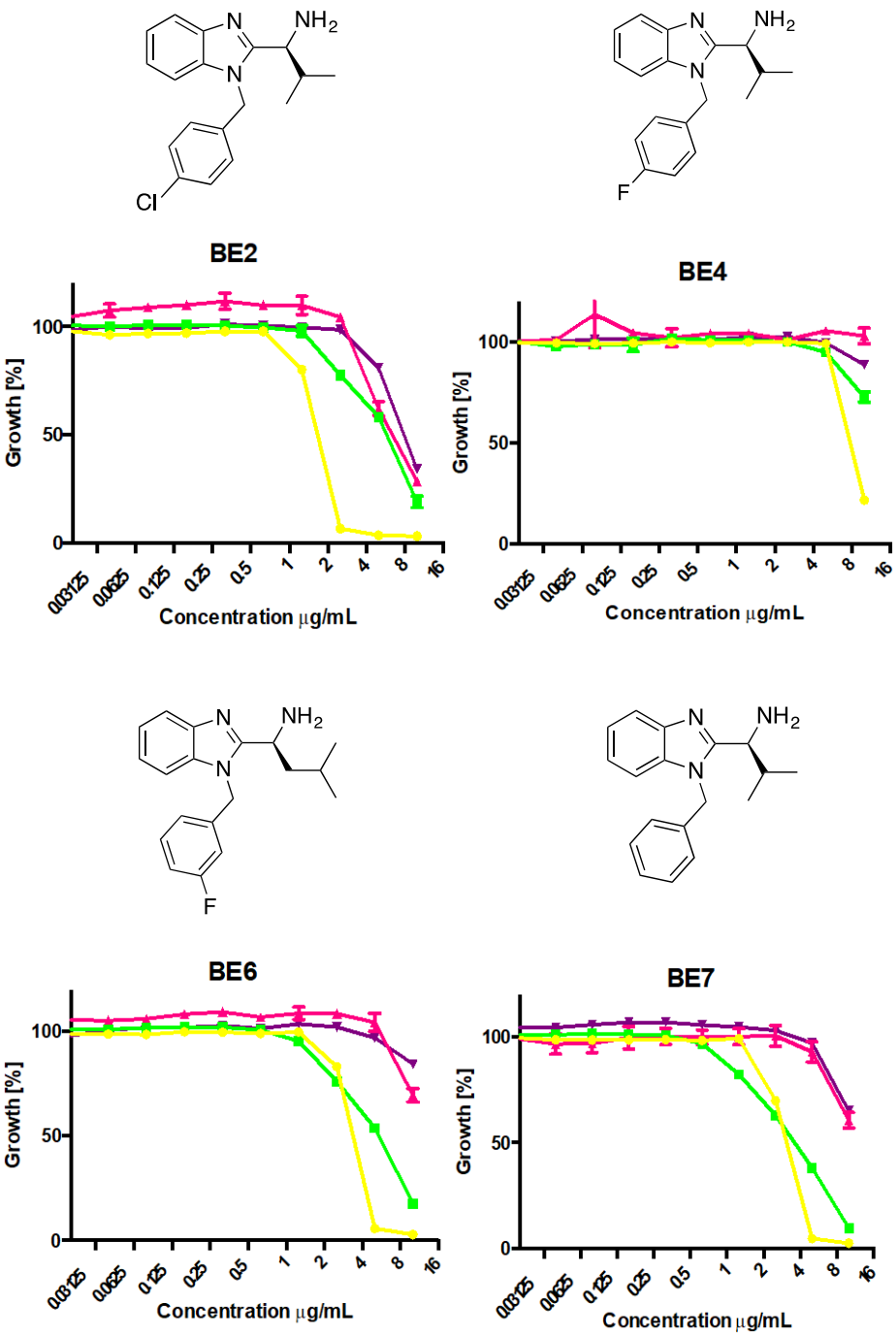

Figure 49. Results extracted from MIC assay. Yellow corresponds to *C. albicans* SC5314; Green corresponds to *C. glabrata* ATCC2001; Pink corresponds to *C. parapsilosis* ATCC22019 and purple corresponds to *C. krusei* ATCC6258.

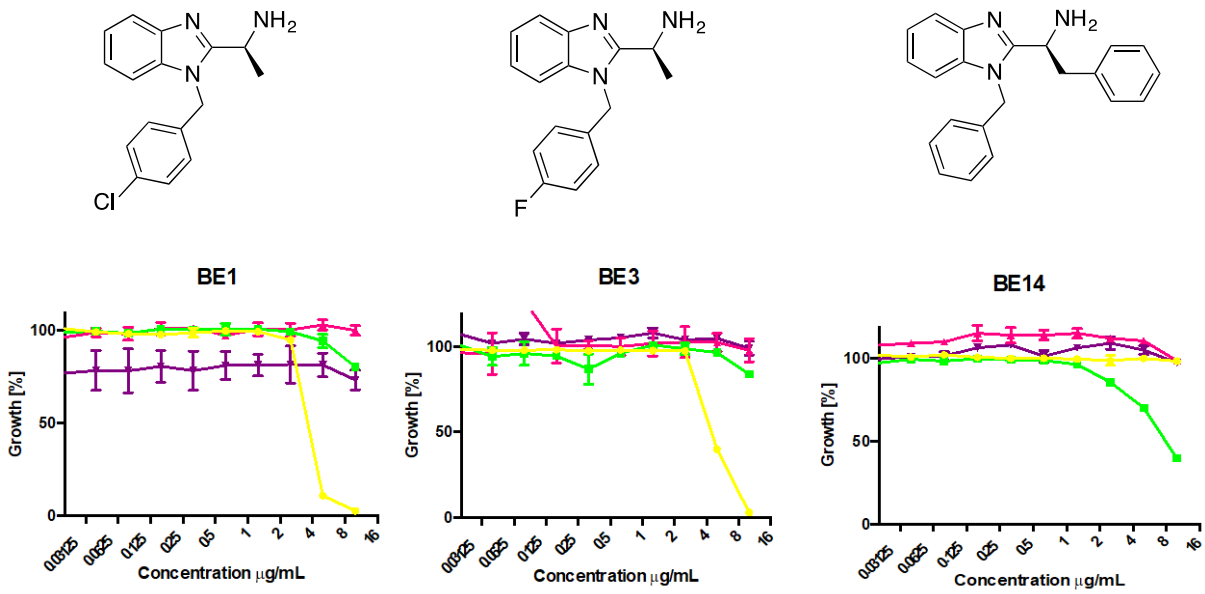

Figure 50. Results extracted from MIC assay. Yellow corresponds to *C. albicans* SC5314; Green corresponds to *C. glabrata* ATCC2001; Pink corresponds to *C. parapsilosis* ATCC22019 and purple corresponds to *C. krusei* ATCC6258.

4.7.5. Screening of clinical *Candida* spp isolates

Only the compounds that showed growth inhibition during the MIC analysis for all four *Candida* species were evaluated for further screening. Those one corresponded to **EMC120B12**, **BE2**, **BE6**, **BE7**, **BE9**, **BE10** and **BE11**.

BE4 was not further studied due to restricted availability of compound.

To investigate the activity on the effect for all four *Candida* species, the concentrations used were:

- 8 µg/ml for **EMC120B12**, **BE2**, **BE6**, **BE7** and **BE11**.
- 4 µg/ml for **BE10**.
- 2 µg/ml for **BE9**.

4.7.5.1. Results

The results of the screening of clinical *Candida* spp isolates were summarized in Table 27 specifying the grade of growth of the fungi with the active compound.

Table 27. Summarized results for the growth of the fungal cells with the compounds at their MIC concentration. Bright green colour indicates that the growth of the fungi was less than 10 % and therefore, almost full inhibition of the fungi growth with the presence of the compound. Pale green colour indicates that the growth of the fungi was between 10-30 %. Skin colour indicates that the growth of the fungi was between 30-40 % and the pale skin colour indicates that the growth of fungi was between 40-50 %. The other green colour collects the other different *Candida* species and corresponding to the growth of the fungi between 0-50 %.

Fungi&	C.&albicans(Isolates&	C.(glabrata(Isolates&	C.(parapsilosis(Isolates&	C.(krusei&solates&	Other&pecies&
Heterocycles&					
EMC120B12& [8&g/mL]&	Very&trong&ffect&	Very&trong&ffect&	Strong&ffect&	Strong&ffect&	Most&f&he&pecies:& C.(lusitaniae(C.(kefyr(C.(tropicalis(
BE2& [8&g/mL]& &	Very&trong&ffect&	Strong&ffect&	Strong&ffect&	Poor&ffect&	Some&pecies:& C.(lusitaniae(C.(tropicalis(C.(kefyr(
BE6& [8&g/mL]& &	Very&trong&ffect&	Strong&ffect&	Poor&ffect&	Very&poor&ffect&	Some&pecies:& C.(kefyr(C.(lusitaniae(
BE7& [8&g/mL]& &	Very&trong&ffect&	Strong&ffect&	Strong&ffect&	Poor&ffect&	Some&pecies:& C.(lusitaniae(C.(kefyr(C.(tropicalis(
BE9& [2&g/mL]& &	Very&trong&ffect&	Very&trong&ffect&	Very&trong&ffect&	Poor&ffect,&nly&ab&train&	Most&f&he&pecies:& C.(lusitaniae(C.(kefyr(C.(tropicalis(C.(lipoly5ka(
BE10& [4&g/mL]& &	Very&trong&ffect&	Very&trong&ffect&	Very&trong&ffect&	Very&poor&ffect&	Most&f&he&pecies:& C.(lusitaniae(C.(kefyr(C.(tropicalis(C.(lipoly5ka(
BE11& [8&g/mL]& &	Very&trong&ffect&	Very&trong&ffect&	Very&trong&ffect&	Poor&ffect&	Most&f&he&pecies:& C.(lusitaniae(C.(kefyr(C.(tropicalis(C.(lipoly5ka(

4.7.6. Proteomic study

4.7.6.1. Objective

This chemical part was separated from antifungal screening section due to its differences in the procedure and objective. In a previous genome study, **EMC120B12** was evidenced to target the ergosterol pathway by showing 15 genes involved in the ergosterol biosynthesis out of 38 upregulated. **EMC120B12** had also an impact on gene products localized in the cell surface, the cell wall and the plasma membrane. [26] Therefore, the main objective in this section was to carry out the quantitative proteomic[4] study of *Candida albicans* cells grown in the absence and presence of **EMC120B12** and **BE10** (Figure 51) and the comparison or resemblance of the genomic study performed previously in presence of **EMC120B12**.

Two experimental conditions were selected for comparison of differential abundance of proteins in *Candida albicans*:

- **Condition A**: *C. albicans* cells were grown in medium RPMI for 3 h with an O.D = 0.4
- **Condition B**: *C. albicans* cells were grown in medium RPMI for 3 h with an O.D = 0.4 and in the presence of compounds **EMC120B12** and **BE10** at their IC_{50} concentrations previously determined: 0.75 and 0.19 µM respectively.

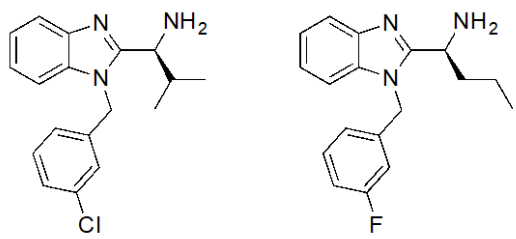

EMC120B12 **BE-10**

Figure 51. Structures of the compounds tested against *Candida albicans*.

4.7.6.2. Introduction

In order to understand cellular processes, proteomics can be useful tool. Its applications varies from large-scale comprehensive study of a specific proteome, including information on protein abundances or their variations and modifications, along with their interacting partners

[4] This analysis was carried out at Universidad Complutense de Madrid, Madrid.

and networks. [98] A proteome is a set of proteins produced in an organism or system. The proteome is not constant, it differs from cell to cell, it changes over time and also when the cell or organism undergoes stress. [99]

Proteomics can provide significant biological information for many biological problems, such as:

1 - Which proteins interact with a particular protein of interest.

2 - Which proteins are localized to a subcellular compartment.

3 - Which proteins are involved in a biological process.

4.7.6.3. Unique challenges for proteomics compared to genomics

The biggest conceptual challenge inherent in proteomics lies in the proteome's increased degree of complexity compared to the genome. [100, 101] For example:

- One gene can encode more than one protein: the human genome contains about 21,000 protein-encoding genes, but the total number of proteins in human cells is estimated to be between 250,000 to one million.
- Proteins are dynamic: proteins are continually undergoing changes such as binding to the cell membrane, partnering with other proteins to form complexes, or undergoing synthesis, post-translational modifications and degradation. The genome, on the other hand, is relatively static.
- Proteins exist in a wide range of concentrations in the cells: this makes it extremely difficult to detect the low abundance proteins in a complex biological matrix.

4.7.6.4. Tools used for proteomics

Mass spectrometry (MS) is the most important technology to detect and quantify proteins in a complex biological matrix. MS methods are very precise, distinguishing proteins that differ in composition by a single hydrogen atom. Despite its potential, common technologies are not yet capable of separating the complex protein mixtures from human biospecimens. Additional technologies such as organelle or protein fractionation or affinity capture have been developed to reduce the complexity of protein mixtures from biospecimens. Furthermore, the continuous improvement of the sensitivity of instrumentation for detection and quantification of proteins can be expected. [102 - 103]

4.7.6.5. Fluorescence microscopy

The viability of *Candida albicans* was visualized by fluorescence microscopy technique [104] in the presence of **EMC120B12** and **BE10** at different times. The two common dyes used for this study were dihydrorhodamine (DHR) and propidium iodide (PI). The viability was determined using an optical-to-electronic coupling system that recorded how the cell scattered incident laser light and emitted fluorescence.

Those two dyes were selected because DHR is an uncharged and nonfluorescent reactive oxygen species (ROS^+) indicator that can passively diffuse across membranes where it is oxidized to cationic rhodamine 123, which localizes in the mitochondria. Its fluorescence wavelength is 596 nm and exhibits green fluorescence. The PI is an intercalating agent that binds to DNA and its detection wavelength is 617 nm exhibiting a red fluorescence.

The study was carried out with:

- *C.albicans* SC5314 with H_2O_2 and MeOH as a positive control for ROS^+ and PI, respectively
- *C.albicans* SC5314 + **EMC120B12**
- *C.albicans* SC5314 + **BE10**

Incubation times used were 1.5 h, 3 h, 4.5 h and 6 h at 37 ºC (180 rpm) and the test compounds were dissolved in RMPI medium with 1 % of DMSO. The viability of the cells was observed by fluorescence microscopy. In total, two biological replicates were performed.

- Incubation time 1.5 h

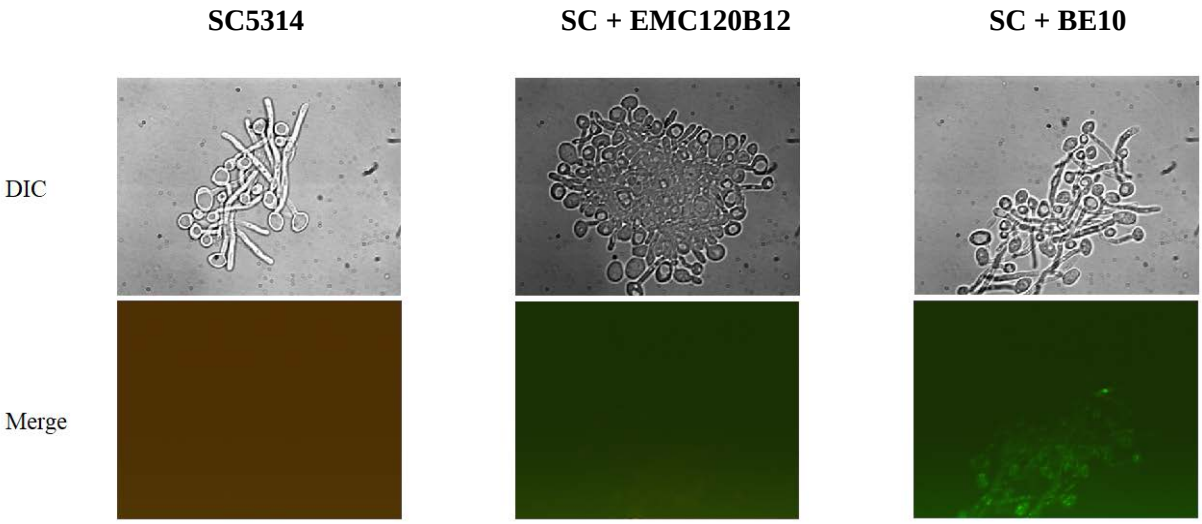

Figure 52. Images obtained from fluorescence microscopy for SC5314, SC5314 + EMC120B12 and SC5314 + **BE10** after 1.5 h. Differential interference contrast (DIC) and merge, as the combination of ROS^+ and PI results.

At 1.5 h, ROS^+ and PI detection was not visualized for any of the two compounds.

- Incubation time 3 h

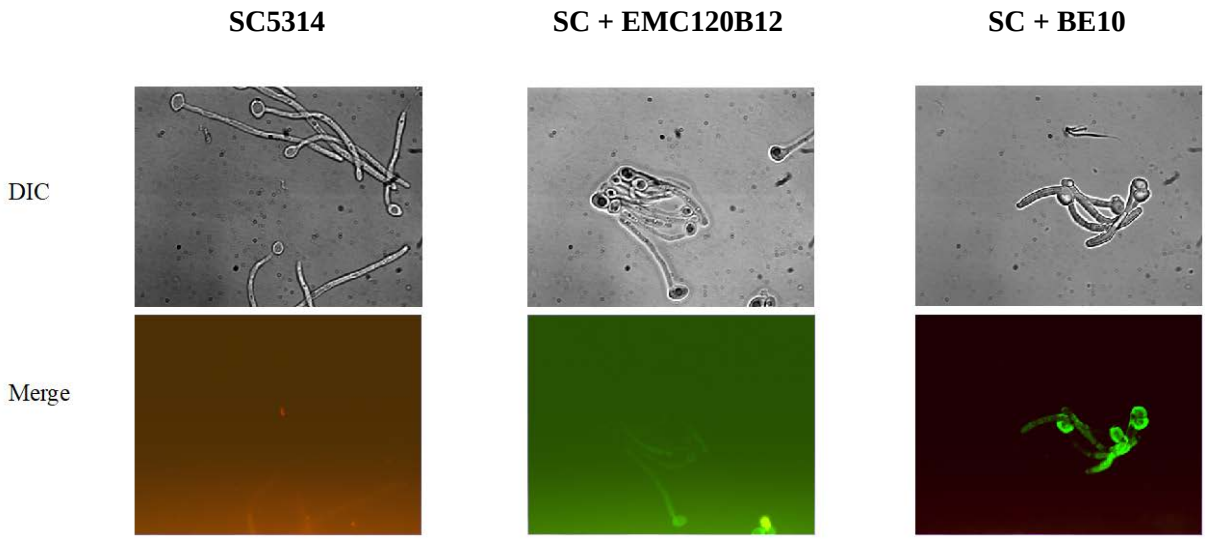

Figure 53. Images obtained from fluorescence microscopy for SC5314, SC5314 + EMC120B12 and SC5314 + BE10 after 3 h. Differential interference contrast (DIC) and merge as the combination of ROS^+ and PI results.

After 3 h, the sample treated with compound **BE10** showed ROS^+ production much stronger than the one caused by compound **EMC120B12**. PI was not visualized.

- Incubation time 4.5 h

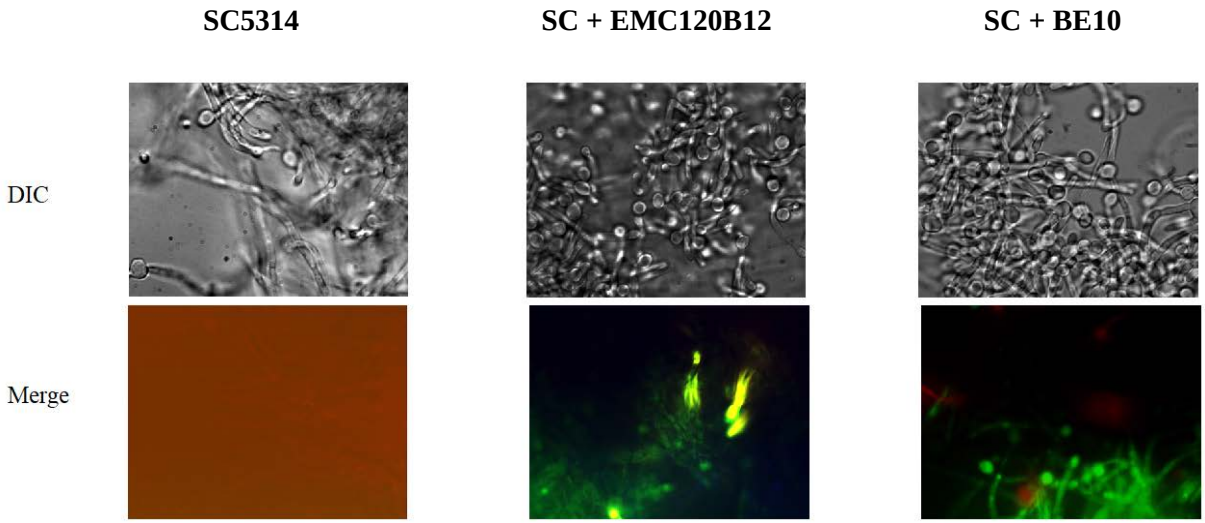

Figure 54. Images obtained from fluorescence microscopy for SC5314, SC5314 + EMC120B12 and SC5314 + BE10 after 4.5 h. Differential interference contrast (DIC) and merge as the combination of ROS^+ and PI images.

At 4.5 h, the cells suffered from stress, as ROS^+ was visualized. The cells with **BE10** started to show some PI.

- Incubation time 6 h

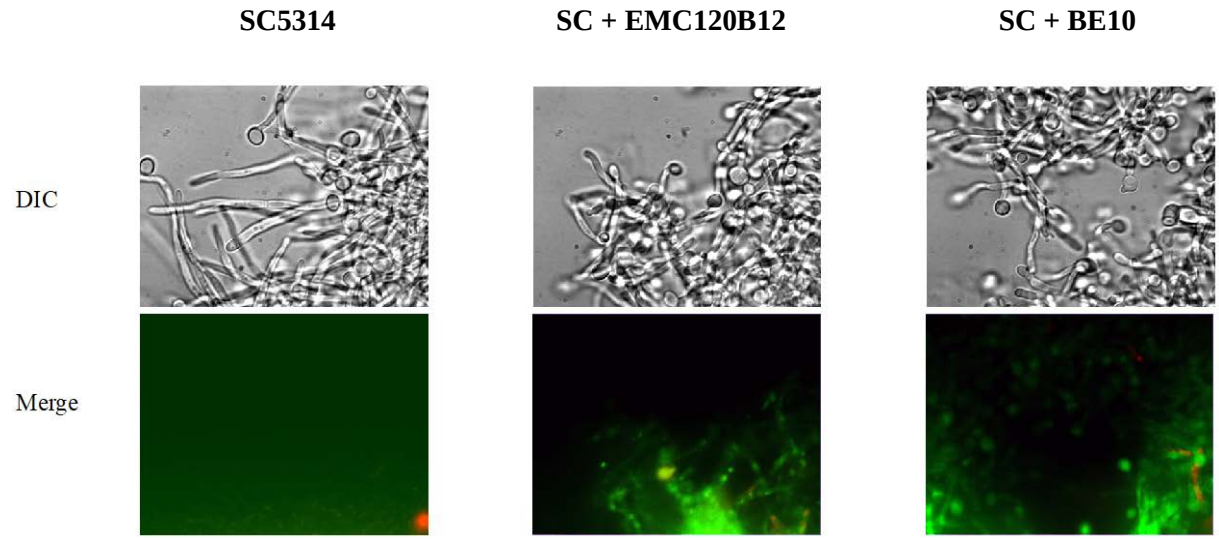

Figure 55. Images obtained from fluorescence microscopy for SC5314, SC5314 + EMC120B12 and SC5314 + BE10 after 6 h. Differential interference contrast (DIC) and merge as the combination of ROS^+ and PI images.

After 6 h, ROS^+ and PI detection was clearly visualized for both compounds in higher levels than the other time points.

This assay confirmed that the compounds **EMC120B12** and **BE10** produced stress to *Candida albicans* SC5314 cells at 3, 4.5 and 6 h. At 1.5 h the ROS^+ effect was not visualized, suggesting that there was still no stress produced for the compounds at that early time. At time point 6 h, it was possible to observe some death cells which was the reason why this time was discarded to perform the proteomic assay. Between 3 and 4.5 h, there was not much difference in cell stress, so to assure better visualization with the study, both time points 3 h and 4.5 h were selected for the proteomic assay.

4.7.6.6. Protein extraction

To study the proteins involved in some processes, it is necessary to extract the proteins. To carry out the assay, cells were mixed with glass beads and were disrupted in the bead beater, to disrupt the cell wall. The debris cells were removed by centrifugation and the protein lysate was stored at -80 °C.

The samples were later quantified and visualized by Bradford method and SDS-PAGE gel, respectively.

4.7.6.7. Protein quantification

The protein quantification is done by Bradford method, which it is used specially to determine the protein content of cell fractions and assessing protein concentrations for gel electrophoresis.

The assay is based on the observation that the absorbance maximum for an acidic solution of Coomassie Brilliant Blue G-250 shifts from 465 nm to 595 nm when binding to protein occurs. Both hydrophobic and ionic interactions stabilize the anionic form of the dye, causing a visible colour change. The assay is useful since the extinction coefficient of a dye-albumin complex solution is constant over a 10-fold concentration range. [105]

To determine the concentration of protein of the cell fractions in our samples, a standard curve was performed with bovine serum albumin (BSA) and proteins with known concentrations.

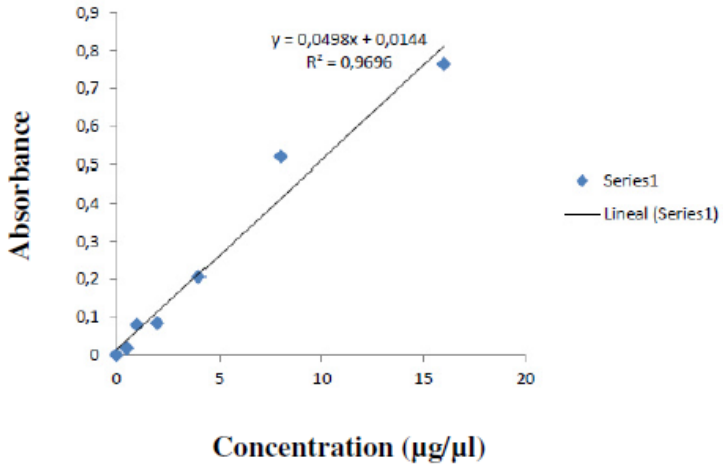

Figure 56. Standard curve with BSA. The regression equation was used to determine the protein concentration of the *Candida albicans* lysates (y = absorbance and x = concentration of the sample).

Table 28. Results obtained after Bradford method to quantify the concentration of proteins. There are 3 replicates for each of the samples. Absorbance values were given and the amount of proteins and concentrations were calculated.

	Samples	Absorbance	Protein amount (µg)	Concentration (µg/µl)
3 h	SC5314	0.502	9.791	1.958
		0.538	10.514	2.102
		0.528	10.313	2.062
	SC5314 + EMC120B12	0.403	7.803	1.560
		0.55	10.755	2.151
		0.503	9.811	1.962
	SC5314 + BE10	0.457	8.887	1.777
		0.471	9.168	1.833
		0.519	10.132	2.026
4.5 h	SC5314	0.539	10.534	2.160
		0.563	11.016	2.203
		0.497	9.690	1.938
	SC5314 + EMC120B12	0.620	12.160	2.432
		0.629	12.341	2.468
		0.563	11.016	2.203
	SC5314 + BE10	0.555	10.855	2.171
		0.631	12.381	2.476
		0.541	10.574	2.114

The values of total concentration (µg/µl) obtained by Bradford method allowed to perform a SDS-PAGE.

4.7.6.8. Protein pattern visualization by SDS-PAGE

Sodium dodecyl sulfate – polyacrylamide gel electrophoresis is a standard technique [106] used to separate proteins. This method uses a discontinuous polyacrylamide gel as a support medium and sodium dodecyl sulfate (SDS) to denature the proteins. Protein separation by SDS-PAGE can be used to estimate relative molecular mass, to determine the relative abundance of major proteins in a sample, and to determine the distribution of proteins. [107]

The SDS is an anionic detergent, meaning that when dissolved its molecules have a net negative charge within a wide pH range. The protein chain binds amounts of SDS in proportion to its relative molecular mass. The negative charges on SDS destroy most of the complex structure of proteins, and are strongly attracted toward an anode (positively-charged electrode) in an electric field. [108, 109]

Polyacrylamide gel restrains larger molecules from migrating as fast as smaller molecules, due to the charge/mass ratio, which it is nearly the same among SDS-denatured polypeptides. The final separation of proteins is dependent almost entirely on the differences in their relative molecular masses.

Two parallel gels were run with SC5314, SC5314 + **EMC120B12** and SC5314 + **BE10** of each one, three biological replicates for the time points 3 and 4.5 h.

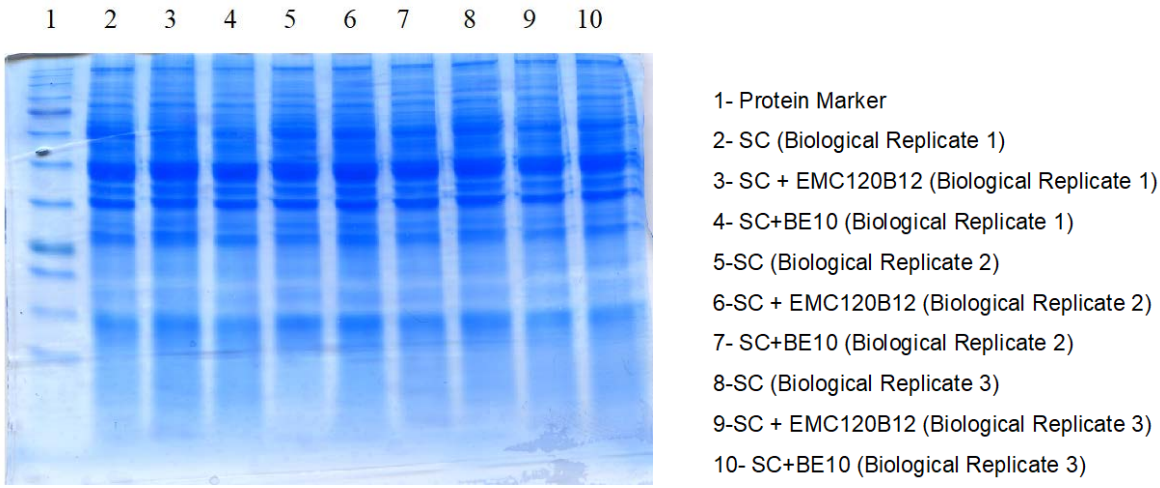

Figure 57. Protein pattern of *Candida albicans* cells grown with **EMC120B12** and **BE-10** and their replicates (up to 3) during 3 h in RPMI medium (complemented with FBS 10%).

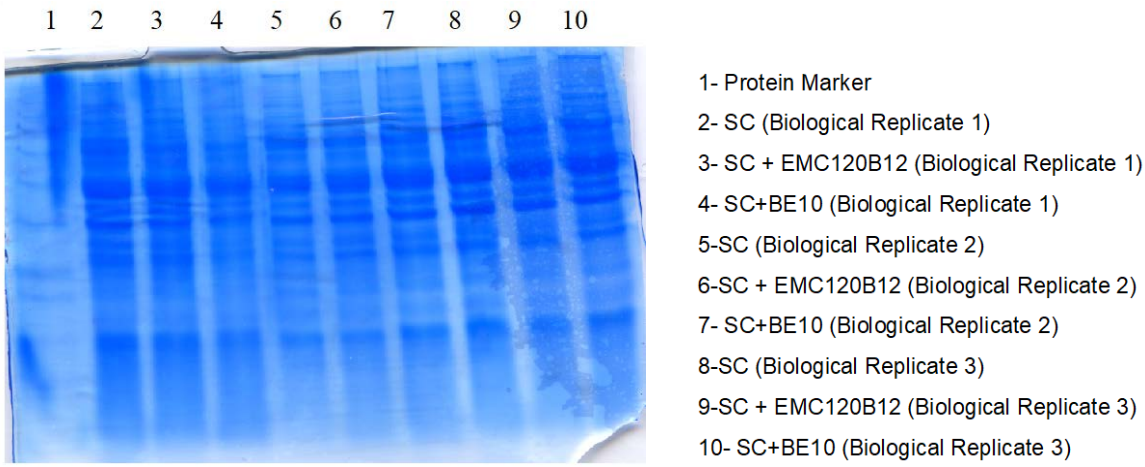

Figure 58. Protein pattern of *Candida albicans* cells grown with **EMC120B12** and **BE-10** and their replicates (up to 3) during 4.5 h in RPMI medium (complemented with FBS 10%).

The protein separation did not indicate much difference between the cells **EMC120B12** and **BE10** neither after 3 h nor 4.5 h. Therefore, *Candida albicans* cells were treated with **EMC120B12** for 3 h to carry out the proteomic study.

4.7.6.9. Protein digestion

After protein quantification, the samples were treated for protein digestion. Serine protease trypsin was employed as it cuts enzymatically peptide chains mainly at the carboxy side of the basic amino acids lysine or arginine. The generated peptides are in the preferred mass range for MS sequencing producing information-rich, easily interpretable peptide fragmentation mass spectra (Scheme 7). [110, 111]

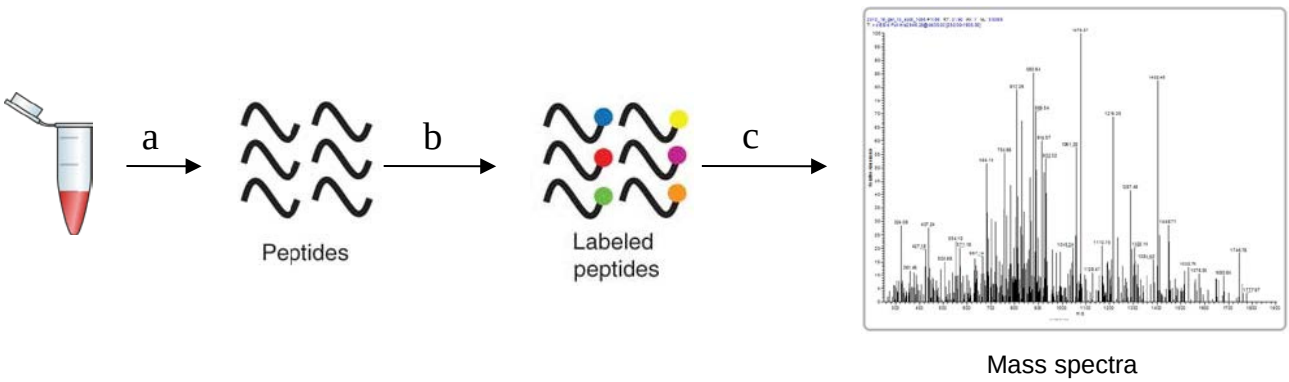

Scheme 7. a) After obtaining the protein concentration, the samples were digested. b) The digested samples were labelled with TMTsixplex Isobaric Mass Tagging Kit. c) The samples were injected to mass spectrometer: Q-TRAP, LTQ and MALDI-TOF/TOF.

4.7.6.10. Peptide labelling with TMT

A mass tag was introduced to the samples after digestion to later quantify the proteins with differences in abundance in the mass spectra.

Tandem mass tag (TMT) (Figure 59) is a chemical label used for mass spectrometry (MS)-based quantification and identification of biological macromolecules such as proteins, peptides or nucleic acids. [112]

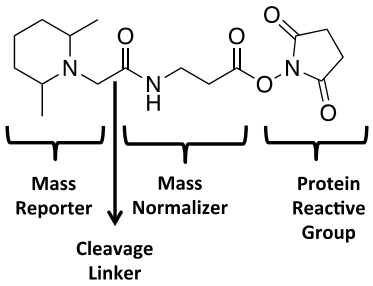

Figure 59. Structure of TMT label reagent

4.7.6.11. Results

The proteomic results are summarized in tables below and in comparison with the genomic study. Statistical significance was adjusted to a P value ≤0,05. Proteins were classified according to their gene and role. Highlighted in green are those that correlate with the gene.

Table 29. [a] Fold expression from the previous genomic study. [b] fold expression from this proteomic study. [c] correlation between the genomic and proteomic studies: Yes means that proteins were correlated to the genes; No was the opposite and (/) means that some correlation was found between proteomic and genomic study at P value ≥0,05. Positive values: up-regulated; negative values: down-regulated.

	Gene	Fold expression (genomic)[a]	Adjusted P value	Fold expression (proteomic)[b]	Adjusted P value	Correlation[c]
Role in ergosterol biosynthesis	ERG1	4,34	0,000108	-	-	No
	ERG10	2,6	0,000948	1,617	9,99999E-07	Yes
	ERG11	8,41	0,000000	-	-	No
	ERG13	4,91	0,000000	0,574	1,1E-05	Yes
	ERG2	2,96	0,006752	-	-	No
	ERG24	3,32	0,001618	-	-	No
	ERG25	2,64	0,000193	-	-	No
	ERG251	4,66	0,000024	-	-	No
	ERG26	2,09	0,000224	-	-	No
	ERG3	6,95	0,000036	-	-	No
	ERG4	3,08	0,001412	-	-	No
	ERG5	3,05	0,000069	-	-	No
	ERG6	11,36	0,000028	1,31	9,99999E-07	Yes
	ERG9	2,57	0,0022424	-	-	No
	UPC2	3,47	0,000159	-	-	No

Table 30. Proteomic results. [a] fold expression from the previous genomic study. [b] fold expression from this proteomic study. [c] correlation between the genomic and proteomic studies: Yes means that proteins were correlated to the genes; No was the opposite and (/) means that some correlation was found between proteomic and genomic study at P value ≥0,05. Positive values: up-regulated; negative values: down-regulated.

	Gene	Fold expression (genomic)[a]	Adjusted P value	Fold expression (proteomic)[b]	Adjusted P value	Correlation[c]
Show changed transcript levels in response to antimycotics	CHT2	-3,90	0,000036	-0,704	0,000589504	Yes
	CRH11	2,02	0,006851	1,255	9,99999E-07	Yes
	CSH1	2,12	0,005475	-	-	No
	DDR48	13,84	0,000000	1,808	9,99999E-07	Yes
	FRP1	2,01	0,00082	-	-	No
	FTH1	2,03	0,000472	-	-	No
	HYR1	2,72	0,003792	0,591	0,000964819	Yes
	NHP6A	-2,04	0,001358	-0,303	0,023372078	/
	orf19.6688	-3,39	0,000147	-	-	No
	orf19.7504	2,46	0,007689	-	-	No
	orf19.3475	-2,20	0,046451	-0,481	7,80E-05	Yes
	orf19.3737	2,15	0,024789	-	-	No
	PGA7	2,46	0,000472	-	-	No
	PHR2	4,38	0,000116	0,103	0,444555445	/
	POL30	-2,00	0,006851	0,064	0,622377622	No
	RTA2	4,18	0,000312	-	-	No
	RTA3	3,18	0,030754	-	-	No

Table 31. Proteomic results. [a] fold expression from the previous genomic study. [b] fold expression from this proteomic study. [c] correlation between the genomic and proteomic studies: Yes means that proteins were correlated to the genes; No was the opposite and (/) means that some correlation was found between proteomic and genomic study at P value ≥0,05. Positive values: up-regulated; negative values: down-regulated.

	Gene	Fold expression (genomic)[a]	Adjusted P value	Fold expression (proteomic)[b]	Adjusted P value	Correlation[c]
Other functions	ARO10	-5,25	0,000734	-0,203	0,13643178	/
	CDG1	-2,04	0,000281	-0,493	0,011528734	Yes
	CHA1	-2,46	0,000734	-	-	No
	CIP1	-2,19	0,026148	-	-	No
	FAV1	2,04	0,028653	-	-	No
	GCV2	-2,18	0,010078	-0,312	0,015921852	/
	HSP31	-2,83	0,016218	-	-	No
	HTA2	-2,32	0,003792	-0,108	0,441558442	/
	MAL2	-2,96	0,000166	-0,658	9,99999E-07	Yes
	PGA23	5,5	0,000009	-	-	No
	PGA26	-3,35	0,00026	-	-	No
	PST3	2,1	0,000028	0,95	9,99999E-07	Yes
	RBT1	-2,63	0,000177	-	-	No
	SET3	3,19	0,000005	-	-	No

4.8. DISCUSSION – SECTION B

- **Chemistry**: **EMC120B12** analogues were synthesized following a method of parallel solid phase organic synthesis based on published procedures. Based on the main benzimidazole hit, **EMC120B12**, compound collections with different cores have been designed and synthesized using the scaffold hopping approach. The triazole compounds were successfully obtained in a two steps reaction in good yields. For the synthesis of the indole family it was necessary to modify the route because the described Grignard step was unsuccessful to obtain intermediate compound (**58**). The new modified route, starting from compound (**56**), allowed the synthesis of indole compounds (**IN1** – **IN7**).

  It was observed, that the functional groups of the most active compounds were similar. In position 2, all four active **EMC120B12** analogues contained a linear alkyl group substituent (Figure 60). Other analogues with a phenyl or methyl substituent (e.g. **BE14** or **BE1**) in that same position were not active. In position 1, the presence of fluoro or chloro in meta position in the phenyl substituent of the benzimidazole had stronger effect compared to analogues where the fluoro or chloro substituents were located in para position of the phenyl substituent (e.g. **BE3** or **BE4**).

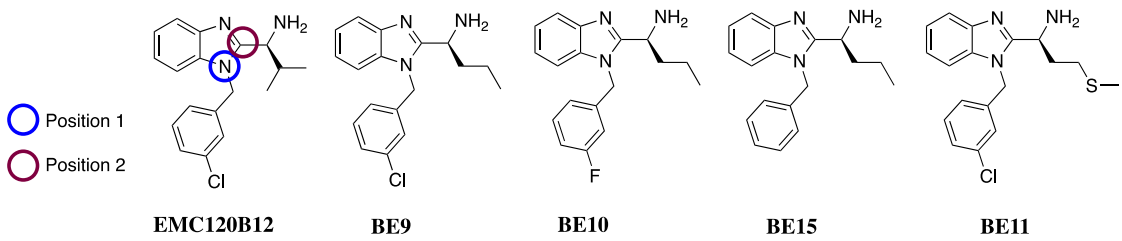

Figure 60. Structures and substitutions of the most active benzimidazole analogues.

The analogues with a phenyl ring in position 1 with no heteroatom substitution were active only if the substituent in position 2 was a linear alkyl group (e.g. **BE15** vs **BE14**). **BE15** was designed to compare the effect of the heteroatom in the phenyl substituent on the antifungal activity (**BE9** or **BE10**). The results showed that the linear alkyl substituent had more effect on the antifungal activity than the phenyl substituent, as **BE15** showed higher cell viability than **BE9**.

All compounds synthesized in this work were tested against *Candida* species and their antifungal activity was evaluated.

- **High-throughput screening**:

  - Benzimidazole: The investigation of 9 out of 16 benzimidazole compounds exhibited strong antifungal activity with more than 40 % of HeLa cell viability at 10 μM. All those hits with high percentage of HeLa cell viability were retested and evaluated in a dose-response assay in order to determine their IC_{50}, and CC_{50}.

  - Indole: The results from the screening at 10 μM revealed that none of the indole compounds tested was active against *Candida albicans*. The HeLa cell viability did not reach the 20 % cut off.

  - Triazole: These compounds showed no antifungal activity against *Candida albicans* at 10 μM. The HeLa cell viability was very low (20 %).

  - The two compounds, imidazo[1,2-a]pyridine and imidazo[1,2-a]pyrimidine were not active against *Candida albicans* at 10 μM.

  Indoles, triazole and imidazole compounds were not further studied.

- **Dose-response assay**: This assay confirmed the high antifungal activity of all benzimidazole compounds previously screened at the high-throughput screening at 10 μM (HTS).

  During the first dose-response assay with concentrations from 250 to 2 μM, positive control **EMC120B12**, **BE2**, **BE9**, **BE10** and **BE11** showed very high antifungal activity at the lowest concentration used (2 μM). **BE4**, **BE6** and **BE7** were not active enough (their cell viability was lower than 50 %) to be considered as an active compound and therefore, their IC_{50} was not calculated.

  To calculate the IC_{50} for the active ones, a second dose-response assay was carried out but in that case, the range of concentration was decreased (4 – 0.0.3125 μM). At concentration of 0.5 and 1 μM, **EMC120B12** and **BE2** reduced the growth of *Candida albicans*, but below those concentrations, the effect was marginal. **BE9**, **BE10** were very active at 0.25 and 0.5 μM with cell viability over 70 %. **BE11** was also active but at higher concentrations, 0.5 and 1 μM.

  A dose-response cytotoxicity assay was performed and it was observed that at lowest concentrations, the active compounds: **EMC120B12**, **BE2**, **BE9**, **BE10** and **BE11** were not toxic to HeLa cells except at highest concentrations (125 – 250 μM).

Table 32. Summary of % cell viability values for the compounds tested in an inhibitory and cytotoxicity dose-response assay. Only lowest concentrations can be visualized; (4, 2 and 1 μM) for the inhibitory assay and (7.8, 4 and 2 μM) for the cytotoxicity assay.

		Dose-Response					
		Inhibitory			Cytotoxicity		
		Concentration (μM)			Concentration (μM)		
		4	2	1	7.8	4	2
Compounds (% cell viability)	**EMC120B12**	74	67	36	80	93	93
	BE2	82	74	60	88	80	91
	BE4	22	7	-	79	83	91
	BE6	5	8	-	82	91	94
	BE7	65	26	-	81	86	96
	BE9	74	98	99	79	87	93
	BE10	76	77	78	80	89	98
	BE11	88	89	87	74	87	96

BE9, though, showed higher cytotoxicity, killing HeLa cells at 62.5 μM.

All their IC_{50} and CC_{50} were calculated (Table 26).

For compounds **BE4**, **BE6** and **BE7**, unlike the dose-response assay for inhibitory concentration, they showed to be not toxic to HeLa cells even at the highest concentration (125 – 250 μM). Either way, their IC_{50} and CC_{50} were not calculated.

- **Minimum inhibitory concentration (MIC)**: All four compounds (**EMC120B12**, **BE9**, **BE10** and **BE11**) were thoroughly active against the *C. albicans* SC5314 at low concentration. Compared to **EMC120B12**, the three analogues, **BE(9-11)**, were more active (0.5 – 1 μM).

  For the remaining fungi species, all four compounds inhibited the growth at the highest concentration (10 μM). **BE9** and **BE10** showed slightly more activity, shown by inhibiting the growth at concentrations (< 10 μM) (Table 33).

Table 33. Summary of the results from minimum inhibitory concentration (MIC) of compounds EMC120B12, BE9, BE10 and BE11 and for all *Candida* species tested.

	***Candida* species**	***albicans* SC5314**	***glabrata* ATCC2001**	***parapsilosis* ATCC22019**	***krusei* ATCC6258**
Compounds	EMC120B12	0.4 µg/ml (1.27 µM)	0.35 µg/ml (1.11 µM)	2 µg/ml (6.3 µM)	
	BE9	0.075 µg/ml (0.24 µM)	0.125 µg/ml (0.40 µM)	0.195 µg/ml (0.62 µM)	0.8 µg/ml (2.55 µM)
	BE10	0.090 µg/ml (0.3 µM)	0.230 µg/ml (0.77 µM)	0.47 µg/ml (1.58 µM)	0.90 µg/ml (3.02 µM)
	BE11	0.095 µg/ml (0.27 µM)	0.45 µg/ml (1.30 µM)	0.37 µg/ml (1.06 µM)	1.98 µg/ml (5.73 µM)

BE2, **BE 4**, **BE6** and **BE7** were active against all *Candida* species too, but at higher concentrations. Analogue **BE2** was more active at lowest concentration in comparison to other analogues (Table 34).

Table 34. Summary of the results from minimum inhibitory concentration (MIC) of compounds **BE2**, **BE6** and **BE7** for all *Candida* species tested.

	***Candida* species**	***albicans* SC5314**	***glabrata* ATCC2001**	***parapsilosis* ATCC22019**	***krusei* ATCC6258**
Compounds	BE2	0.97 µg/ml (3.1 µM)	2.0 µg/ml (6.37 µM)	3.2 µg/ml (10.2 µM)	4.2 µg/ml (13.4 µM)
	BE4	6.5 µg/ml (21.8 µM)	10 µg/ml (33.6 µM)		
	BE6	1.97 µg/ml (6.32 µM)	1.5 µg/ml (4.81 µM)	6.2 µg/ml (19.90 µM)	
	BE7	1.98 µg/ml (7.08 µM)	1.0 µg/ml (3.58 µM)	6.2 µg/ml (22.2 µM)	

The compounds (**BE1**, **BE3** and **BE14)** were active at highest concentrations and active against one *Candida* species (Table 35). **BE1** and **BE3** were active for *C.albicans* and **BE14** for *C.glabrata*.

Table 35: Summary of the results from minimum inhibitory concentration (MIC) of compounds **BE1**, **BE3** and **BE14** for all *Candida* species tested.

	***Candida* species**	***albicans* SC5314**	***glabrata* ATCC2001**	***parapsilosis* ATCC22019**	***krusei* ATCC6258**
Compounds	BE1	3.5 µg/ml (12.3 µM)	11.5 µg/ml (40.2 µM)	No activity	
	BE3	3.7 µg/ml (13.74 µM)	No activity		
	BE14	No activity	1.98 µg/ml (6.05 µM)	No activity	

- **Screening of clinical *Candida* spp isolates**: Only the active compounds in the MIC study were screened further against clinical Candida spp isolates. The selected compounds were **EMC120B12**, **BE (2, 6**, **7**, **9**, **10** and **11**) and they were tested with the minimum inhibitory concentration obtained from the previous study.
  As it had been shown in the previous assays, **BE9**, **BE10** and **BE11** gave a very strong response against *C. albicans*, *C. glabrata* and *C. parapsilosis*, inhibiting the growth of these fungi over 90 %. However, for *C. krusei*, the inhibition was in the range of 50-70 %. **EMC120B12** was also very active and gave good activity against all *Candida* species, inhibiting from 70 to 90 % of the fungi growth.
  BE2 and **BE7** showed inhibition over 90 % only for *C. albicans* and an inhibition between 70-90 % for *C. glabrata* and *C. parapsilosis*. For *C. krusei*, the inhibition was lower, between 60-70 %. **BE6** gave very good activity against *C. albicans* and *C. glabrata* (inhibition of the fungi growth between 70-90 %). However, for *C. parapsilosis* and *C. krusei*, the inhibition was not exceeding the 70 %.
  For all the compounds studied, the antifungal activity against other *Candida* species, like *C. lusitaniae* or *C. tropicalis*, among others, was very good, inhibiting at least over the 60 % of the fungi growth.

- **Proteomic study**: This assay was only carried out for the hit compounds **EMC120B12** and **BE10**. **BE10** was selected because it was the most active compound so far, even showing better results than the compound we used as a control, **EMC120B12**. The initial hit (**EMC120B12**) was chosen for the final proteomic study, to compare and/or confirm with the genomic study already published. [26] **BE10** was treated but was not further studied.
  The results showed that some proteins were upregulated correlating with the genes in the genomic study. Those genes were assigned to play a role in the ergosterol biosynthesis, to show changed transcript levels in response to antimycotics and also related to other functions.
  This first approach showed the presence of other proteins linked to the ergosterol biosynthesis that were not upregulated in the genomic study.
  In conclusion of this study, gene ontology (GO) analysis revealed that most of the upregulated genes (q value ≤0,05) were localized to the cell surface, the cell wall and

the plasma membrane, indicating that **EMC120B12** has strong impact on membrane and cell wall biosynthesis similar to some azoles like fluconazole.

On the opposite, the GO analysis for the downregulated genes, showed that they were located in the extracellular region and nucleus, indicating that **EMC120B12** does not have much effect on that regions.

CONCLUSIONS

5. CONCLUSIONS

In an effort to discover novel antifungal compounds, different peptides and heterocycles have been designed, synthesized and tested for their antifungal activity.

The conclusions reached in this thesis are the following:

- Several analogues of the peptide **LL-37** have been designed and synthesized using automated solid phase peptide synthesis (SPPS). These novel peptides have been studied for their antifungal activity. During the primary high-throughput screening (HTS) assay, only analogue **KS-30-NH2 (16)** gave remarkable activity. Minimum inhibitory concentration (MIC) for the **LL-37** peptide analogues was also determined. However, **(16)** did not show any positive results, whereas, analogues **FK-13**, **(31)** and **(32)** did inhibit the growth of all four *Candida* species used at the highest concentration.
- Several benzimidazole analogues from a previous hit, **EMC120B12** [20, 26] were synthesized following the procedures established at EMC microcollections GmbH. Eight out of fifteen benzimidazole analogues exhibited a very high activity against *Candida albicans, C.glabrata, C.parapsilosis and C.krusei*. From those active analogues **BE10** was the most active with an IC_{50} below 0.5 μM and a CC_{50} over 200 μM; **BE9** and **B11** were also active, but their IC_{50} and CC_{50} were higher than 0.5 μM and less than 200 μM, respectively and therefore, less active than **BE10**.

  BE15 showed activity at the HTS with cell viability almost 70 % at 10 μM.

  Different analogues of **EMC120B12** were synthesized by scaffold hopping. The heterocycles chosen were indole, triazole, imidazo[1,2-a]pyridine and imidazo[1,2-a]pyrimidine. All compounds were synthesized in solution phase combinatorial organic chemistry. Unfortunately, these compounds synthesized were not active against *Candida albicans* in the high-throughput screening (HTS) at 10 μM.

EXPERIMENTAL PART

6. EXPERIMENTAL PART

6.1. Section A – Chemical synthesis of LL-37 analogues

6.1.1. Materials

6.1.1.1. Solvents

All solvents used were reagent grade quality unless stated otherwise and used without further purification. Milli-Q water with a resistively superior to 18.2 MΩ/cm.

Solvent	Supplier
ACN	VWR
$CHCl_3$	Acros Organics
DCM	VWR
DMF peptide synthesis quality	Acros Organics
Et_2O technical grade	VWR
EtOH	Merck
H_2O (Milli-Q)	Millipore
MeOH quality HPLC	VWR

6.1.1.2. Reagents

Reagent	Supplier
Rink amide resin Chloro-(2'-chloro)trityl resin	Rapp Polymere
Ac_2O 98 %	Fluka
DIPEA 99 %	Acros Organics
DIC 99 %	Iris Biotech
DMSO 99 %	Acros Organics
HCl 37%	VWR
HOBt	Biosolve
NMP 99.5 %	Acros Organics
Ninhydrin	Merck
OxymaPure®	Iris Biotech
Piperidine	Acros Organics
TCTU 98 %	Iris Biotech
TFA technical grade	VWR
TFA HPLC grade	Fisher
TIS	Acros Organics

6.1.1.3. Instruments

Instrument	Supplier and Model
Centrifuge	Hettich, Universal 30 F
Lyophilizer	Christ, Alpha 1-4, Pump Edwards RV5
Sonicator	Elma, Transsonic T780/H
Spectrometer	Pharmacia Biotech, Ultrospec ® 2000
Peptide Synthesizer	Syro II, Dual robotic arm
RP-HPLC-MS	Waters Alliance 2795, Chromolith FastGradient RP-18e 50 x 2 mm column, 2489 UV detector and 3100 mass detector
HPLC-Analytical	Gilson 322 UV/VIS detector (ReproSil-Pur ODS (3-5 µm, 50 x 4.6 mm) column
HPLC-Preparative	Gilson 151 UV/VIS detector; reprospher C18 (5µm, 120 x 20 mm) column
Balance	Acculab Sartorius group Ohaus, Analytical Plus

6.1.2. Methods

6.1.2.1. Qualitative ninhydrin assay

This assay allows the qualitative evaluation of the efficiency of the couplings of the amino acids in solid phase peptide synthesis, by means of the colorimetric detection of the free amino groups in the N-terminal side of the growing peptide chain. In the assay three different reagents are used:

- Solution I: KCN solution (0.66 mg in 1 mL H_20) in pyridine (w/v)
- Solution II: Ninhydrin in ethanol (w/v) (2 g in 40 mL)
- Solution III: Phenol in ethanol (w/v) (30 g in 7.5 mL)

The assay is carried out by introducing, in an Eppendorf cup, some clean and dry beads with the polymer-bound peptide. One drop of each solution is added, and the mixture is heated at 105 °C for 3 min. Developing blue colour of the solution and the resin indicates the presence of free primary amino groups (positive assay), therefore the coupling is incomplete and it is necessary to repeat the coupling, while a yellow colour indicates the absence of free primary amino groups (negative assay) (reaction in Scheme 8).

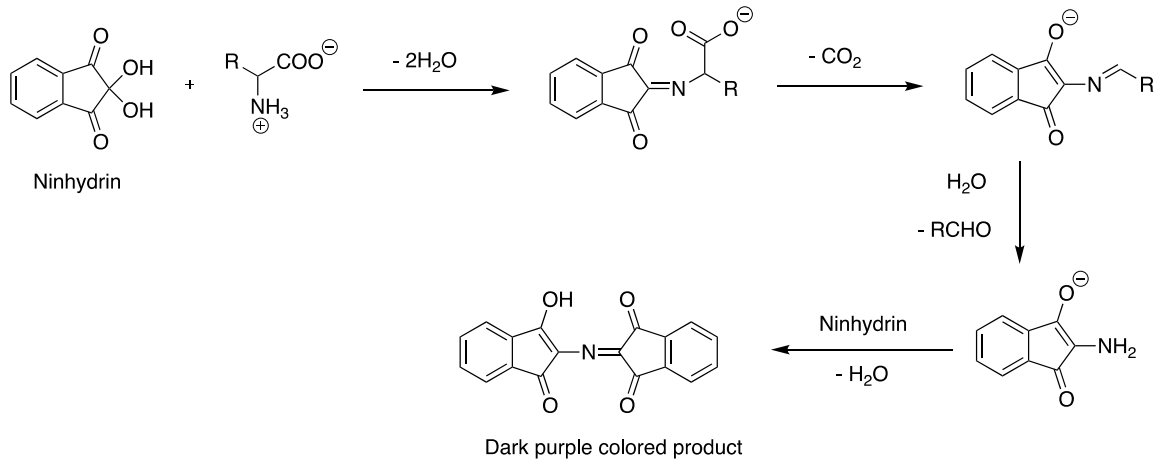

Scheme 8: Reaction between a free primary amino group and the ninhydrin to yield the blue compound Ruhemann's purple (positive assay).

6.1.2.2. Fmoc quantification

This quantification is used to determine the loading of the resin with the first amino acid. The resin (50 mg, 15 µmol) was swollen with DCM and DMF (3 mL). After filtration, Et_3N in DMF (3 mL) was added for 2 min and discarded. To the resin, the first amino acid (3 eq) of the sequence was dissolved in DMF (1 mL) and added, together with DIPEA (3 eq). The reactor with resin was left for 1.5 h with continuous shaking.

The resin was washed with DMF, MeOH, DCM and Et_2O (3x). Before quantifying the amount of Fmoc, the resin was very well dried and put into the desiccator for 2 h or overnight. A resin sample (8-12 mg) was transferred to a falcon tube and DMF with piperidine (30 %) (500 µl) was added and left for 45 min with constant shaking.

That solution (100 µl) was transferred to a new falcon tube and DMF (5900 µl) was added. The absorbance was obtained using a spectrometer and the concentration was calculated based on Lambert-Beer formula:

$$A = \varepsilon\, l\, c \;\rightarrow\; c = A/\varepsilon\, l$$

A = absorbance; ε = molar attenuation coefficient; c = concentration and l = path-length

The blank used corresponded to DMF with piperidine (30 %) (100 µl), diluted in DMF (5900 µl). This procedure was repeated 3 times.

The optimal concentration corresponded to >0.45 mmol/g. If the test showed concentration below 0.45 mmol/g, the coupling of the amino acid was repeated.

6.1.2.3. Solid Phase Peptide Synthesis (SPPS)

The peptides were synthesized using a fully automated parallel synthesizer (Syro II, MultiSynTech, Bochum, Germany) with a reactor block of 96 positions and a software control computer, which not only controls the instrument functions, but also calculates all amounts and volumes of required amino acids and reagents. The reactors were filled with Rink Amide or trityl resins (depending on the desired C-terminal end; Rink Amide for a C-terminal amide or trityl for a C-terminal carboxylic acid). The protocol used was previously optimized at EMC microcollections GmbH. The peptide synthesis was controlled during the synthesis after cleavage by HPLC-MS. 5 mg of resins were collected and a mixture of TFA/Reagent K^*/H_2O (80:15:5, v/v) (500 µL) was added for 1 h at room temperature. (* The Reagent K composition is: phenol (5 %, v/v), thioanisole (5 %, v/v) and 1,2-ethanedithiol (5 %, v/v).

The peptide was precipitated with Et_2O (1 mL) and the solvent was decanted. This procedure was repeated 3 times. The peptide was then lyophilized with tBuOH/H_2O (4:1, v/v) and analysed with HPLC-MS (214 nm).

Protocol for coupling - deprotection and washing steps:

Coupling Steps	Text/Command
1	Flush needle (DMF) for 1 cycle
2	Fill reactor with 40 µL reagent 3M DIPEA
3	Fill reactor with 60 µL reagent 3M DIC
4	Fill reactor with 200 µL building block (amino acid residue)
5	Hold for 50 min
6	Empty for 0.50 min into waste container
7	Wash system: DMF; 1 cycle 300 µL 0.50 min into waste container
8	Fill reactor with 40 µL reagent 3M DIPEA
9	Fill reactor with 100 µL building block (amino acid residue)
10	Fill reactor with 200 µL reagent TCTU
11	Hold for 60 min
12	Empty for 0.50 min into waste container
13	Wash system: DMF; 4 cycles 300 Fill reactor with 200 µL 0.50 min into waste container
14	Fill reactor with 200 µL reagent: Piperidine 30%
15	Hold for 5.0 min
16	Empty for 0.50 min into waste container
17	Wash system: DMF; 1 cycle 300 µL 0.50 min into waste container

18	Fill reactor with 300 µL reagent: Piperidine 30 %
19	Hold for 10 min
20	Empty for 0.50 min into waste container
21	Wash system: DMF; 8 cycles 300 µL 0.50 min into waste container

6.1.2.4. Cleavage and deprotection

The reactors were taken out from the Syro II synthesizer after synthesis and washed several times with diethyl ether. Cleavage and full deprotection of the linear peptides from the resin was carried out by acidolysis with a mixture of TFA/triisopropylsilane/H_2O (95:3:2, v/v) or TFA/Reagent K/H_2O (80:15:5, v/v) for 90 min. After cleavage, the resin was filtered off and washed with pure TFA and DCM (1 mL, 2x). The combined filtrates were evaporated to a reduced volume under a gentle stream of air. The crude peptide was precipitated with cold Et_2O (3 mL), centrifuged for 3 min (4800 rpm) and separated by decantation from the supernatant. This procedure was repeated 3 times. Before purification, the compounds were dissolved in a mixture of tBuOH/H_2O (4:1, v/v) and lyophilized.

6.1.2.5. RP-HPLC purification

The peptides were purified by preparative RP-HPLC. The instrument used was a Gilson 151 UV/VIS detector; Reprospher C18 (5µm, 120 x 20 mm) column, and the detection was carried out at 214 nm. The samples were eluted at a flow rate of 10 mL/min using linear gradients (0 – 100 %; 45 – 100 %; 30 – 75 %) of the following solvents:

A: H_2O – 0.1 % TFA

B: ACN – 0.1 % TFA

The peptides were characterized by analytical RP-HPLC and RP-HPLC-MS. The columns used were a ReproSil-Pur ODS (3-5 µm, 50 x 4.6 mm) for analytical HPLC and Chromolith FastGradient RP-18e (50 x 2 mm) with a 2489 UV detector and 3100 mass detector. The detections were carried out at 214 nm for both HPLCs.

The samples were eluted at a flow rate of 1 mL/min using linear gradient of the following solvents:

For RP-HPLC:	For RP-HPLC-MS:
A: H_2O – 0.1 % TFA	C: H_2O – 0.1 % FA
B: ACN – 0.1 % TFA	D: ACN – 0.1 % FA

6.2. SECTION B – Chemical synthesis of heterocyclic compounds

6.2.1. Materials

6.2.1.1. Solvents

All solvents used were reagent grade quality unless stated otherwise and used without further purification. Milli-Q water with a resistively superior to 18.2 MΩ/cm.

Solvent	Supplier
ACN 99 %	VWR
$CHCl_3$	Acros Organics
DCM technical grade	VWR
Dioxane	Acros Organics
DMF technical grade	Acros Organics
DMSO 99 %	Acros Organics
Et_2O technical grade	VWR
EtOH 99 %	Merck
H_2O (Milli-Q)	Millipore
MeOH 98 %	VWR
THF 99.9 %	Acros Organics
Toluene	Fisher

6.2.1.2. Reagents

All reagents used were of the maximum purity available

Reagent	Supplier
Wang resin	Rapp Polymere
2,6-lutidine	Fluka
2-aminopyridine	Acros Organics
2-iodoaniline	ChemPur
3-chlorobenzylamine	Alfa Aesar
3-fluorobenzylamine	Aldrich
4-chlorobenzylamine	Acros Organics
Ac_2O	Fluka
Boc_2O	Acros Organics
CDI	Fluka
Citric acid	Fluka
Cs_2CO_3	Fluka
CuI	Riedel-deHaen
DIPEA	Acros Organics

DIC	Iris Biotech
DMFDMA	Acros Organics
DSMO	Acros Organics
ECF	Fluka
EDC·HCl	Biotech
Et_3N	Fisher
HCl 37%	VWR
Hydrazine hydrate	Sigma Aldrich
HOBt	Biosolve
L-Pro	Fluka
MeNHOMe-HCl	Acros Organics
$NaHCO_3$	Acros Organics
NBS	Acros Organics
NMP	Acros Organics
Ninhydrin	Merck
Oxyma Pure	Sigma Aldrich
Piperidine	Acros Organics
PyBOP	Iris Biotech
TFA technical grade	VWR
TEA	Acros Organics
TIS	Acros Organics

6.2.2. Methods

6.2.2.1. General procedure for benzimidazoles

Syntheses of benzimidazoles were carried out by methods of parallel solid phase organic synthesis and following the protocol from EMC microcollections GmbH. [20] Activation of Wang resin (**77**) to *p*-nitrophenyl carbonate Wang resin (**40**) (Scheme 9) was achieved by addition of 4-nitrophenylchloroformate in DCM for 15 h. After washing the resin with DMF, MeOH, DCM and Et_2O (4x) and drying under high vacuum, 2-nitroaniline in presence of NaH was added to give the corresponding 2-nitrophenyl carbamates (**41**). Alkylation of the carbamate with the desired benzyl bromides using lithium tert-butoxide as a base gave the alkyl-(2-nitrophenyl) carbamate Wang resin (**42**). Analysis was done by HPLC-MS after cleavage of the intermediate from a small amount of resin (3 mg) (**42**) by TFA (25 %) in DCM . The nitro group was reduced by a solution of 1M of stannous chloride dihydrate in dry DMF to afford polymer bound carbamoyl anilines (**43**). Further acylation of the weakly nucleophilic aniline could be achieved most efficiently by PyBrOP mediated activation of N-

Fmoc-α- amino acids in the presence of DIPEA in NMP. Complete conversion of the anilines (**44**) was determined colorimetrically by treatment of the resin with ninhydrin (Kaiser test). Acidolytic cleavage (25 % TFA in DCM) and evaporation of the reagents provided N-Fmoc-α-amino acid anilides (**45**).

The N-α-protected benzimidazol-2-yl-alkylcarbamates (**46**) were obtained by heating (**45**) in glacial acetic acid at 80 °C for 16 h. Deprotection of the primary amino group by a mixture of piperidine/DCM afforded (S)-2-aminoalkyl-benzimidazoles **BE(1-15)**. The purification of the benzimidazoles was carried out by column chromatography using a mixture of DCM:MeOH (3-5 %) and monitored by TLC.

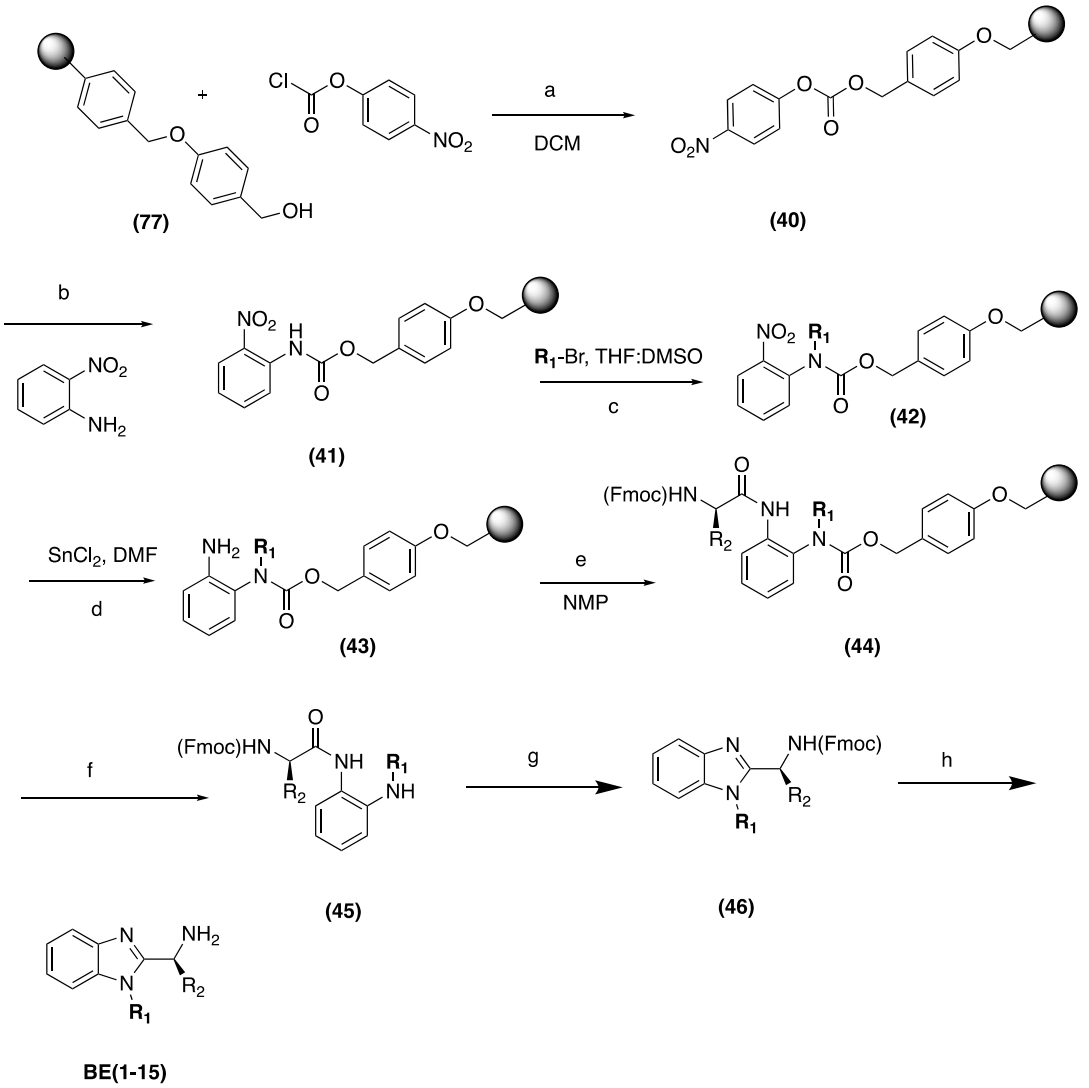

Scheme 9: Reagents and conditions: (a) 1.6 eq pyridine, 10 eq 4-nitrophenylchloroformate in DCM; (b) 3 eq NaH, DMF, 2.5 eq nitroaniline, 12h; (c) 5 eq alkylbromide, 8 eq LiO^tBu, THF/DMSO (1:1, v/v), 16h; (d) 1M $SnCl_2$ in DMF, 16 h; (e) 2.5 eq Fmoc-amino acid, 5 eq DIPEA, 2.5 eq PyBrOP, NMP, 16 h; (f) 25% TFA/DCM, 1 h; (g) HOAc, 80 °C, 16 h; (h) 5% piperidine, DCM, 2 h.

6.2.2.2. Wang resin activation (40)

Wang resin (77) (200 mg, 1.28 mmol·g^{-1}) was suspended in DCM (2.1 mL) at 0°C. Pyridine (33 µL, 0.40 mmol) and 4-nitrophenylchloroformate (516 mg, 2.56 mmol) were added dropwise. The suspension was stirred for 30 min at 0°C and 15 h at room temperature. The resin was washed with DMF, MeOH, DCM and Et_2O (4x) and dried under high vacuum.

6.2.2.3. Loading of Wang resin (41)

2-Nitroaniline (88.4 mg, 0.64 mmol) and a solution of NaH (18.4 mg 0.77 mmol) in DMF were added to p-nitrophenyl carbonate Wang resin (200 mg) (**40**) and stirred at room temperature 16 h.

The solution was washed with DMF until the washing solution was almost colorless. After washing, NH_4OH (25 % water) in DMF (1.5 mL per 100 mg of resin approximately) was added and shaken for 1 h at room temperature.

The resin (**41**) was washed with DMF, MeOH, THF, DCM and Et_2O (4x) and dried in an evacuated desiccator.

6.2.2.4. 3-Chlorobenzyl-(2-nitrophenyl)carbamate Wang resin (42)

3-Chlorobenzyl bromide (168 µL, 1.28 mmol) was added to a suspension of 2-nitrophenyl-carbamate Wang resin (**41**) in a mixture of dry THF and DMSO (3 mL, 1:1, v/v). Lithium tert-butoxide (164 mg, 2.04 mmol) was added and the suspension was agitated for 16 h at room temperature. The resin was collected by filtration, washed with DMF, MeOH, DCM and Et_2O (4x) and dried in an evacuated desiccator.
The intermediate (**42**) was analyzed using HPLC-MS (214 nm) after cleavage of a small amount (5 mg) of the resin with 25% TFA in DCM (1 h) followed by evaporating the solvents.

6.2.2.5. 3-Chlorobenzyl-(2-aminophenyl)carbamate Wang resin (43)

A 1M solution of stannous chloride dihydrate in dry DMF (3 mL) was added to the 3-chlorobenzyl (2-nitrophenyl)carbamate Wang resin (**42**) and the suspension was agitated for 16 h at room temperature. The resin (**43**) was collected by filtration, washed with DMF, MeOH, DCM and Et_2O (4x) and dried in high vacuum. The reduction was monitored by cleavage of a small amount (5 mg) of the intermediate compound (**43**) with 25% of TFA in DCM (1 h) evaporating the solvents and analyzed by HPLC-MS (214 nm).

6.2.2.6. 3-Chlorobenzyl-(2-(Fmoc-L-valylamino)phenyl)carbamate Wang resin (44)

Fmoc-L-valine (217 mg, 0.64 mmol), N,N-diisopropylethylamine (0.223 mL, 1.28 mmol) and PyBrOP (298 mg, 0.64 mmol) were dissolved in dry NMP (1.5 mL) and added to a suspension of 3-chlorobenzyl(2-aminophenyl)carbamate Wang resin (**43**) in dry NMP (2.25 mL). The suspension was agitated for 16 h in a shaker at room temperature. The resin (**44**) was collected by filtration, washed with DMF, MeOH, DCM and Et_2O (4x) and dried in high vacuum for at 4.5 h. The complete acylation was proven by chloranil test of a small amount of resin (2-5 mg) and it was observed that the resin (in contrast to a non-acylated control sample) did not show the typical blue-stained resin beads indicating the conversion of the aniline.

6.2.2.7. (9*H*-Fluoren-9-yl)methyl (*R*)-(1-((2-((3-chlorobenzyl)amino)phenyl)amino)-3-methyl-1-oxobutan-2-yl)carbamate (45)

3-Chlorobenzyl(2-(Fmoc-L-valylamino)phenyl)carbamate Wang resin (200 mg) (**44**) was suspended in 25 % TFA in DCM (3.2 mL). The suspension was agitated for 1 h and then filtrated. The resin was washed with DCM and MeOH (5 mL, 3x) and all the filtrates were combined. Solvents were removed by evaporation and the crude product (**45**) was lyophilized from tert-butylalcohol/water (4:1 v/v) to yield a pale yellow solid.
Yield: 64 %, $C_{33}H_{32}ClN_3O_3$, MW: 554 g/mol

6.2.2.8. (9*H*-Fluoren-9-yl)methyl (*S*)-(1-(1-(3-chlorobenzyl)-1*H*-benzo[*d*]imidazol-2-yl)-2-methylpropyl)carbamate (46)

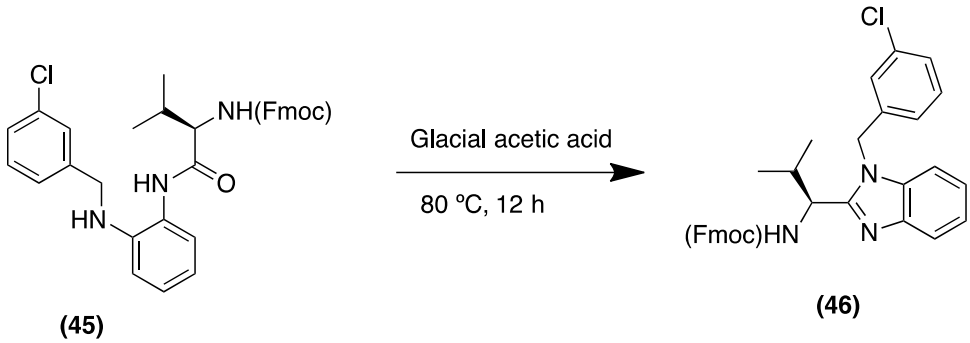

(45) **(46)**

Compound **(45)** (74.7 mg, 0.13 mmol) was dissolved in glacial acetic acid (3 mL) and heated at 80 °C for 16 h. Solvents were removed by evaporation and the crude product **(46)** was lyophilized from tert-butylalcohol/water (4:1, v/v) to yield a dark oil.

6.2.2.9. (*S*)-2-(1-Aminoisobutyl)-1-(3-chlorobenzyl)benzimidazole (EMC120B12)

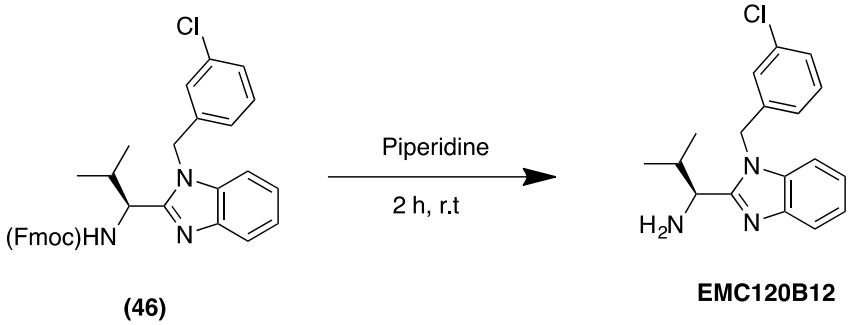

(46) **EMC120B12**

(9*H*-Fluoren-9-yl)methyl(*S*)-(1-(1-(3-chlorobenzyl)-1*H*-benzo[*d*]imidazol-2-yl)-2-methylpropyl) carbamate (74.7 mg, 0.14 mmol) (**46**) was dissolved in DCM (6.1 mL). Piperidine (303 µL, 3.03 mmol) was added and the reaction was stirred for 2 h at room temperature. Solvents were removed by evaporation and the crude product (**EMC120B12**) was purified by column chromatography (silica gel, 3 % of MeOH in DCM) to yield the pure compound.

Yield: 65 %; brown solid; 97% purity; Rf (3 % MeOH/DCM)= 0.24, $C_{18}H_{20}ClN_3$, MW: 313.83 g/mol; HPLC-ESI-MS, 214 nm: $[M+H]^+$ = 314 m/z.

^{1}H-NMR (400 MHz, $CDCl_3$) δ 0.66 (d, 3H), 1.22 (d, 3H), 2.95 (m, 1H), 4.22 (d, 1H), 5.42 (dd, 2H), 6.95-6.90 (m, 2H), 7.32-7.21 (m, 5H), 7.80 (d, 1H).

6.2.2.10. EMC120B12 analogues

(*S*)-2-(1-Aminoethyl)-1-(4-chlorobenzyl)benzimidazole (BE1)

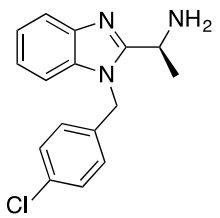

BE1

(*S*)-2-(1-Aminoethyl)-1-(4-chlorobenzyl)benzimidazole (**BE1**) was synthesized analogously to compound **EMC120B12**. Purification by chromatography on silica gel; MeOH (3 %) in DCM.

Yield: 85 %; Pale brown solid; DCM:MeOH (3 %) Rf = 0.3, $C_{16}H_{16}ClN_3$, MW: 285.78 g/mol, purity: 91 % (HPLC-ESI-MS, 214 nm), $[M+H]^+$ = 286 m/z

^{1}H-NMR (400 MHz, $CDCl_3$) δ 1.55 (d, 3H), 2.36 (m, 1H), 5.27 (dd, 2H), 6.93-6.91 (m, 3H), 7.26-7.21 (m, 4H), 7.76 (d, 1H).

(*S*)-2-(1-Aminoisobutyl)-1-(4-chlorobenzyl)benzimidazole (BE2)

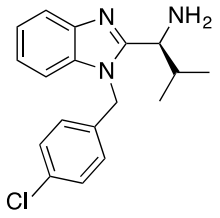

BE2

(*S*)-2-(1-Aminoisobutyl)-1-(4-chlorobenzyl)benzimidazole (**BE2**) was synthesized analogously to compound **EMC120B12**. Purification by chromatography on silica gel; MeOH (3 %) in DCM.

Yield: 66 %; Brown solid; MeOH (3 %) in DCM Rf = 0.24, $C_{18}H_{20}ClN_3$, MW: 313.83 g/mol, purity: 96 % (HPLC-ESI-MS, 214 nm), $[M+H]^+$ = 314 m/z.

^{1}H-NMR (400 MHz, $CDCl_3$) δ 0.64 (d, 3H), 0.94 (d, 3H), 2.23 (m, 1H), 4.48 (d, 1H), 5.46 (dd, 2H), 7.02-7.05 (m, 2H), 7.18-7.22 (m, 2H), 7.26-7,3 (m, 3H), 7.68 (d, 1H).

(*S*)-2-(1-Aminoethyl)-1-(4-fluorobenzyl)benzimidazole (BE3)

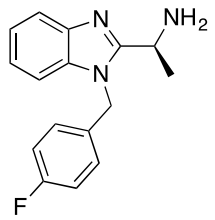

BE3

(*S*)-2-(1-Aminoethyl)-1-(4-fluorobenzyl)benzimidazole (**BE3**) was synthesized analogously to compound **EMC120B12**. Purification by chromatography on silica gel; MeOH (3 %) in DCM.

Yield: 82 %; Pale brown solid; MeOH (3 %) in DCM Rf = 0.38, $C_{18}H_{20}FN_3$, MW: 297.38 g/mol, purity: 91 % (HPLC-ESI-MS, 214 nm), $[M+H]^+$ = 298 m/z.

^{1}H-NMR (400 MHz, $CDCl_3$) δ 1.42 (d, 3H), 2.66 (m, 1H), 5.45 (dd, 2H), 7.03-6.98 (m, 2H), 7.13-7.05 (m, 2H), 7.31-7.27 (m, 3H), 7.76 (d, 1H).

(*S*)-2-(1-Aminoisobutyl)-1-(4-fluorobenzyl)benzimidazole (BE4)

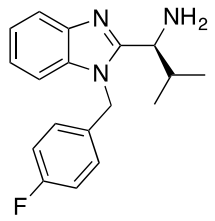

BE4

(*S*)-2-(1-Aminoisobutyl)-1-(4-fluorobenzyl)benzimidazole (**BE4**) was synthesized analogously to compound **EMC120B12**. Purification by chromatography on silica gel; MeOH (3 %) in DCM.

Yield: 76 %; Brown solid; MeOH (3 %) in DCM Rf = 0.25, $C_{16}H_{16}FN_3$, MW: 269.32 g/mol, purity: 96 % (HPLC-ESI-MS, 214 nm), $[M+H]^+$= 270 m/z.

^{1}H-NMR (400 MHz, $CDCl_3$) δ 0.42 (d, 3H), 1.11 (d, 3H), 2.45 (m, 1H), 4.63 (d, 1H), 5.47 (dd, 2H), 7.24-7.17 (m, 2H), 7.33-7.29 (m, 3H), 7.64-7,57 (m, 2H), 7.79 (d, 1H).

(*S*)-2-(1-Aminoethylindolyl)-1-(3-chlorobenzyl)benzimidazole (BE5)

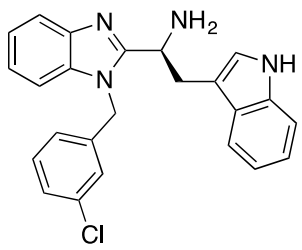

BE5

(*S*)-2-(1-Aminoethylindolyl)-1-(3-chlorobenzyl)benzimidazole (**BE5**) was synthesized analogously to compound **EMC120B12**. Purification by chromatography on silica gel; MeOH (3 %) in DCM.

Yield: 25 %; Dark brown solid; MeOH (4 %) in DCM Rf = 0.27, $C_{24}H_{21}ClN_4$, MW: 400.91 g/mol, purity: 76 % (HPLC-ESI-MS, 214 nm), $[M+H]^+$ = 401 m/z.

(*S*)-2-(1-Aminoisopentyl)-1-(3-fluorobenzyl)benzimidazole (BE6)

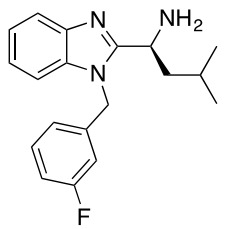

BE6

(*S*)-2-(1-Aminoisopentyl)-1-(3-fluorobenzyl)benzimidazole (**BE6**) was synthesized analogously to compound **EMC12012**. Purification by chromatography on silica gel; MeOH (3 %) in DCM.

Yield: 77 %; Pale brown solid; MeOH (3 %) in DCM Rf = 0.21, $C_{19}H_{22}FN_3$, MW: 311.41 g/mol, purity: 97 % (HPLC-ESI-MS, 214 nm), $[M+H]^+$ = 312 m/z.

^{1}H-NMR (400 MHz, $CDCl_3$) δ 0.63 (d, 3H), 0.69 (d, 3H), 1.32 (m, 1H), 1.58 (dd, 2H), 4.36 (t, 1H), 5.22 (dd, 2H), 6.87-7.03 (m, 2H), 7.13-7.09 (m, 2H), 7.26-7,37 (m, 3H), 7.72 (d, 1H).

(*S*)-2-(1-Aminoisobutyl)-1-(benzyl)benzimidazole (BE7)

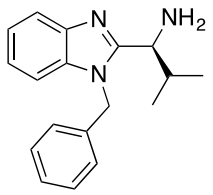

BE7

(*S*)-2-(1-Aminoisobutyl)-1-(benzyl)benzimidazole (**BE7**) was synthesized analogously to compound **EMC120B12**. Purification by chromatography on silica gel; MeOH (3 %) in DCM.

Yield: 74 %; Brown solid; MeOH (3 %) in DCM Rf = 0.22, $C_{18}H_{21}N_3$, MW: 279.39 g/mol, purity: 81 % (HPLC-ESI-MS, 214 nm), $[M+H]^+$ = 280 m/z.

^{1}H-NMR (400 MHz, $CDCl_3$) δ 0.89 (d, 3H), 1.11 (d, 3H), 2.33 (m, 1H), 4.37 (d, 1H), 5.36 (dd, 2H), 7.27-7.23 (m, 2H), 7.52-7.31 (m, 6H), 7.61 (d, 1H).

(*S*)-2-(1-Aminoisopentyl)-1-(3-chlorobenzyl)benzimidazole (BE8)

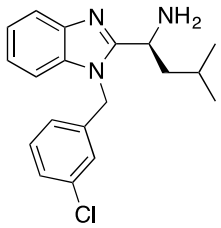

BE8

(*S*)-2-(1-Aminoisopentyl)-1-(3-chlorobenzyl)benzimidazole (**BE8**) was synthesized analogously to compound **EMC120B12**. Purification by chromatography on silica gel; MeOH (3 %) in DCM.

Yield: 73 %; Brown solid; MeOH (3 %) in DCM Rf = 0.28, $C_{19}H_{22}ClN_3$, MW: 327.86 g/mol, purity: 92 % (HPLC-ESI-MS, 214 nm), $[M+H]^+$ = 328 m/z.

(*S*)-2-(1-Aminobutyl)-1-(3-chlorobenzyl)benzimidazole (BE9)

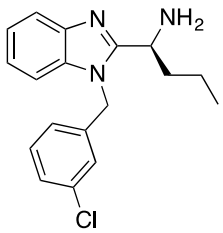

BE9

(*S*)-2-(1-Aminobutyl)-1-(3-chlorobenzyl)benzimidazole (**BE9**) was synthesized analogously to compound **EMC120B12**. Purification by chromatography on silica gel; MeOH (3.5 %) in DCM.

Yield: 55 %; Pale brown solid; MeOH (3.5 %) in DCM Rf = 0.31, $C_{18}H_{20}ClN_3$, MW: 313.16 g/mol, purity: 99 % (HPLC-ESI-MS, 214 nm), $[M+H]^+$ = 314 m/z.

^{1}H-NMR (400 MHz, $CDCl_3$) δ 0.74 (t, 3H), 1.27-1.21 (m, 2H), 1.65 (dt, 2H), 4.10 (t, 1H), 5.47 (dd, 2H), 6.91-6.89 (m, 2H), 7.20-7.16 (m, 2H), 7.48-7.32 (m, 3H), 7.80 (d, 1H).

(*S*)-2-(1-Aminobutyl)-1-(3-fluorobenzyl)benzimidazole (BE10)

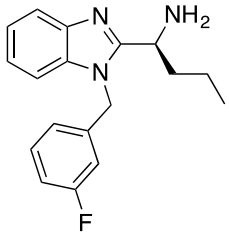

BE10

(*S*)-2-(1-Aminobutyl)-1-(3-fluorobenzyl)benzimidazole (**BE10**) was synthesized analogously to compound **EMC120B12**. Purification by chromatography on silica gel; MeOH (3 %) in DCM.

Yield: 51 %; Pale brown solid; MeOH (3 %) in DCM Rf = 0.24, $C_{18}H_{20}FN_3$, MW: 298 g/mol, purity: 95 % (HPLC-ESI-MS, 214 nm), $[M+H]^+$ = 299 m/z.

^{1}H-NMR (400 MHz, $CDCl_3$) δ 0.86 (t, 3H), 1.33-1.21 (m, 2H), 1.80 (dt, 2H), 4.12 (t, 1H), 5.48 (dd, 2H), 6.80 (dd, 2H), 6.96 (dt, 1H), 7.30-7.20 (m, 4H), 7.78 (d, 1H).

(*S*)-2-(1-Aminomethylthiopropyl)-1-(3-chlorobenzyl)benzimidazole (BE11)

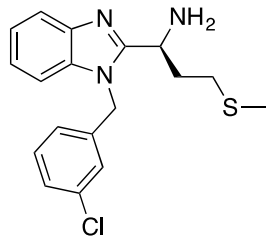

BE11

(*S*)-2-(1-Aminomethylthiopropyl)-1-(3-chlorobenzyl)benzimidazole (**BE11**) was synthesized analogously to compound **EMC120B12**. Purification by chromatography on silica gel; MeOH (4 %) in DCM.

Yield: 31 %; Dark brown solid, MeOH (4 %) in DCM Rf = 0.26, $C_{18}H_{20}ClN_3S$, MW: 345.90 g/mol, purity: 97 % (HPLC-ESI-MS, 214 nm), $[M+H]^+$ = 346 m/z.

^{1}H-NMR (400 MHz, $CDCl_3$) δ 0.91 (s, 3H), 2.22-2.14 (m, 2H), 2.5 (dt, 2H), 4.51 (t, 1H), 5.46 (dd, 2H), 6.95 (d, 2H), 7.32-7.21 (m, 5H), 7.79 (d, 1H).

(*S*)-2-(1-Amino-4-hydroxiphenylethyl)-1-(3-chlorobenzyl)benzimidazole (BE12)

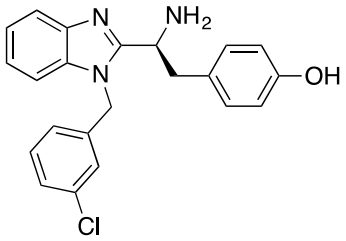

BE12

(*S*)-2-(1-Amino-4-hydroxiphenylethyl)-1-(3-chlorobenzyl)benzimidazole (**BE12**) was synthesized analogously to compound **EMC120B12**. Purification by chromatography on silica gel; MeOH (3 %) in DCM.

Yield: 34 %; Pale brown solid, MeOH (3 %) in DCM Rf = 0.17, $C_{22}H_{20}ClN_3O$, MW: 377.88 g/mol, purity: 98 % (HPLC-ESI-MS, 214 nm), $[M+H]^+$ = 378 m/z.

(*S*)-2-(1-Aminoethyl)-1-(benzyl)benzimidazole (BE13)

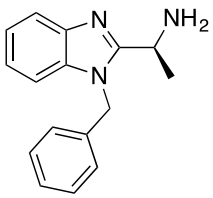

BE13

(*S*)-2-(1-Aminoethyl)-1-(benzyl)benzimidazole (**BE13**) was synthesized analogously to compound **EMC120B12**. Purification by chromatography on silica gel; MeOH (3.5 %) in DCM.

Yield: 86 %; Pale brown solid; MeOH (3.5 %) in DMC Rf = 0.13, $C_{16}H_{17}N_3$, MW: 251.33 g/mol, purity: 92 % (HPLC-ESI-MS, 214 nm), $[M+H]^+$ = 252 m/z.

^{1}H-NMR (400 MHz, $CDCl_3$) δ 1.23 (d, 3H), 3.99 (q, 1H), 5.33 (dd, 2H), 7.21-7.17 (m, 2H), 7.62-7.29 (m, 6H), 7.77 (d, 1H).

(*S*)-2-(1-Aminobenzylmethyl)-1-(benzyl)benzimidazole (BE14)

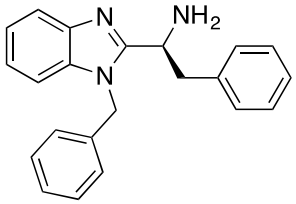

BE14

(*S*)-2-(1-Aminobenzylmethyl)-1-(benzyl)benzimidazole (**BE14**) was synthesized analogously to compound **EMC120B12**. Purification by chromatography on silica gel; MeOH (3.5 %) in DCM.

Yield: 46 %; Pale yellow solid; MeOH (3.5 %) in DCM Rf = 0.27, $C_{22}H_{21}N_3$, MW: 327.43 g/mol, purity: 96 % (HPLC-ESI-MS, 214 nm), $[M+H]^+$ = 328 m/z.

^{1}H-NMR (400 MHz, $CDCl_3$) δ 3.06 (dd, 2H), 4.28 (t, 1H), 5.21 (dd, 2H), 6.96 (dd, 2H), 7.06 (dd, 3H), 7.28-7.21 (m, 8H), 7.83 (d, 1H).

(*S*)-2-(1-Aminobutyl)-1-(benzyl)benzimidazole (BE15)

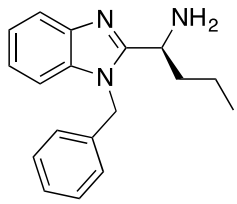

BE15

(*S*)-2-(1-Aminobutyl)-1-(benzyl)benzimidazole (**BE15**) was synthesized analogously to compound **EMC120B12.** Purification by chromatography on silica gel; MeOH (3.5 %) in DCM.

Yield: 73 %; Pale brown solid; MeOH (3.5 %) in DCM Rf = 0.21, $C_{18}H_{21}N_3$, MW: 279.39 g/mol, purity: 96 % (HPLC-ESI-MS, 214 nm), $[M+H]^+$ = 280 m/z.

^{1}H-NMR (400 MHz, $CDCl_3$) δ 0.81 (t, 3H), 1.32-1.22 (m, 2H), 1.85 (dt, 2H), 4.21 (t, 1H), 5.57 (dd, 2H), 7.01 (dd, 2H), 7.33 (dt, 1H), 7.21-7.16 (m, 5H), 7.58 (d, 1H).

6.2.2.11. Boc protection

Boc_2O (0.588 mL, 1.2 eq, 2.56 mmol, **80**) and Et_3N (0.862 mL, 2.9 eq, 6.2 mmol) were added to L-valine (250 mg, 2.13 mmol, **79**) in a single-necked, round-bottomed flask, diluted in dioxane:H_2O (1:1, 10 mL) and the mixture was left stirring for 18 h at room temperature. The solution was extracted with petroleum ether and the aqueous phase was cooled on ice and carefully acidified to pH = 3 by addition of 10 % citric acid aqueous solution. The organic phase was extracted with EtOAc (8 mL, 3x) and the combined extracts were washed with sat. NaCl (2x), dried with Na_2SO_4, filtered and concentrated under reduced pressure to give the protected α-amino acid (**81**) in 83 % yields.

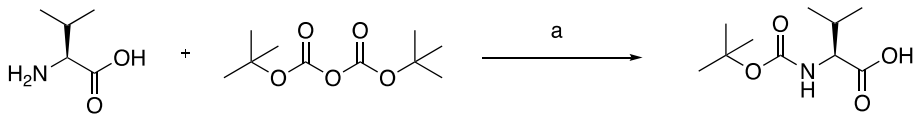

(79) **(80)** **(81)**

Scheme 10: Conditions: a) Et_3N (2.9 eq), Boc_2O (1.2 eq), dioxane:H_2O (1:1), 18 h, room temperature

6.2.2.11.1. Preparation of 4-Boc-amino-3-ketoester (54)

CDI (1.1 g, 1.35 eq, 6.2 mmol) was added to a stirred solution of Boc-valine (1 g, 4.6 mmol) in THF at room temperature under Ar atmosphere for 40 min. A freshly prepared solution of lithium tert-butoxycarbonylmethanide (**78**) was prepared in parallel by addition of nBuLi (16.6 mL, 4.2 eq, 179.8 mmol) with a syringe to a solution of diisopropylamine (6 mL, 42.8 mmol) in dry THF (8 mL), under argon and cooled to 0 ºC. This mixture was stirred at 0 ºC for 10 min and then cooled to -78 ºC. Tert-butyl acetate dissolved in dry THF was added dropwise by syringe and the resulting mixture was stirred for 15 min.

The acyl imidazole solution prepared previously was then added dropwise to the pale yellow solution of the lithium enolate at -78 ºC under Ar. The reaction mixture was stirred for 40 min and then the reaction was quenched with 1 N HCl (10 mL). After extraction with EtOAc (2x), the combined organic extracts were washed with brine (3x), dried over Na_2SO_4, filtered and concentrated by rotary evaporation to provide the Boc-amino-3-ketoester. The crude product *tert*-butyl (*S*)-4-((*tert*-butoxycarbonyl)amino)-5-methyl-3-oxohexanoate (**54**) was purified by chromatography on a colum using cyclohexane:EtOAc (4:1) as solvents. Yield: 67 %.

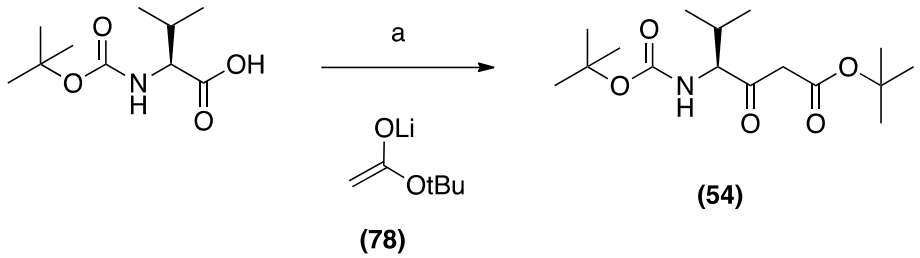

Scheme 11: Conditions: a) CDI (1.35 eq), THF, 40 min at room temperature; BuLi (4.2 eq), DIPA (1 eq), TBAc (1 eq), under Ar, 40 min, -78 ºC.

6.2.2.12. General procedure for indoles (IN1-IN7)

A solution of the corresponding β-ketoester intermediate (**54**) (100 mg, 1 eq, 0.32 mmol) in dry DMSO (5 mL) was treated with 2-iodoaniline (69.5 mg, 1 eq, 0.32 mmol), CuI (12 mg, 0.2 eq, 0.06 mmol), L-Pro (14.6 mg, 0.4 eq, 0.12 mmol) and Cs_2CO_3 (103.3 mg, 1 eq, 0.32 mmol) and stirred at 50 °C for 12 h (Scheme 12). The reaction mixture was neutralized with 1M HCl (8 mL) and extracted with EtOAc (2x). The organic phase was washed with brine (3x) and dried over Na_2SO_4, the solvent was evaporated and the crude material (**55**) was purified by precipitation (Petroleum Ether:EtOAC). After purification, the ester and also Boc were cleaved by an acidic mixture composed of TFA/DCM/TIS/H_2O (80:20:5:1) for 1 h at room temperature to yield the indole intermediate **55a**. **55a** was again protected, following

procedure explained in **6.2.2.11.** to obtain the protected indole intermediate (**56**) in 86 % yield. Without any previous purification and in a single-necked, round-bottomed flask, (**56**) (100 mg, 0.3 mmol) was charged with EDC·HCl (63.4 mg, 1.1 eq, 0.33 mmol) and dissolved in DCM/DMF (1:1) (5 mL). The colourless solution of the carbodiimide was then stirred at room temperature for approximately 20 min to allow complete dissolution of the reactant, followed by cooling in an ice bath to 0 °C. Then, the indole intermediate (**56**) and Oxyma (Pure) (47 mg, 1.1 eq, 0.33 mmol) were added to the cold solution of EDC·HCl. Two min after the addition of the reactants, the corresponding substituted amine was added to the preactivated (**56**), followed by addition of DIPEA (63 μL, 1.2 eq, 0.57 mmol) and allowed to stir in an ice bath for 1 h. To assure a complete coupling, Oxyma and DIPEA were again added and the reaction was left overnight at room temperature. After 14-15 h, the solvent was removed and the crude oily residue was diluted in chloroform and transferred to a separatory funnel. The organic solution was extracted and washed with 1 N HCl, sat. Na_2CO_3 and saturated NaCl. The resulting pale yellow organic fraction was dried over Na_2SO_4, filtered and concentrated by rotary evaporation. The amino group (**59**) was deprotected with a mixture composed of TFA/DCM/TIS/H_2O (80:20:5:1). Finally, the crude products (**IN(1-7)**) were purified by column chromatography with DCM:MeOH (4 %) as a eluents.

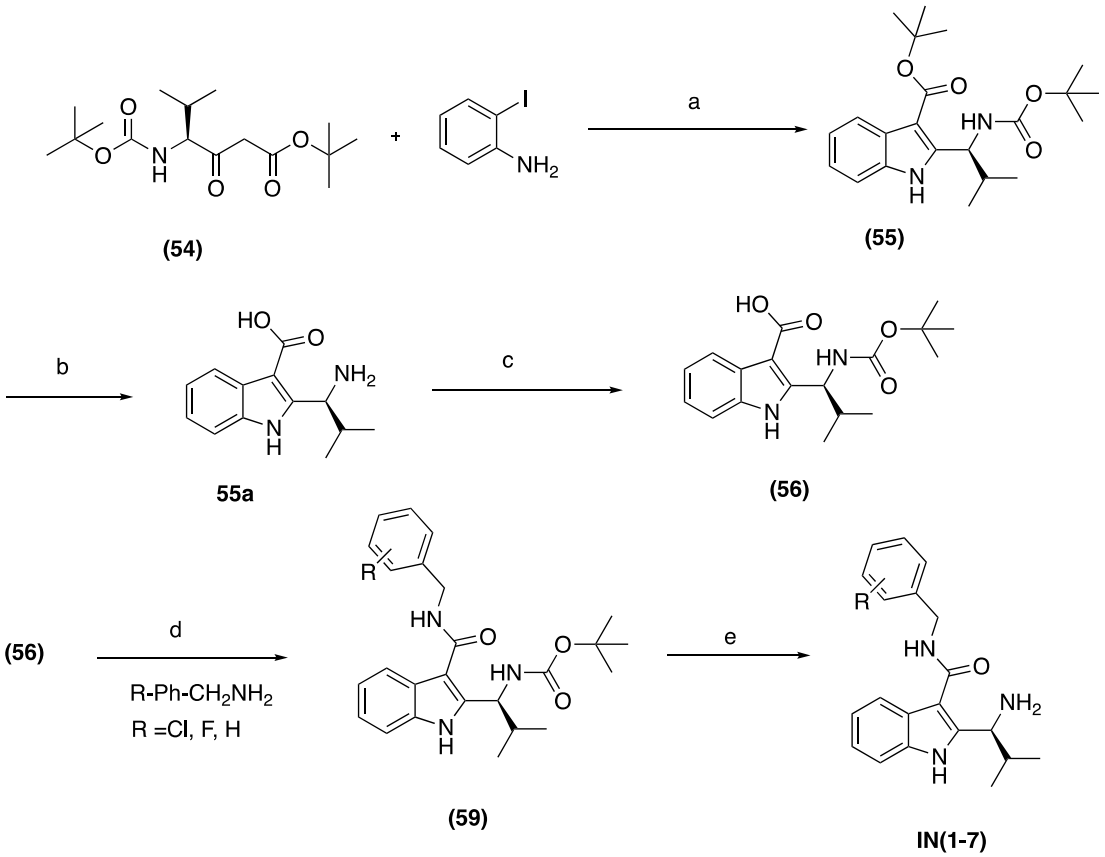

Scheme 12: Conditions: a) CuI (0.2 eq), Cs_2CO_3 (1 eq), L-Pro (0.4 eq) in dry DMSO, 50 ºC overnight, b) Mixture: TFA/DCM/TIS/H_2O (80/20/5/1), 1 h, room temperature, c) Boc_2O (1 eq), Et_3N (2.9 eq), dioxane:H_2O (1:1), 18 h at room temperature, d) EDC:HCl (1.1 eq), Oxyma Pure (1.1 eq), DCM:DMF (1:1), R-NH_2 (1.1 eq), DIPEA (1.2 eq), 0 ºC for 1 h, and then overnight at room temperature, e) Mixture: TFA/DCM/TIS/H_2O (80/20/5/1), 1 h, room temperature.

6.2.2.12.1. Indole analogues

(*S*)-2-(Aminoisobutyl)-3-(carboxylic acid)indole (55a)

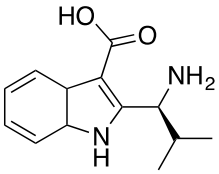

55a

(*S*)-2-(Aminoisobutyl)-3-(carboxylic acid)indole (**55a**) was obtained as described in 6.1.2.1.4.4. Purified by precipitation EtOAc/Cyclohexane. Yield: 65 %, Brownish oil; $C_{13}H_{18}N_2O_2$, MW: 234.14 g/mol; purity: 98 % (HPLC-ESI-MS, 214), $[M+H]^+$ = 235 m/z.

^{1}H-NMR (400 MHz, $CDCl_3$) δ 0.86 (d, 3H), 1.03 (d, 3H), 1.24-1.13 (m, 1H), 4.83 (d, 1H), 7.25-7.20 (m, 2H), 7.50 (d, 1H), 8.05 (d, 1H), 12.27 (s, 1H).

(*S*)-2-(Aminoisobutyl)-3-(N-3-chlorobenzylcarbamoyl)indole (IN1)

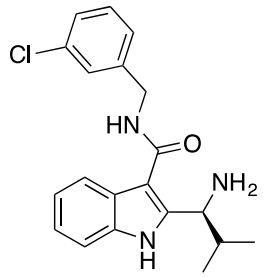

IN1

(*S*)-2-(Aminoisobutyl)-3-(N-3-chlorobenzylcarbamoyl)indole (**IN1**) was obtained as described in **6.2.2.12**. Purification by silica gel chromatography MeOH (3.5 %) in DCM.
Yield: 85 %; Green oil; MeOH (3.5 %) in DCM; Rf = 0.21, $C_{20}H_{22}ClN_3O$, MW: 355.87 g/mol; purity: 94 % (HPLC-ESI-MS, 214 nm), $[M+H]^+$ = 356 m/z.
^{1}H-NMR (400 MHz, $CDCl_3$) δ 0.91 (d, 3H), 1.01 (d, 3H), 1.17-1.11 (m, 1H), 4.66 (d, 1H), 4.88 (dd, 2H), 7.10-7.06 (m, 2H), 7.22-7.14 (m, 2H), 7.66-7.32 (m, 3H), 7.81 (d, 1H).

(*S*)-2-(Aminoisobutyl)-3-(N-3-fluorobenzylcarbamoyl)indole (IN2)

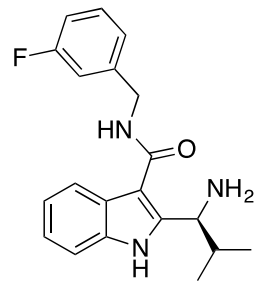

IN2

(S)-2-(Aminoisobutyl)-3-(N-3-fluorobenzylcarbamoyl)indole (**IN2**) was obtained as described in **6.2.2.12**. Purification by silica gel chromatography MeOH (3.5 %) in DCM.
Yield: 66 %; Dark green oil; MeOH (3.5 %) in DCM; Rf = 0.15, $C_{20}H_{22}FN_3O$, MW: 339.41 g/mol; purity: 95 % (HPLC-ESI-MS, 214 nm), $[M+H]^+$ = 340 m/z.

(*S*)-2-(Aminoisobutyl)-3-(N-benzylcarbamoyl)indole (IN3)

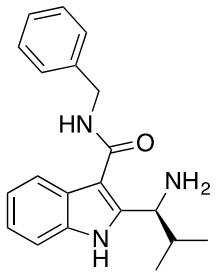

IN3

(*S*)-2-(Aminoisobutyl)-3-(N-benzylcarbamoyl)indole (**IN3**) was obtained as described in **6.2.2.12**. Purification by silica gel chromatography MeOH (3.5 %) in DCM.

Yield: 82 %; Pale green oil; MeOH (3-4 %) in DCM; Rf = 0.37, $C_{20}H_{23}N_3O$, MW: 321.42 g/mol; purity: 98 % (HPLC-ESI-MS, 214 nm), $[M+H]^+$ = 322 m/z.

(*S*)-2-(Aminoisobutyl)-3-(N-4-chlorobenzylcarbamoyl)indole (IN4)

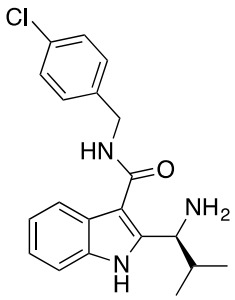

IN4

(*S*)-2-(Aminoisobutyl)-3-(N-4-chlorobenzylcarbamoyl)indole (**IN4**) was obtained as described in **6.2.2.12**. Purification by silica gel chromatography MeOH (3 %) in DCM.

Yield: 76 %; Dark green oil; MeOH (3 %) in DCM; Rf = 0.26, $C_{20}H_{22}ClN_3O$, MW: 355.87 g/mol; purity: 93 % (HPLC-ESI-MS, 214 nm), $[M+H]^+$ = 356 m/z.

^{1}H-NMR (400 MHz, $CDCl_3$) δ 0.97 (d, 3H), 1.10 (d, 3H), 1.22-1.15 (m, 1H), 4.73 (d, 1H), 5.26 (dd, 2H), 7.13-7.10 (m, 2H), 7.21-7.16 (m, 2H), 7.61-7.39 (m, 3H), 7.77 (d, 1H).

(*S*)-2-(Aminoisobutyl)-3-(N-3-fluorobenzylcarbamoyl)indole (IN5)

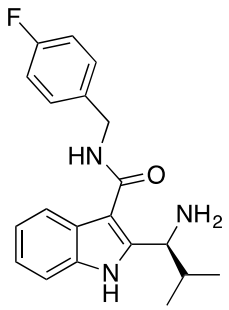

IN5

(*S*)-2-(Aminoisobutyl)-3-(N-3-fluorobenzylcarbamoyl)indole (**IN5**) was obtained as described in **6.2.2.12**. Purification by silica gel chromatography MeOH (3.5 %) in DCM.
Yield: 26 %; Dark brown oil; MeOH (3.5 %) in DCM; Rf = 0.32, $C_{20}H_{22}FN_3O$, MW: 339.41 g/mol; purity: 96 % (HPLC-ESI-MS, 214 nm), $[M+H]^+$ = 340 m/z.

(*S*)-2-(Aminoisobutyl)-3-(N-2,4-dichlorobenzylcarbamoyl)indole (IN6)

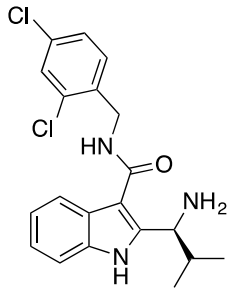

IN6

(*S*)-2-(Aminoisobutyl)-3-(N-2,4-dichlorobenzylcarbamoyl)indole (**IN6**) was obtained as described in **6.2.2.12**. Purification by silica gel chromatography MeOH (4 %) in DCM.
Yield: 77 %; Dark brown oil; MeOH (4 %) in DCM; Rf = 0.26, $C_{20}H_{21}Cl_2N_3O$, MW: 390.31 g/mol; purity: 95 % (HPLC-ESI-MS, 214 nm), $[M+H]^+$ = 391 m/z.

(*S*)-2-(Aminoisobutyl)-3-(N-3,5-difluorobenzylcarbamoyl)indole (IN7)

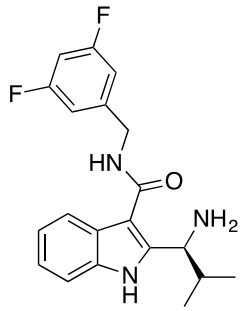

IN7

(*S*)-2-(Aminoisobutyl)-3-(N-3,5-difluorobenzylcarbamoyl)indole (**IN7**) was obtained as described in **6.2.2.12**. Purification by silica gel chromatography MeOH (4 %) in DCM.

Yield: 74 %; Brown oil; MeOH (4 %) in DCM; Rf = 0.28, $C_{20}H_{21}F_2N_3O$, MW: 357.40 g/mol; purity: 89 % (HPLC-ESI-MS, 214 nm), $[M+H]^+$ = 358 m/z.

6.2.2.13. General procedure for triazoles (TR1-TR8)

Syntheses of triazoles were carried out as follows (Scheme 13**)**: The first step was the protection of an α-amino acid (100 mg) with Boc. The conditions are described above in **6.2.3.** [113] Activation of (**64**) by Et_3N (1.05 eq), ethyl chloroformate (ECF, 1.05 eq) in THF (at - 20 ºC. The $Et_3N{\cdot}HCl$ formed during the reaction was filtered off), led to intermediate anhydrides (**65**) which were immediately reacted with $NH_2NH_2{\cdot}H_2O$ (2 eq) in MeOH (5 mL) at 0 ºC and left to warm up to room temperature, to yield the hydrazides (**66**). The solvents were evaporated and EtOAc (8 mL) was added. The organic phase was washed with $NaHCO_3$ (sat) (3x) and NaCl (sat) (3x), dried over $MgSO_4$ and concentrated to afford the N-protected amino acid hydrazides (**66**) in 75-90 % yield. Triazole formation (**67**) was carried out by stirring the hydrazides in ACN (6 mL) and DMF-DMA (1 eq) at 50 ºC for 1 h. A substituted amine (0.91 eq) was added in ACN (3 mL) and HOAc (10 eq). The temperature was increased from 50 to 120 ºC and the reaction mixture was left for 2.5 h, cooled, concentrated by evaporation of the solvents. The N-protected group was cleaved with a mixture composed of TFA/DCM/TIS/H_2O (80:20:5:1) for 1 h to give the triazole compounds **TR(1-8)**. Purification was carried out on silica gel eluting with DCM:MeOH (3-5 %). The compounds were obtained in 65-85 % yield.

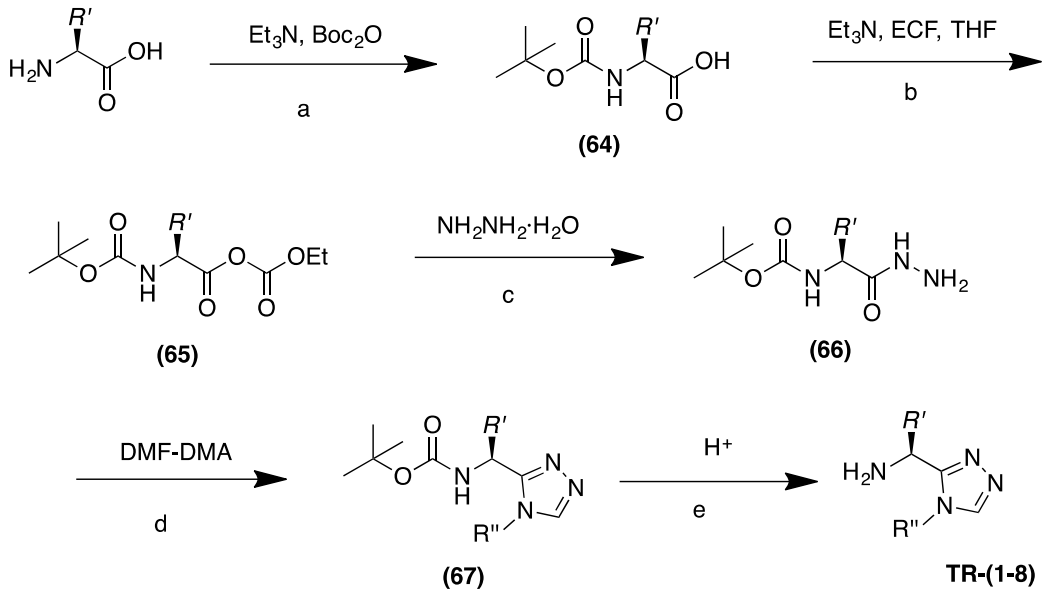

Scheme 13: Reagents and conditions: a) 2.9 eq Et_3N, 1.2 eq Boc_2O, dioxane:H_2O (1:1), r.t, 18 h. b) Et_3N (1.05 eq), ECF (1.05 eq), THF, 0 ºC, 1 h. c) $NH_2NH_2 \cdot H_2O$ (2 eq), MeOH, 0 ºC to r.t. d) i) DMF-DMA (1 eq), ACN, 50 ºC, 1 h. ii) Substituted amine (0.91 eq), ACN, HOAc (10 eq), 120 ºC, 2.5 h. f) Deprotection conditions: TFA/DCM/TIS/H_2O (80:20:5:1).

6.2.2.13.1. Triazole analogues

(*S*)-3-(Aminoisobutyl)-4*H*-(3-chlorobenzyl)triazole (TR1)

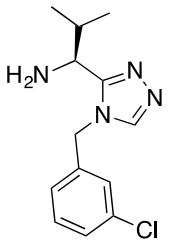

TR1

(*S*)-3-(Aminoisobutyl)-4*H*-(3-chlorobenzyl)triazole (**TR1**) was synthesized as it was described in **6.2.2.13**. Purification by silica gel chromatography MeOH (2 %) in DCM.

Yield: 65 %; Grey oil; MeOH (2 %) in MeOH, Rf = 0.38, $C_{13}H_{17}ClN_4$, MW: 264.76 g/mol

Purity: 97 % (HPLC-ESI-MS, 214 nm), $[M+H]^+$ = 265 m/z.

^{1}H-NMR (400 MHz, $CDCl_3$) δ 0.81 (d, 3H), 0.94 (d, 3H), 1.63-1.47 (m, 1H), 4.33 (d, 1H), 5.46 (dd, 2H), 7.11 (d, 1H), 7.25 (d, 1H), 7.41 (dd, 2H), 8.79 (s, 1H).

(*S*)-3-(Aminobutyl)-4*H*-(3-chlorobenzyl)triazole (TR2)

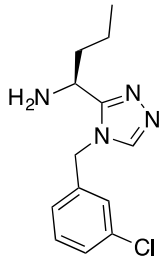

TR2

(*S*)-3-(Aminobutyl)-4*H*-(3-chlorobenzyl)triazole (**TR2**) was synthesized as it was described in **6.2.2.13**. Purification by silica gel chromatography MeOH (2 %) in DCM.

Yield: 87 %; Pale gray oil; MeOH (2 %) in DCM Rf = 0.18, $C_{13}H_{17}ClN_4$, MW: 264.76 g/mol

Purity: 97 % (HPLC-ESI-MS, 214 nm), $[M+H]^+$ = 265 m/z.

^{1}H-NMR (400 MHz, $CDCl_3$) δ 0.75 (t, 3H), 0.89-0.85 (m, 2H), 1.87 (dt, 2H), 4.74 (t, 1H), 5.29 (dd, 2H), 7.13 (d, 1H), 7.20 (d, 1H), 7.37 (dd, 2H), 8.48 (s, 1H).

(*S*)-3-(Aminobutyl)-4*H*-(3-fluorobenzyl)triazole (TR3)

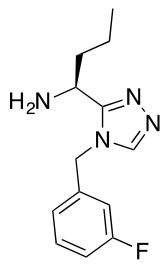

TR3

(*S*)-3-(Aminobutyl)-4*H*-(3-fluorobenzyl)triazole (**TR3**) was synthesized as it was described in **6.2.2.13**. Purification by silica gel chromatography MeOH (2 %) in DCM.

Yield: 88 %; Gray oil; MeOH (2 %) in DCM Rf = 0.22, $C_{13}H_{17}FN_4$, MW: 264.76 g/mol

Purity: 98 % (HPLC-ESI-MS, 214 nm), $[M+H]^+$ = 265 m/z.

^{1}H-NMR (400 MHz, $CDCl_3$) δ 0.66 (t, 3H), 0.87-0.84 (m, 2H), 1.79 (dt, 2H), 4.71 (t, 1H), 5.31 (dd, 2H), 7.11 (d, 1H), 7.18 (d, 1H), 7.29 (dd, 2H), 8.51 (s, 1H).

(*S*)-3-(Aminomethylthiopropyl)-4*H*-(3-chlorobenzyl)triazole (TR4)

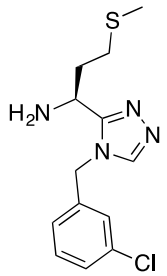

TR4

(*S*)-3-(Aminomethylthiopropyl)-4*H*-(3-fluorobenzyl)triazole (**TR4**) was synthesized as it was described in **6.2.2.13**. Purification by silica gel chromatography MeOH (3.5 %) in DCM.
Yield: 89 %; Gray oil; MeOH (3.5 %) in DCM Rf = 0.26, $C_{13}H_{17}ClN_4$, MW: 296.82 g/mol
Purity: 94 % (HPLC-ESI-MS, 214 nm), $[M+H]^+$ = 297 m/z.
^{1}H-NMR (400 MHz, $CDCl_3$) δ 0.78 (s, 3H), 0.88 (t, 2H), 1.83 (dt, 2H), 4.79 (t, 1H), 5.46 (dd, 2H), 7.09 (d, 1H), 7.15 (d, 1H), 7.32 (dd, 2H), 8.46 (s, 1H).

(*S*)-3-(Aminoisopentyl)-4*H*-(3-fluorobenzyl)triazole (TR5)

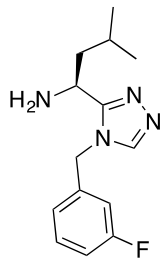

TR5

(*S*)-3-(Aminoisopentyl)-4*H*-(3-fluorobenzyl)triazole (**TR5**) was synthesized as it was described in **6.2.2.13**. Purification by silica gel chromatography MeOH (2 %) in DCM.
Yield: 71 %; Pale gray oil; MeOH (2 %) in DCM Rf = 0.33, $C_{14}H_{19}FN_4$, MW: 262.33 g/mol
Purity: 95 % (HPLC-ESI-MS, 214 nm), $[M+H]^+$ = 293 m/z.

(*S*)-3-(Aminoisobutyl)-4*H*-(benzyl)triazole (TR6)

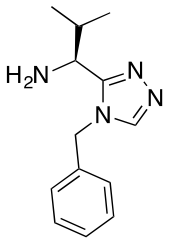

TR6

(*S*)-3-(Aminoisobutyl)-4*H*-(benzyl)triazole (**TR6**) was synthesized as it was described in **6.2.2.13**. Purification by silica gel chromatography MeOH (2 %) in DCM.

Yield: 54 %; Pale gray oil; MeOH (2 %) in DCM Rf = 0.17, $C_{13}H_{18}N_4$, MW: 230.32 g/mol

Purity: 93 % (HPLC-ESI-MS, 214 nm), $[M+H]^+$ = 231 m/z.

^{1}H-NMR (400 MHz, $CDCl_3$) δ 0.87 (d, 3H), 0.93 (d, 3H), 1.66-1.44 (m, 1H), 4.41 (d, 1H), 5.41 (dd, 2H), 7.16 (d, 1H), 7.32 (d, 2H), 7.48 (dd, 2H), 8.81 (s, 1H).

(*S*)-3-(Aminoisobutyl)-4*H*-(4-chlorobenzyl)triazole (TR7)

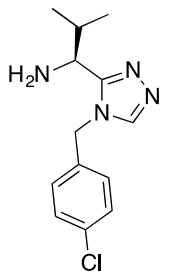

TR7

(*S*)-3-(Aminoisobutyl)-4*H*-(4-chlorobenzyl)triazole (**TR7**) was synthesized as it was described in **6.2.2.13**. Purification by silica gel chromatography MeOH (2.5 %) in DCM.

Yield: 77 %; Gray oil; MeOH (2.5 %) in DCM Rf = 0.26, $C_{13}H_{17}ClN_4$, MW: 264.76 g/mol

Purity: 97 % (HPLC-ESI-MS, 214 nm), $[M+H]^+$ = 265 m/z.

(*S*)-3-(Aminoethyl)-4*H*-(4-fluorobenzyl)triazole (TR8)

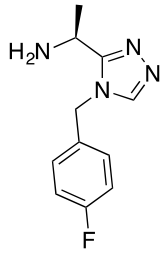

TR8

(*S*)-3-(Aminoethyl)-4*H*-(4-fluorobenzyl)triazole (**TR8**) was synthesized as it was described in **6.2.2.13**. Purification by silica gel chromatography MeOH (2.5 %) in DCM.

Yield: 85 %; Pale gray oil; MeOH (2.5 %) in DCM Rf = 0.23, $C_{11}H_{13}FN_4$, MW: 220.25 g/mol. Purity: 96 % (HPLC-ESI-MS, 214 nm), $[M+H]^+$ = 221 m/z.

6.2.2.14. Synthesis of *tert*-butyl (4*S*)-2-bromo-4-((*tert*-butoxycarbonyl)amino)-5-methyl-3-oxohexanoate (75)

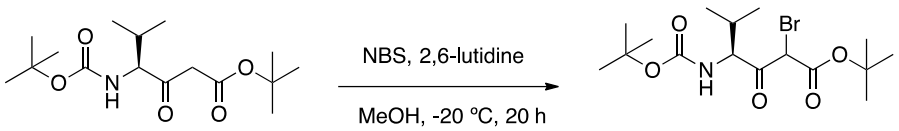

(54) **(75)**

The starting reagent **(54)** (200 mg, 1 eq, 0.63 mmol) was brominated with N-bromosuccinimide (90.3 mg, 0.8 eq, 0.5 mmol) in a solution of 2,6-lutidine (7.5 µL, 10 mol %, 0.063 mmol) in MeOH (7 mL) and stirred for 2.5 h at room temperature. Then, the solution was cooled at -20 ºC for 20 h. The reaction mixture was extracted with 50 % saturated NaCl (3x) and saturated NaCl (3x), dried over Na_2SO_4 and the solvents were evaporated to give the 2-bromo-β-ketone ester as crude product **(75)**. It was purified by silica gel chromatography with cyclohexane:EtOAc (4:1) as eluents and obtained in yield 77 %. The core intermediate **(75)** was used for the synthesis of compounds **ImPn1** and **ImPm1**.

Rf = 0.21, $C_{16}H_{28}BrNO_5$, MW: 393.12 g/mol. Purity: 89 % (HPLC-ESI-MS, 214 nm), $[M+H]^+$ = 394 m/z.

6.2.2.15. Synthesis of (*S*)-2-(Aminoisobutyl)-3-(carboxylic acid)imidazo[1,2-*a*]pyridine (ImPn1)

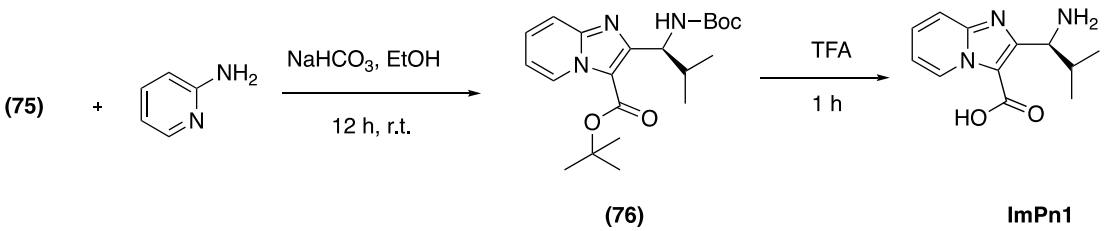

Compound (**75**) (95 mg, 1 eq, 0.24 mmol) was dissolved in EtOH (10 mL). 2-Aminopyridine (18.2 mg, 0.8 eq, 0.2 mmol) and $NaHCO_3$ (13.2 mg, 0.65 eq, 0.15 mmol) were added and the solution was stirred for 12 h at room temperature. The solution was evaporated in vacuo and destilled water (5 mL) was added to the residue and extracted twice with $CHCl_3$. This solution was washed with brine (2x) and dried over Na_2SO_4. The filtrate (**76**) was evaporated in vacuo. Cleavage of Boc protecting group was carried out with a mixture of TFA/DCM/TIS/H_2O (85/20/5/1) to give the crude product **ImPn1**. The compound was purified by silica gel chromatography using MeOH (4 %) in DCM as eluents.

Yield: 54 %; Rf = 0.26, $C_{12}H_{15}N_3O_2$, MW = 233.12 g/mol

Purity: 73 % (HPLC-ESI-MS, 214 nm), $[M+H]^+$ = 234 m/z.

6.2.2.16. Synthesis of (*S*)-2-(Aminoisobutyl)-3-(carboxylic acid)imidazo[1,2-*a*]pyrimidine (ImPm1)

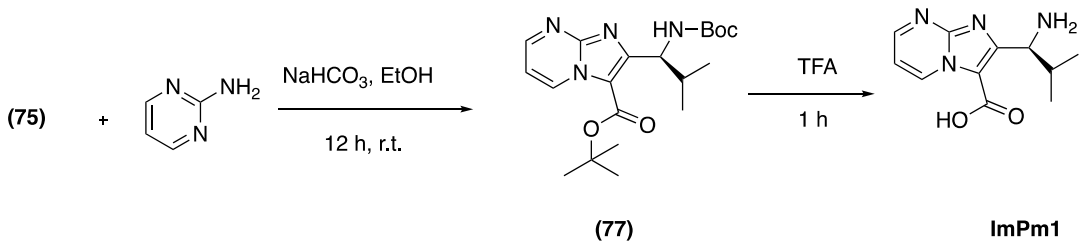

Compound (**75**) (90 mg, 1 eq, 0.22 mmol) was dissolved in EtOH (10 mL). 2-aminopyrimidine (17.4 mg, 0.8 eq, 0.18 mmol) and $NaHCO_3$ (12.5 mg, 0.65 eq, 0.14 mmol) were added and the solution was stirred for 12 h at room temperature. The solution was evaporated in vacuo and deionized water (5 mL) was added to the residue and extracted twice with $CHCl_3$. This solution was washed with brine (2x) and dried over Na_2SO_4. The filtrate

(**77**) was evaporated in vacuo. Cleavage of Boc protecting group was carried out with a mixture of TFA/DCM/TIS/H_2O (85/20/5/1) to give the crude product **ImPm1**. The compound was purified by silica gel chromatography using MeOH (4 %) in DCM as eluent.

Yield: 56 %; Rf = 0.28, $C_{11}H_{14}N_4O_2$, MW: 234.26 g/mol

Purity: 61 % (HPLC-ESI-MS, 214 nm), $[M+H]^+$ = 235 m/z.

6.3. Antifungal screenings

6.3.1. Materials

6.3.1.1. Reagents

All reagents used were of the maximum purity available.

Reagent	Supplier
RPMI medium	Invitrogen
FBS (fetal bovine serum)	Lonza
YPD medium	Home made
Propidium Iodide (PI)	---
DHR (dihydrorhodamine)	Sigma Aldrich
Tris-HCl	Invitrogen
EDTA (Ethylenediaminetetraacetate acid)	Panreac
NaCl	Panreac
DTT (dithiothreitol)	AppliChem
Phosphate-buffered saline (PBS)	Thermo Scientific
phenylmethane sulfonyl fluoride **(**PMSF)	Sigma Aldrich
Protease Inhibitors	Thermo Scientific
Coomassie Blue staining	Biorad
Tetramethylethylenediamine (TEMED)	Sigma Aldrich
Sodium dodecyl sulfate (SDS)	Duchefa Biochemie
Ammonium persulfate (APS)	Amersham Bioscience
Acrylamide-Bis-Acrylamide	Panreac
β-Mercaptoethanol	Sigma Aldrich
Bromophenol blue	Panreac
YP (Yeast peptone)	VWR international
FDA (Fluorescein diacetate)	---

6.3.1.2. Instruments

Instrument	Supplier and Model
Centrifuge	Eppendorf 5810R
Sonicator	P-selecta
Spectrometer	Beckman DU 640
Bead beater	Millipore
Incubator	Infors HT
Fluoresence microscope	Nikon MicroscopyU
Microlayout machine	Victor^3

6.3.2. Methods

6.3.2.1. Primary high-throughput screening

For HeLa cell culture, the following medium was used: RPMI 1640 medium with 10 % heat inactivated fetal calf serum (FCS), 2 mM L-glutamine and penicillin/streptomycin (P/S).

Remarks: FCS is a common additive in most cell cultures and provides growth factors, hormones and other essential nutrients. Heat inactivation consists of heating the serum at 56 ºC for 30 min to destroy components of the complement system. L-Glutamine tends to degrade in the medium; therefore it is always supplemented with some fresh extra L-glutamine when opening a new bottle of medium. P/S is another common additive used routinely in cell culture, to prevent microbial infections. For this assay, HeLa cells were cultivated initially with P/S, and medium without P/S was used when the test compounds were added, to avoid any interference.

- Medium preparation:

  FBS was thawed in a warm water bath, homogenizing the solution from time to time by gently inverting the tube. P/S and L-glutamine were also thawed but at room temperature.

  From a 500 ml RPMI 1640 medium bottle, 60 ml were removed (which could be discarded or saved for posterior use) and 50 ml of PBS as added. Then, 5 ml of P/S and 5 ml o fL-glutamine were added.

- Splitting the cells (passaging):

  Splitting the cells, in case of HeLa and other adherent cell lines (cells that attach to the bottom of the flask), means detaching them from the bottom of the flask. The protocol followed was: addition of trypsin, accutase, collagenase or other enzymatic/non-enzymatic agent, diluting and transferring them to a larger flask.

  Before to start the procedure it was necessary to inspect the flask visually to make sure it was not contaminated meaning that the medium should not be cloudy. Also, the confluency was checked under the microscope, to be almost 100 % confluent.

  The medium was aspirated from the flask with disposable glass pipette; the flask was washed with 10 ml PBS (37 ºC or room temperature) and the PBS aspirated. Addition then of 1 ml of one-time trypsin solution as cell detaching agent. After making sure that the whole surface of the flask was covered by trypsin solution, the flask was put back in the incubator and checked it after 10 min. To help to detach the cells, the flask

was shacked by tapping gently at the side of the flask. The flask was put into the incubator at 37 ºC to assure all cells were detached.

Afterwards, 5 ml of media was added to stop the trypsinization and the cells were moved up and down a few times with pipette to dissolve clumps of cells. 500 µl of that cell suspension was transferred to an Eppendorf tube and the cells were counted.

Then, the required volume of cell suspension was transferred to a new flask (1 million cells); the volume was completed up to 10 ml with medium, gently homogenized and put it in the incubator at 37 ºC.

- Counting the cells with CASY:
    - 10 ml of CASY ton buffer was added to a disposable counting vial.
    - 100 µl of cell suspension was added to the vial, mixed by inverting 3 times.
    - The vial then was placed under the capillary and "start" bottom was pressed. In the current settings of that equipment, the value given was the number of cells per ml. If the sample was too concentrated, only 50 µl of cell suspension was used.
- Preparation of stock solutions

  As the compounds to be tested were already weighed and stored into Eppendorf tubes, the diluent required to obtain a standard solution was calculated for a final 10 µM concentration.

  The compounds were diluted in DMSO into the calculated volume to obtain the desired stock solution.
- Preparation of working solution

  From the stock solution, the calculated amount necessary to obtain a final concentration of 20 µM was pipetted.

  From that working solution, 20 µl were pipetted and transferred to the well-plate.

- First day of assay:

  The assay was performed in a 96- well tissue culture plate, with a total volume of 200 µl per well (50 µl of cells solution + 50 µl of fungus solution + 100 µl of screening compound solution). The procedure was simply to add all the components (cell + fungus + drug) to the well and then incubated the plate for 5 days at 37 ºC in a 5 % CO_2 humidified incubator (standard cell culture condition).

In addition to all test compounds, three controls were necessary in this assay: cell viability control, fungus control and drug control. The cell viability control contained only HeLa cells; the fungus control contained HeLa cells + fungus, but no drug and the drug control contained HeLa cells + fungus + the drug amphotericin B.
Everything was done in RPMI 10 % FC and 1 % L-glutamine (no antibiotics)

- HeLa cells: 10.000 cells per well (50 µl of a 200.000 cells /ml suspension
- Test compound: 50 µM (100 µl of a 100 µM stock solution
- Fungi: 50 CFU per well (50 µl of a 1000 CFU/ml suspension)
- Drug control: amphotericin B at 1 µg/ml (100 µl of a 2 µg/ml stock solution)

Layout of the 96 well-plate:

	1	2	3	4	5	6	7	8	9	10	11	12
A	Cell viability control	Fungus control										
B												
C												
D												
E		Drug control										
F												
G												
H												
I												

- Read-out of the plate (after 5 days)

  To assess the reading of cell viability, a spectrofluorometer was used and the dye fluorescein diacetate (FDA) excitation and emission wave-length was: 485 nm, and 538 nm, respectively.

  FDA stock solution was diluted in DMSO to a concentration of 10 mg/ml.

  Afterwards, the FDA working solution was diluted in PBS: 1:1000 dilutions from the stock.

  The cells were washed with PBS (2x 100 µl), 100 µl of FDA working solution was added per well and the reading was performed.

6.3.2.2. Dose-Response assay

This assay followed exactly the same protocol as the highthrough put screening. The difference in this case, was that instead of working with only one concentration, a range of concentrations was done from 250 to 0.1953 µM.

6.3.2.3. Minimum inhibitory concentration (MIC)

- Preparation of medium YPD

  For a liter of medium 25 g Bacto ™ Peptone and 12.5 g Bacto ™ Yeast Extract were dissolved in 800 ml of distilled water. The total volume was adjusted to 900 ml once all the components were completely dissolved. The YP solution was then autoclaved immediately and all the following steps were performed in a sterile workspace. To 900 ml of YP solution 100 ml of 20 % glucose solution was added to obtain a final concentration of 2 % glucose.

- Preparation of stock solutions

  The solution required to obtain a standard solution was calculated for two plates and for a concentration of 12.8 g/ml for peptides and 1.6 mg/ml for the heterocyclic compounds.

  The compounds to screen were dissolved with deionized water for peptides and with DMSO for heterocyclic compounds into the calculated volume to obtain the desired stock solution. The stock solutions were stored at -80 ºC until usage.

- Preparation of working solutions

  The concentrations used in the adapted assay were based on the concentrations that were currently used for other azole antifungals (EUCAST protocol). The test range was 64 to 0.125 µg/ml for peptides and 10 to 0.0195 µg/ml for heterocyclic compounds.

  10 Falcon tubes were used to prepare the work solutions. The tube number one (D1, Table 35) was prepared by pippeting 36 µl from the stock solution and diluted with 3564 µl of YPD medium to obtain a final volume of 3600 µl and therefore, a concentration of 128 µg/ml. The falcon tubes, 2-10, were prepared by pipetting 1800 µl from the previous falcon tube into a new one with 1800 µl of YPD medium to get the final volume of 3600 µl (Table 36).

Table 36. Calculation of the final concentration for each falcon tube.

Falcon nº Tube	µl transferred to falcon	Final concentration in the falcon tube	Total Volume (µl)
D1	36	128	3600
D2	1800	64	3600
D3	1800	32	3600
D4	1800	16	3600
D5	1800	8	3600
D6	1800	4	3600
D7	1800	2	3600
D8	1800	1	3600
D9	1800	0.5	3600
D10	1800	0.125	3600

- Colony suspension

  The inocolum was prepared by harvesting a single colony form an YPD-agar plate. The cells were transferred to an Eppendorf tube with 1 ml of sterile distilled water. The OD_{600} was measured on a photometer and adjusted with YPD medium to an OD_{600} of 0,01. In *C. glabrata*, this OD_{600} correlates to a cell density of 2.5×10^6 CFU per ml.

- Inoculation of the plates

  For the assay, sterile 96 well microdilution plates with flat bottom and a capacity of 200 µl were used. 100 µl of the antifungal dilutions were pipetted to the first ten columns of the 96 well plates (Table 36). The preparation mixture with the highest concentration was placed in column 1 while that with the lowest concentration was placed in column 10. Each well in column 11 was filled with 100 µl of YPD medium as a positive control and column 12 served as negative control with 200 µl of YPD medium. The whole plate layout is shown in Table 37.

  Afterwards, 100 µl of cell suspension were added to the wells in columns 1 to 11. For each strain two rows were used as duplicates. The plates were then incubated for 24 h at 30 ºC without agitation. As further positive control, two plates were filled only with YPD medium.

Table 37: Scheme of the plate layout. Green: solutions. Yellow: 100 % growth drug free. Orange 0 % growth (no inoculation).

	1	2	3	4	5	6	7	8	9	10	11	12
A	D1	D2	D3	D4	D5	D6	D7	D8	D9	D10	100	0
B	D1	D2	D3	D4	D5	D6	D7	D8	D9	D10	%	%
C	D1	D2	D3	D4	D5	D6	D7	D8	D9	D10	C	C
D	D1	D2	D3	D4	D5	D6	D7	D8	D9	D10	T	T
E	D1	D2	D3	D4	D5	D6	D7	D8	D9	D10	R	R
F	D1	D2	D3	D4	D5	D6	D7	D8	D9	D10	L	L
G	D1	D2	D3	D4	D5	D6	D7	D8	D9	D10		
H	D1	D2	D3	D4	D5	D6	D7	D8	D9	D10		

- Reading of the plates

  After incubating the plates for 24 h at 30 ºC, the OD_{600} values were measured using a plate reader (Victor^3). Table 38 shows exemplary results for such measurement.

Table 38: Scheme of the results obtained after OD_{600} measurement.

		Relative growth									
		1	2	3	4	5	6	7	8	9	10
SC5314	A	99,7	101,7	100,4	100,3	99,6	99,9	100,1	99,3	99,2	99,4
SC5314	B	100,3	100,8	100,0	99,8	100,2	100,0	101,0	100,6	100,0	99,8
ATCC2001	C	100,6	100,6	99,8	99,9	99,3	99,3	99,7	100,0	99,9	99,9
ATCC2001	D	100,2	100,5	99,6	99,7	99,7	99,0	100,1	99,9	99,5	99,7
ATCC22019	E	104,4	101,3	96,3	97,5	100,9	101,9	101,6	98,8	97,9	99,0
ATCC22019	F	103,6	101,0	95,8	97,4	100,1	101,2	102,6	100,2	99,7	98,1
ATCC6258	G	106,2	102,5	100,0	100,6	100,3	100,2	100,8	99,5	99,8	100,9
ATCC6258	H	106,1	103,1	100,3	106,8	100,5	101,6	101,0	100,6	100,2	100,0
	µg.ml^{-1}	64	32	16	8	4	2	1	0,5	0,25	0,125

6.3.2.4. Screening of clinical *Candida* spp isolates

The screening plates with 100 µl of medium YPD were supplemented with 100 µl of the respective antifungal compound (all wells except the last 4 of the plates) with the concentration determinate based on the previous MICs assay.

The clinical isolates were arrayed in a 96-well pattern on a solid media square plate. Using a Singer RoTor HDA robot, they were transferred to the 96-well plate holding the 200 µl (YPD media + peptide) and incubated at 30 °C for 24 h.

The readings were carried out after those 24 h of incubation by measuring the OD_{600} at Victor^3 plate reader.

The empty wells containing only media was used as a blank for the growth.

6.3.2.5. Proteomic assay

6.3.2.5.1. Fluorescence microscopy

A preinoculum culture of *C. albicans* SC5314 was cultivated overnight in YPD medium (50 ml) at 30 ºC and adjusted to an optical density (OD) of 0.4.

To reveal the influence of EMC120B12 and BE10 on the proteomic level on *C. albicans*, 50 ml RPMI 1640 medium with 10 % FBS was inoculated with the preinoculum of *C. albicans* SC5314 and adjusted to an optical density (OD) of 0.4 and grown for 1.5 h, 3 h, 4.5 h and 6 h at 37 ºC with and without the compounds using their IC_{50} previously determined (0.75 µM and 0.194 µM, respectively).

Therefore, 3 inoculations for each time corresponding to SC5314; SC5314 + **EMC120B12** (0.75 µM) and SC5314 + **BE10** (0.194 µM) (Scheme 14) were prepared.

30 min before the time points, 1 ml of each culture was transferred to three laboratory tubes, which were treated as follows:

- Lab tubes **A**: Addition of 60 µl H_2O_2 (30 %) to induce a positive control of oxidative stress with 25 µl DHR.
- Lab tubes **B**: no addition.
- Lab tubes **C**: Addition of 25 µl DHR.

After the time points, the samples were transferred to Eppendorf-cups and centrifuged at 7000 rpm for 10 min discarding the medium.

- To tub **A**: After centrifugation, the Eppendorf-cup contents were washed by 1 ml of PBS (3x).
- To tub **B**: After centrifugation, 1 ml of EtOH was added and kept at 4 ºC for 10 min. After removing EtOH, 1 ml of PBS and 10 µl (100 µg/ml) of PI were added. The solutions were kept at room temperature for 5 min and later discarded and washed with PBS (3x).
- To tub **C**: After centrifugation, 10 µl of PI was added and the mixture was kept at room temperature for 5 min. Later the tubs were washed with PBS (3x).

This procedure was repeated three times.

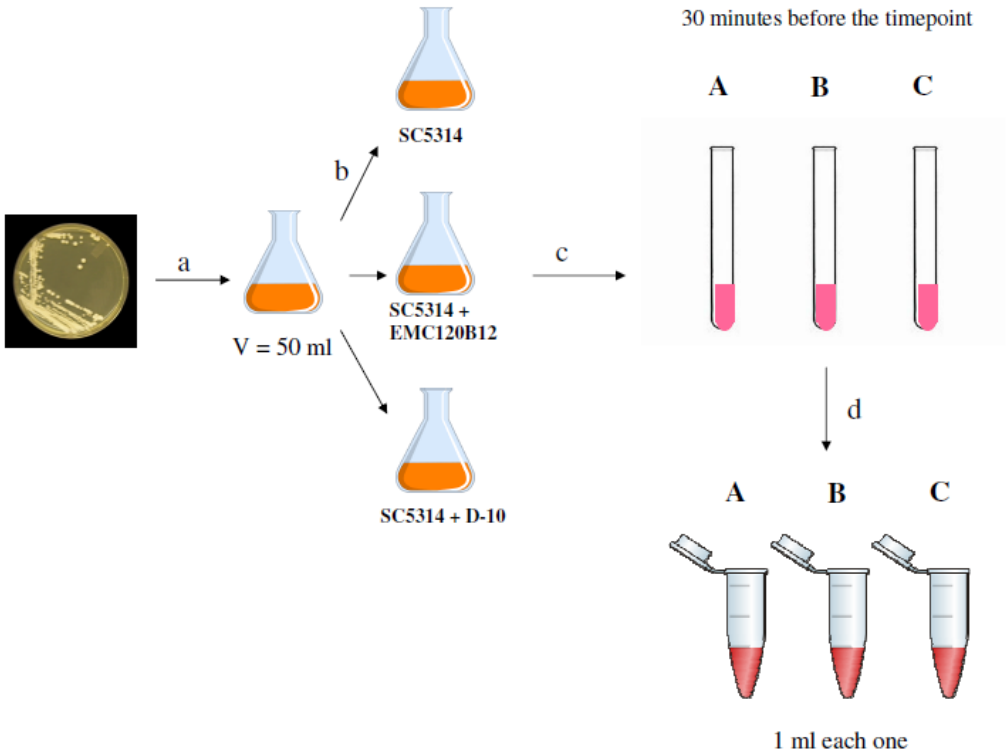

Scheme 14: a) preinoculum culture of *C. albicans* SC5314 was prepared overnight at 30 °C and adjusted to an OD of 0.4. b) 50 ml of RMPI was inoculated with the compounds to study (**EMC120B12** and **BE10**) with the preinoculum of *C. albicans* early prepared and left at 37 °C to the corresponding times (1.5; 3; 4.5 and 6 h). c) 30 min before the time points, 1 ml of each culture was transferred to 3 laboratory tubes and they were treated as it is described. d) after the time points, the solutions were transferred to 3 Eppendorf-cups.

These samples were examined using a fluorescence microscope at 596 nm for ROS^+ and 617 nm for PI.

6.3.2.5.2. Protein extraction by cell lysis

A preinoculum culture of *C. albicans* SC5314 was prepared in YPD medium (50 ml) at 30 ºC for 12 h and adjusted to an optical density (OD) of 0.4.

To reveal the influence of **EMC120B12** and **BE10** on the proteomic level and on *C. albicans*, 50 ml RPMI 1640 medium with 10 % FBS was inoculated with the preinoculum of *C. albicans* SC5314 and adjusted to an optical density (OD) of 0.4 and grown for 1.5 h, 3 h, 4.5 h and 6 h at 37 ºC with and without the compounds using their IC_{50} previously studied (0.75 µM and 0.194 µM, respectively).

Therefore, 3 inoculations for each time corresponding to SC5314; SC5314 + **EMC120B12** (0.75 µM) and SC5314 + **BE10** (0.194 µM) were prepared (Scheme 15).

After time points of 3 and 4.5 h, the solutions were centrifuged at 4 ºC for 10 min (2500 rpm) and the supernatant was removed. The cells were washed with PBS (3x) and transferred to Eppendorf-cups. After washing, the samples were resuspended in a lysis buffer composed by Tris-Hcl 50 mM (pH 7.5), 1 mM EDTA, 150 mM NaCl, 1 mM DTT, 0.5 % PMSF and 1 % of proteinases inhibitor.

To assure the rupture of the cells, glass beads were added and the samples were treated to 10 cycles of rupture in a bead beater. For each cycle of 20 s, the samples were cooled down for 2 min. After the lysate, the suspensions were centrifuged (2x) and the supernatant was recollected.

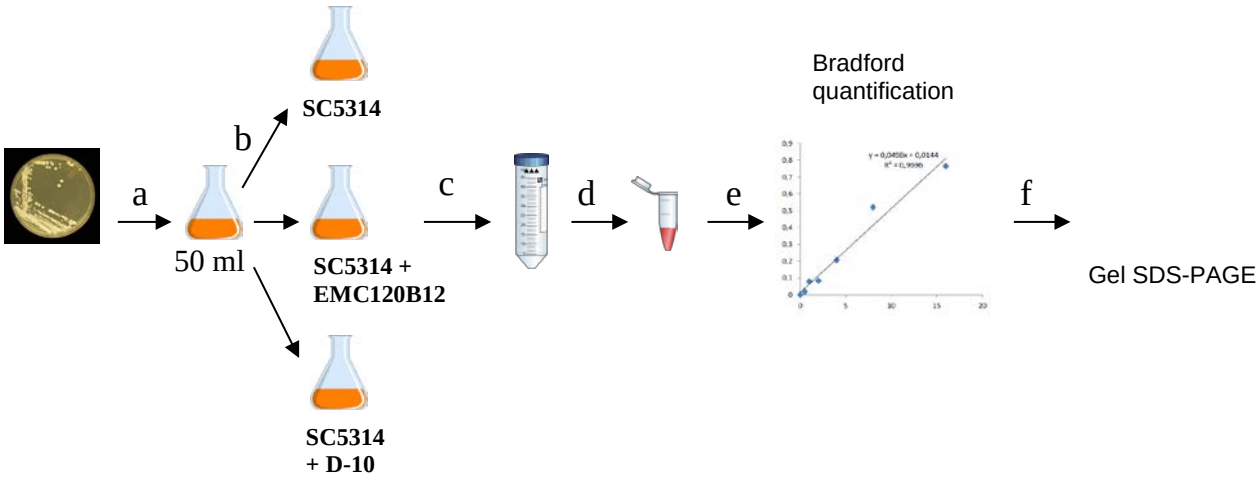

Scheme 15: a) Preinoculum culture of *C. albicans* SC5314 was prepared at 30 °C for 12 h and adjusted to an OD of 0.4. b) 50 ml of RMPI was inoculated with the compounds to study (**EMC120B12** and **BE10**) with the preinoculum of *C. albicans* early prepared and left at 37 °C to the corresponding times of 3 and 4.5 h. c) The 50 ml were transferred to falcons and centrifuged. d) The supernatant was removed and the pellets were washed with PBS and transferred to Eppendorf-cups. e) After cell lysis, the proteins were quantified by Bradford quantification. f) To visualize the proteins, a SDS-PAGE gel was carried out for all samples and replicates.

6.3.2.5.3. Protein quantification by Bradford method

To prepare the standard curve, a BSA protein sample concentration was used:

Eppendorf	**1**	**2**	**3**	**4**	**5**	**6**	**7**	**Sample**
BSA (V) 1 mg/ml	0 µl	0.5 µl	1 µl	2 µl	4 µl	8 µl	16 µl	5 µl
Protein	0 µl	1 µl	2 µl	4 µl	8 µl	16 µl	32 µl	X
Bradford reagent	200 µl	200 µl	200 µl	200 µl	200 µl	200 µl	200 µl	200 µl
H_2O	800 µl	799.5 µl	799 µl	798 µl	796 µl	792 µl	784 µl	795 µl

The Eppendorf-cups were incubated for 15 min in a dark box at room temperature. Then, the absorbances were measured at 595 nm and the regression line was made. To obtain the sample concentration, the following regression formula was applied:

$$y = 0.0498x + 0.0144$$

(X is the concentration and Y the absorbance).

6.3.2.5.4. Protein visualization by SDS-PAGE gel

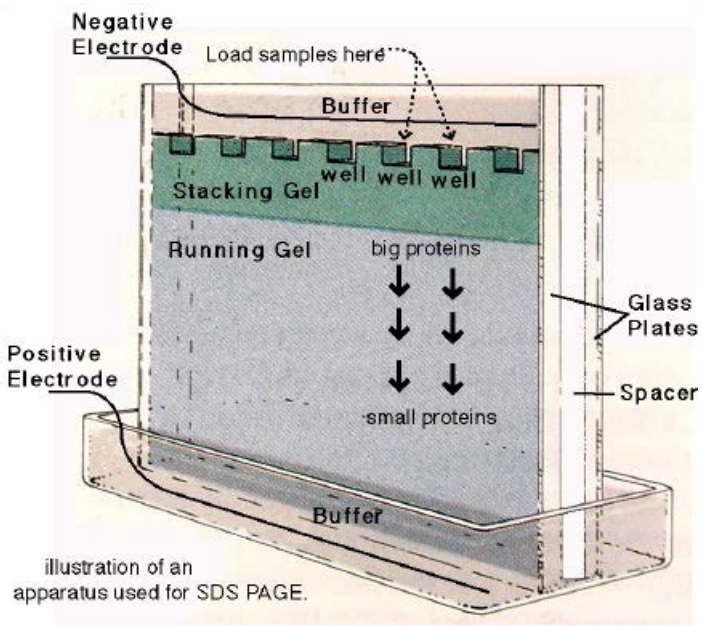

- Gel preparation:

	Stacking Gel (stock 50 ml)	Resolving Gel
H_2O	31.25 ml	5 ml
Tris-HCl (1.5 M pH 8.8)	---	2.5 ml
Tris-HCl (1.5 M pH 6.8)	12.50 ml	---
Acrylamide-bis-acrylamide Solution (40 %)	6.25 ml	2.5 ml
SDS (10 %)	250 µl	50 µl
APS (10 %) for 10 ml	100 µl	100 µl
TEMED (for 10 ml)	10 µl	10 µl

The resolving gel was prepared and immediately loaded in the integrated space of the glass plates. After addition of methanol to avoid polymerization inhibition, the plates were incubated for 30 min. Meanwhile, the stacking gel was prepared without the addition of TEMED and APS.

Methanol was then removed and then TEMED and APS were added to the concentration gel and loaded to the plates. They were incubated for 30 min to allow the polymerization.

The glass plate sandwiches were placed in the electrode assembly and the electrode assembly was filled with running buffer composed of 250 nM Tris-HCl, 1.92 M glycine and 1 % SDS.

40 µg of each sample was dissolved in sample buffer consisting of 30 nM Tris-HCl pH 6.8, 10 % SDS, 50 % glycerol, 3.5 M β-mercaptoethanol, bromophenol blue traces. The samples were heated at 100 °C for 10 min and later incubated on ice for further 10 min. The samples were centrifuged at 13.000 rpm for 2 min and then loaded to the gel. Then, the electric source was started at 100 V and left running until the bromophenol blue reached the edge of the gels.

The gels were extracted and dyed with bromophenol blue for 2-3 h and washed with methanol.

6.3.2.5.5. Protein digestion

After running the gel, some bands were cut out as closely as possible with a sharp scalpel and then cut into smaller pieces that were approximately 1 mm^2 to 2 mm^2.

The bands were transferred to Eppendorfs and washed 2 times with 50 µl of ACN during 5 min. The samples were dried in the Speed-vac for 15 min.

To reduce the samples, 50 µl of DTT solution (10 mM dithiothreitol) was added and incubated at 56 °C for 30 min.

DTT was removed by pipetting and washed with 50 µl of ACN (100 %) for 5 min. It was important to have the samples well dried, therefore the samples were dried again in the Speed-vac for 30 – 45 min.

To start the digestion, 1 µg of trypsin in 100 µl of Ambi 25 nM were added and incubated at 4 °C for 45 min.

After removing the excess of trypsin that was not incorporated in the gel, 50 µl of

Ambi 25 mM was added and incubated this time at 37 °C overnight.

On the next day, the samples were centrifuged for 1 min at 12.000 rpm. The peptide solutions in Ambi buffer were transferred to a fresh Eppendorf to extract the peptides as follows:

- 30 µl of ACN was added for 5 min. Then, ACN was removed.
- 20 µl of Ambi + 20 µl of ACN were added for 5 min. Then, all the mixture was removed and transferred to a new Eppendorf.

REFERENCES

7. REFERENCES

1. Bajwa, S. J. & Kulshrestha, A. Fungal Infections in Intensive Care Unit: Challenges in Diagnosis and Management. *Ann. Med. Health Sci. Res.* **3,** 238–244 (2013).
2. de Pauw, B. E. What Are Fungal Infections? *Mediterr. J. Hematol. Infect. Dis.* **3,** e2011001 (2011).
3. Keller, P. *et al.* An Antifungal Benzimidazole Derivative Inhibits Ergosterol Biosynthesis and Reveals Novel Sterols. *Antimicrob. Agents Chemother.* **59,** 6296–6307 (2015).
4. Badiee, P. & Hashemizadeh, Z. Opportunistic invasive fungal infections: diagnosis & clinical management. *Indian J. Med. Res.* **139,** 195–204 (2014).
5. Ramana, K. V *et al.* Invasive Fungal Infections: A Comprehensive Review. *Am. J. Infect. Dis. Microbiol.* **1,** 64–69 (2013).
6. Enoch, D. A., Ludlam, H. A. & Brown, N. M. Invasive fungal infections: a review of epidemiology and management options. *J. Med. Microbiol.* **55,** 809–818 (2006).
7. Kabir, M. A., Hussain, M. A. & Ahmad, Z. Candida albicans: A Model Organism for Studying Fungal Pathogens. *Int. Sch. Res. Netw. Microbiol.* **2012,** 1–15 (2012).
8. Höfs, S., Mogavero, S. & Hube, B. Interaction of Candida albicans with host cells: virulence factors, host defense, escape strategies, and the microbiota. *J. Microbiol.* **54,** 149–169 (2016).
9. Weindl, G., Wagener, J. & Schaller, M. Epithelial Cells and Innate Antifungal Defense. *J. Dent. Res.* **89,** 666–675 (2010).
10. Taff, H. T., Mitchell, K. F., Edward, J. A. & Andes, D. R. Mechanisms of Candida biofilm drug resistance. *Future Microbiol.* **8,** 10.2217/fmb.13.101 (2013).
11. Fauci, A. S. Infectious Diseases: Considerations for the 21st Century. *Clin. Infect. Dis.* **32,** 675–685 (2001).
12. Srinivasan, A., Lopez-Ribot, J. L. & Ramasubramanian, A. K. Overcoming antifungal resistance. *Drug Discov. Today Technol.* **11,** 65–71 (2014).
13. Balkis, M. M., Leidich, S. D., Mukherjee, P. K. & Ghannoum, M. A. Mechanisms of Fungal Resistance. *Drugs* **62,** 1025–1040 (2002).
14. Ghannoum, M. A. & Rice, L. B. Antifungal Agents: Mode of Action, Mechanisms of Resistance, and Correlation of These Mechanisms with Bacterial Resistance. *Clin. Microbiol. Rev.* **12,** 501–517 (1999).

15. Sheehan, D. J., Hitchcock, C. A. & Sibley, C. M. Current and Emerging Azole Antifungal Agents. *Clin. Microbiol. Rev.* **12,** 40–79 (1999).
16. Denning, D. W. Echinocandins: a new class of antifungals. *J. Antimicrob. Chemother.* **49,** 889–891 (2002).
17. Eschenauer, G., DePestel, D. D. & Carver, P. L. Comparison of echinocandin antifungals. *Ther. Clin. Risk Manag.* **3,** 71–97 (2007).
18. Butler, M. S., Blaskovich, M. A. & Cooper, M. A. Antibiotics in the clinical pipeline in 2013. *J Antibiot*. **66,** 571–591 (2013).
19. Brown, G. D. *et al.* Hidden Killers: Human Fungal Infections. *Sci. Transl. Med.* **4,** 165rv13 LP-165rv13 (2012).
20. Bauer, J. *et al.* High-Throughput-Screening-Based Identification and Structure–Activity Relationship Characterization Defined (S)-2-(1-Aminoisobutyl)-1-(3-chlorobenzyl)benzimidazole as a Highly Antimycotic Agent Nontoxic to Cell Lines. *J. Med. Chem.* **54,** 6993–6997 (2011).
21. Sun, H., Tawa, G. & Wallqvist, A. Classification of Scaffold Hopping Approaches. *Drug Discov. Today* **17,** 310–324 (2012).
22. Kaitin, K. I. Deconstructing the drug development process: the new face of innovation. *Clin. Pharmacol. Ther.* **87,** 356–61 (2010).
23. Schneider, G., Neidhart, W., Giller, T. & Schmid, G. 'Scaffold-Hopping' by Topological Pharmacophore Search: A Contribution to Virtual Screening. *Angew. Chemie Int. Ed.* **38,** 2894–2896 (1999).
24. Tsunoyama, K., Amini, A., Sternberg, M. J. E. & Muggleton, S. H. Scaffold Hopping in Drug Discovery Using Inductive Logic Programming. *J. Chem. Inf. Model.* **48,** 949–957 (2008).
25. Wang, L. *et al.* Accurate Modeling of Scaffold Hopping Transformations in Drug Discovery. *J. Chem. Theory Comput.* **13,** 42–54 (2017).
26. Burger-Kentischer, A. *et al.* A Screening Assay Based on Host-Pathogen Interaction Models Identifies a Set of Novel Antifungal Benzimidazole Derivatives. *Antimicrob. Agents Chemother.* **55,** 4789–4801 (2011).
27. Alksne, LE, D. P. Target-based antimicrobial drug discovery. *Methods Mol. Biol.* **431,** 271–283 (2008).
28. Zasloff, M. Antimicrobial peptides of multicellular organisms. *Nature* **415,** 389–395 (2002).

29. Campistany, A. G. Design, synthesis and study of the biological and biophysical activity of antimicrobial peptides. (Unpublished dissertation). *Universitat de Barcelona (UB)*, **2014**.
30. Brown, K. L. & Hancock, R. E. Cationic host defense (antimicrobial) peptides. *Curr. Opin. Immunol.* **18,** 24–30 (2006).
31. Aerts, A. M., François, I. E. J. A., Cammue, B. P. A. & Thevissen, K. The mode of antifungal action of plant, insect and human defensins. *Cell. Mol. Life Sci.* **65,** 2069–2079 (2008).
32. Kavanagh, K. & Dowd, S. Histatins: antimicrobial peptides with therapeutic potential. *J. Pharm. Pharmacol.* **56,** 285–289 (2004).
33. Ganz, T. Defensins: antimicrobial peptides of innate immunity. *Nat. Rev. Immunol.* **3,** 710–720 (2003).
34. Kościuczuk, E. M. *et al.* Cathelicidins: family of antimicrobial peptides. A review. *Mol. Biol. Rep.* **39,** 10957–10970 (2012).
35. Zanetti, L. T. and M. The Cathelicidins - Structure, Function and Evolution. *Current Protein & Peptide Science* **6,** 23–34 (2005).
36. Zanetti, M. Cathelicidins, multifunctional peptides of the innate immunity. *J. Leukoc. Biol.* **75,** 39–48 (2004).
37. Zanetti, M., Gennaro, R. & Romeo, D. Cathelicidins: a novel protein family with a common proregion and a variable C-terminal antimicrobial domain. *FEBS Lett.* **374,** 1–5 (1995).
38. Currie, S. M. *et al.* The Human Cathelicidin LL-37 Has Antiviral Activity against Respiratory Syncytial Virus. *PLoS One* **8,** e73659 (2013).
39. Seil, M., Nagant, C., Dehaye, J.-P., Vandenbranden, M. & Lensink, M. F. Spotlight on Human LL-37, an Immunomodulatory Peptide with Promising Cell-Penetrating Properties. *Pharmaceuticals* **3,** (2010).
40. Vandamme, D., Landuyt, B., Luyten, W. & Schoofs, L. A comprehensive summary of LL-37, the factotum human cathelicidin peptide. *Cell. Immunol.* **280,** 22–35 (2012).
41. Gudmundsson, G. H. *et al.* The Human Gene FALL39 and Processing of the Cathelin Precursor to the Antibacterial Peptide LL-37 in Granulocytes. *Eur. J. Biochem.* **238,** 325–332 (1996).
42. Murakami, M., Lopez-Garcia, B., Braff, M., Dorschner, R. A. & Gallo, R. L. Postsecretory Processing Generates Multiple Cathelicidins for Enhanced Topical

Antimicrobial Defense. *J. Immunol.* **172,** 3070–3077 (2004).

43. Zaiou, M., Nizet, V. & Gallo, R. L. Antimicrobial and Protease Inhibitory Functions of the Human Cathelicidin (hCAP18/LL-37) Prosequence. *J. Invest. Dermatol.* **120,** 810–816 (2017).
44. Johansson, J. Conformation-dependent Antibacterial Activity of the Naturally Occurring Human Peptide LL-37. *J. Biol. Chem.* **273,** 3718–3724 (1998).
45. Turner, J., Cho, Y., Dinh, N.-N., Waring, A. J. & Lehrer, R. I. Activities of LL-37, a Cathelin-Associated Antimicrobial Peptide of Human Neutrophils. *Antimicrob. Agents Chemother.* **42,** 2206–2214 (1998).
46. De Smet, K. & Contreras, R. Human Antimicrobial Peptides: Defensins, Cathelicidins and Histatins. *Biotechnol. Lett.* **27,** 1337–1347 (2005).
47. den HERTOG, A. L. *et al.* Candidacidal effects of two antimicrobial peptides: histatin 5 causes small membrane defects, but LL-37 causes massive disruption of the cell membrane. *Biochem. J.* **388,** 689 LP-695 (2005).
48. Barlow, P.G; Svodoba, P; Mackellar, A; Nash, A.A; York, J; Pohl, D.J; Davidson, R. . No Title. *PLoS One* (2011).
49. Wong, J. H. *et al.* Effects of cathelicidin and its fragments on three key enzymes of HIV-1. *Peptides* **32,** 1117–1122 (2011).
50. Büchau, A. S. *et al.* The Host Defense Peptide Cathelicidin Is Required for NK Cell-Mediated Suppression of Tumor Growth. *J. Immunol.* **184,** 369 LP-378 (2009).
51. Wu, W. K. K. *et al.* The host defense peptide LL-37 activates the tumor-suppressing bone morphogenetic protein signaling via inhibition of proteasome in gastric cancer cells. *J. Cell. Physiol.* **223,** 178–186 (2010).
52. Amer, L. S., Bishop, B. M. & van Hoek, M. L. Antimicrobial and antibiofilm activity of cathelicidins and short, synthetic peptides against Francisella. *Biochem. Biophys. Res. Commun.* **396,** (2010).
53. Steinstraesser, L. *et al.* Host Defense Peptides in Wound Healing. *Mol. Med.* **14,** 528–537 (2008).
54. Mookherjee, N. *et al.* Systems biology evaluation of immune responses induced by human host defence peptide LL-37 in mononuclear cells. *Mol. Biosyst.* **5,** 483–496 (2009).
55. Oppenheim, J. J. & Yang, D. Alarmins: chemotactic activators of immune responses. *Curr. Opin. Immunol.* **17,** 359–365 (2005).

56. Porcelli, F. *et al.* NMR Structure of the Cathelicidin-Derived Human Antimicrobial Peptide LL-37 in Dodecylphosphocholine Micelles. *Biochemistry* **47,** 5565–5572 (2008).
57. Burton, M. F. & Steel, P. G. The chemistry and biology of LL-37. *Nat. Prod. Rep.* **26,** 1572–1584 (2009).
58. Wang, G. Structures of Human Host Defense Cathelicidin LL-37 and Its Smallest Antimicrobial Peptide KR-12 in Lipid Micelles. *J. Biol. Chem.* **283,** 32637–32643 (2008).
59. Zelezetsky, I. *et al.* Evolution of the Primate Cathelicidin: Correlation between structural variations and antimicrobial activity. *J. Biol. Chem.* **281,** 19861–19871 (2006).
60. Braff, M. H. *et al.* Structure-Function Relationships among Human Cathelicidin Peptides: Dissociation of Antimicrobial Properties from Host Immunostimulatory Activities. *J. Immunol.* **174,** 4271 LP-4278 (2005).
61. Oren, Z., Lerman, J. C., Gudmundsson, G. H., Agerberth, B. & Shai, Y. Structure and organization of the human antimicrobial peptide LL-37 in phospholipid membranes: relevance to the molecular basis for its non-cell-selective activity. *Biochem. J.* **341,** 501–513 (1999).
62. Wang, G. Tool Developments for Structure-Function Studies of Host Defense Peptides. *Protein & Peptide Letters* **14,** 57–69 (2007).
63. Nell, M. J. *et al.* Development of novel LL-37 derived antimicrobial peptides with LPS and LTA neutralizing and antimicrobial activities for therapeutic application. *Peptides* **27,** 649–660 (2006).
64. Li, X., Li, Y., Han, H., Miller, D. W. & Wang, G. Solution Structures of Human LL-37 Fragments and NMR-Based Identification of a Minimal Membrane-Targeting Antimicrobial and Anticancer Region. *J. Am. Chem. Soc.* **128,** 5776–5785 (2006).
65. Li, Y., Li, X. & Wang, G. Cloning, expression, isotope labeling, and purification of human antimicrobial peptide LL-37 in Escherichia coli for NMR studies. *Protein Expr. Purif.* **47,** 498–505 (2006).
66. Meijer, A. B., Spruijt, R. B., Wolfs, C. J. A. M. & Hemminga, M. A. Configurations of the N-Terminal Amphipathic Domain of the Membrane-Bound M13 Major Coat Protein. *Biochemistry* **40,** 5081–5086 (2001).
67. Oren, Z., Hong, J. & Shai, Y. A repertoire of novel antibacterial diastereomeric

peptides with selective cytolytic activity. *J. Biol. Chem.* **272,** 14643–14649 (1997).

68. Sevcsik, E. *et al.* Interaction of LL-37 with Model Membrane Systems of Different Complexity: Influence of the Lipid Matrix. *Biophys. J.* **94,** 4688–4699 (2017).
69. Silhavy, T. J., Kahne, D. & Walker, S. The Bacterial Cell Envelope. *Cold Spring Harb. Perspect. Biol.* **2,** a000414 (2010).
70. Lau, Y. E., Bowdish, D. M. E., Cosseau, C., Hancock, R. E. W. & Davidson, D. J. Apoptosis of Airway Epithelial Cells: Human Serum Sensitive Induction by the Cathelicidin LL-37. *Am. J. Respir. Cell Mol. Biol.* **34,** 399–409 (2006).
71. Lai, Y. & Gallo, R. L. AMPed up immunity: how antimicrobial peptides have multiple roles in immune defense. *Trends Immunol.* **30,** 131–141 (2017).
72. von Haussen, J. *et al.* The host defence peptide LL-37/hCAP-18 is a growth factor for lung cancer cells. *Lung Cancer* **59,** 12–23 (2008).
73. Avrahami, D., Oren, Z. & Shai, Y. Effect of Multiple Aliphatic Amino Acids Substitutions on the Structure, Function, and Mode of Action of Diastereomeric Membrane Active Peptides. *Biochemistry* **40,** 12591–12603 (2001).
74. Tjabringa, G. S. *et al.* The Antimicrobial Peptide LL-37 Activates Innate Immunity at the Airway Epithelial Surface by Transactivation of the Epidermal Growth Factor Receptor. *J. Immunol.* **171,** 6690 LP-6696 (2003).
75. Mitchell, A. R. Bruce Merrifield and solid-phase peptide synthesis: A historical assessment. *Pept. Sci.* **90,** 175–184 (2008).
76. Nilsson, B. L., Soellner, M. B. & Raines, R. T. Chemical Synthesis of Proteins. *Annu. Rev. Biophys. Biomol. Struct.* **34,** 91–118 (2005).
77. Chan, W.C and White, P., Fmoc solid phase peptide synthesis; a practial approach. *Oxford (NY)* (2000).
78. Borgia, J. A. & Fields, G. B. Chemical synthesis of proteins. *Trends Biotechnol.* **18,** 243–251 (2000).
79. Kleymann, G. & Werling, H.-O. A Generally Applicable, High-Throughput Screening–Compatible Assay to Identify, Evaluate, and Optimize Antimicrobial Agents for Drug Therapy. *J. Biomol. Screen.* **9,** 578–587 (2004).
80. Jacoby, N. B. and E. On Scaffolds and Hopping in Medicinal Chemistry. *Mini-Reviews in Medicinal Chemistry* **6,** 1217–1229 (2006).
81. Hu, Y., Stumpfe, D. & Bajorath, J. Recent Advances in Scaffold Hopping. *J. Med. Chem.* **60,** 1238–1246 (2017).

82. Lloyd, D. G. Approaches to Scaffold Hopping. *Drug Discov. Today Technol.* **10,** e451–e452 (2013).
83. Vainio, M. J., Kogej, T., Raubacher, F. & Sadowski, J. Scaffold Hopping by Fragment Replacement. *J. Chem. Inf. Model.* **53,** 1825–1835 (2013).
84. Gomtsyan, A. Heterocycles in drugs and drug discovery. *Chem. Heterocycl. Compd.* **48,** 7–10 (2012).
85. Vitaku, E., Smith, D. T. & Njardarson, J. T. Analysis of the Structural Diversity, Substitution Patterns, and Frequency of Nitrogen Heterocycles among U.S. FDA Approved Pharmaceuticals. *J. Med. Chem.* **57,** 10257–10274 (2014).
86. Bansal, Y. & Silakari, O. The therapeutic journey of benzimidazoles: A review. *Bioorg. Med. Chem.* **20,** 6208–6236 (2012).
87. Singla, P., Luxami, V. & Paul, K. Benzimidazole-biologically attractive scaffold for protein kinase inhibitors. *RSC Adv.* **4,** 12422–12440 (2014).
88. Kaushik, N. K. *et al.* Biomedical importance of indoles. *Molecules* **18,** 6620–62 (2013).
89. Vaitla, J., Bayer, A. & Hopmann, K. H., Synthesis of Indoles and Pyrroles Utilizing Iridium Carbenes Generated from Sulfoxonium Ylides. *Angew. Chemie Int. Ed.* **56**, 4277- 4281(2017).
90. El-sayed, M. T., Hamdy, N. A., Osman, D. A. & Ahmed, K. M. Indoles as anticancer agents. *Adv. Mod. Oncol. Res.* **1,** 20 (2015).
91. Hong, W. *et al.* Synthesis and biological evaluation of indole core-based derivatives with potent antibacterial activity against resistant bacterial pathogens. *J. Antibiot.* **70**, 832-844 (2017).
92. Stocks, M. J., Cheshire, D. R. & Reynolds, R. Efficient and Regiospecific One-Pot Synthesis of Substituted 1,2,4-Triazoles. *Org. Lett.* **6,** 2969–2971 (2004).
93. Gudmundsson, K. S., Williams, J. D., Drach, J. C. & Townsend, L. B. Synthesis and Antiviral Activity of Novel Erythrofuranosyl Imidazo[1,2-a]pyridine C-Nucleosides Constructed via Palladium Coupling of Iodoimidazo[1,2-a]pyridines and Dihydrofuran. *J. Med. Chem.* **46,** 1449–1455 (2003).
94. Gueiffier, A. *et al.* Synthesis of Acyclo-C-nucleosides in the Imidazo[1,2-a]pyridine and Pyrimidine Series as Antiviral Agents. *J. Med. Chem.* **39,** 2856–2859 (1996).
95. Sebaugh, J. L. Guidelines for accurate EC50/IC50 estimation. *Pharm. Stat.* **10,** 128–134 (2011).

96. Frank, S. A. Input-output relations in biological systems: measurement, information and the Hill equation. *Biol. Direct* **8,** 31 (2013).
97. Lehar, J. *et al.* Synergistic drug combinations tend to improve therapeutically relevant selectivity. *Nat. Biotech.* **27,** 659–666 (2009).
98. Anderson, N. L. & Anderson, N. G. Proteome and proteomics: new technologies, new concepts, and new words. *Electrophoresis* **19,** 1853–61 (1998).
99. Wilkins, M. R. *et al.* From proteins to proteomes: large scale protein identification by two-dimensional electrophoresis and amino acid analysis. *Biotechnology. (N. Y).* **14,** 61–5 (1996).
100. Stojnev, S. *et al.* Challenges of Genomics and Proteomics in Nephrology. *Ren. Fail.* **31,** 765–772 (2009).
101. Chandramouli, K. & Qian, P.-Y. Proteomics: Challenges, Techniques and Possibilities to Overcome Biological Sample Complexity. *Hum. Genomics Proteomics* **2009,** 239204 (2009).
102. Weston, A. D. & Hood, L. Systems Biology , Proteomics , and the Future of Health Care : Toward Predictive , Preventative , and Personalized Medicine Introduction : Paradigm Changes in Health Care. *J. Proteome Res.* **3,** 179–96 (2004).
103. Lössl, P., van de Waterbeemd, M. & Heck, A. J. R. The diverse and expanding role of mass spectrometry in structural and molecular biology. *EMBO J.* **35,** 2634–2657 (2016).
104. Sanderson, M. J., Smith, I., Parker, I. & Bootman, M. D. Fluorescence Microscopy. *Cold Spring Harb. Protoc.* **10**, 1-36, (2014).
105. Bradford, M. M. A rapid and sensitive method for the quantitation of microgram quantities of protein utilizing the principle of protein-dye binding. *Anal. Biochem.* **72,** 248–254 (1976).
106. Marshall, T. Sodium dodecyl sulfate polyacrylamide gel electrophoresis of serum after protein denaturation in the presence or absence of 2-mercaptoethanol. *Clin. Chem.* **30,** 475 LP-479 (1984).
107. Shapiro, A. L., Viñuela, E. & V. Maizel, J. Molecular weight estimation of polypeptide chains by electrophoresis in SDS-polyacrylamide gels. *Biochem. Biophys. Res. Commun.* **28,** 815–820 (1967).
108. Laemmli, U. K. Cleavage of Structural Proteins during the Assembly of the Head of Bacteriophage T4. *Nature* **227,** 680–685 (1970).

109. Gundry, R. L. *et al.* Preparation of Proteins and Peptides for Mass Spectrometry Analysis in a Bottom-Up Proteomics Workflow. *Curr. Protoc. Mol. Biol.* **10**, 1-29, (2009).
110. Rawlings, N. D. & Barrett, A. J. [2] Families of serine peptidases. *Methods Enzymol.* **244,** 19–61 (1994).
111. Shevchenko, A., Tomas, H., Havlis, J., Olsen, J. V & Mann, M. In-gel digestion for mass spectrometric characterization of proteins and proteomes. *Nat. Protoc.* **1,** 2856–2860 (2007).
112. Thompson, A. *et al.* Tandem Mass Tags: A Novel Quantification Strategy for Comparative Analysis of Complex Protein Mixtures by MS/MS. *Anal. Chem.* **75,** 1895–1904 (2003).
113. Webster, K. L., Maude, A. B., O'Donnell, M. E., Mehrotra, A. P. & Gani, D. Design and preparation of serine-threonine protein phosphatase inhibitors based upon the nodularin and microcystin toxin structures. Part 3. *J. Chem. Soc. Perkin Trans.* **1,** 1673–1695 (2001).